INVESTIGATION OF BLAST ACTIONS ON MASONRY STRUCTURES USING NON-LINEAR FINITE ELEMENT ANALYSIS AND DEEP LEARNING TECHNIQUES

By

Sipho Gcinangaye Thango

Submitted in fulfilment of the academic requirements for the degree of Doctor of Philosophy in Civil Engineering, College of Agriculture, Engineering and Science University of KwaZulu-Natal, Durban

December 2023

Supervisor: Prof. Georgios A. Drosopoulos

PREFACE

The research presented in this thesis was carried out under the supervision of Prof. Georgios A. Drosopoulos of the School of Civil Engineering, Surveying and Construction, University of KwaZulu-Natal, Durban, South Africa. This thesis is comprised of a set of distinct journal articles and has been compiled in accordance with The Guidelines for the Writing of a PhD, prepared by the College of Agriculture, Engineering and Science at the University of KwaZulu-Natal, Durban and represents work written by Sipho Gcinangaye Thango, unless otherwise stated in the text.

Signed: …  ..

Prof. Georgios A. Drosopoulos

Date:

DECLARATION 1 - PLAGIARISM

I, Sipho Gcinangaye Thango, declare that:

1. The research reported in this thesis, except where otherwise indicated, is my original research.

2. This thesis has not been submitted for any degree or examination at any other university.

3. This thesis does not contain other persons' data, pictures, graphs, or other information, unless specifically acknowledged as being sourced from other persons.

4. This thesis does not contain other persons' writing, unless specifically acknowledged as being sourced from other researchers. Where other written sources have been quoted, then:

a. Their words have been re-written, but the general information attributed to them has been referenced.

b. Where their exact words have been used, then their writing has been placed in italics and inside quotation marks and referenced.

5. This thesis does not contain text, graphics or tables copied and pasted from the Internet, unless specifically acknowledged, and the source being detailed in the thesis and in the References sections.

Candidate:

……  …… 05/04/2024

Sipho Gcinangaye Thango Date

Supervisor:

As the candidate's supervisor I approve the submission of this thesis for examination.

…… 05/04/2024

Prof. Georgios A. Drosopoulos Date

DECLARATION 2 - PUBLICATIONS

This section presents the articles that form part and/or include the research presented in this thesis. This doctoral thesis is a compilation of international journal articles that are accredited by the South African Department of Higher Education and Training (DHET) and SCOPUS indexed.

Publication 1

Thango, S.G., Stavroulakis, G.E and Drosopoulos, G.A. (2023). Investigation of the Failure Response of Masonry Walls Subjected to Blast Loading Using Nonlinear Finite Element Analysis. *Computation,* 11, 165. https://doi.org/10.3390/computation11080165

Publication 2

Thango, S.G., Motsa, S.M., Stavroulakis, G.E and Drosopoulos, G.A. Investigating the effect of brickwork patterns on the response of masonry wall subjected to in-plane loading and blast loading.

(Article has been submitted for publication and is currently under review).

Publication 3

Thango, S.G., Motsa, S.M., Stavroulakis and G., Drosopoulos (2024). Prediction of the response of masonry walls under blast loading using Artificial Neural Networks.

Infrastructures, 9, 5. https://doi.org/10.3390/infrastructures9010005

Authorship contribution

In all the above listed papers, **Sipho Gcinangaye Thango** was the lead author who conducted the research, creating numerical simulations, machine learning models, coding and wrote the manuscripts. Prof. Georgios A. Drosopoulos is the supervisor of this PhD. The other authors assisted with finite element modelling, machine learning models and reviewed the papers.

Signed:

…… 05/04/2024……

Sipho Gcinangaye Thango Date

ACKNOWLEDGEMENTS

First of all, all glory belongs to the almighty God for His faithfulness, mercy, grace and for giving me knowledge and wisdom to start and finish this research work.

I express my sincere gratitude to my supervisor, Professor Georgios Drosopoulos, his continuous guidance, and support have been instrumental in shaping this research work. Your encouragement and mentorship enriched my academic journey. You have always made time for us to meet, and you have always given valuable feedback on all the drafts I have sent to you. Your attention to detail has really improved my writing skills. Thank you for believing in me when I sometimes felt like I am letting you down. Thank you, Prof.

I am also deeply thankful to Prof. Georgios E. Stavroulakis, for the research collaborations, comments and your computational mechanics knowledge came in handy. I would also like to thank Prof. Georgios E. Stavroulakis, for allowing me to remotely use the university of Crete's ABAQUS and MATLAB for my numerical simulations.

I would like to thank Dr. Siphesihle Mpho Motsa for the wonderful collaborations we had. Your knowledge on MATLAB and ABAQUS came in handy and for all the words of encouragement. I look forward to more research collaborations.

I would also like to my family (*boBhiyoza*) for the love and support. My parent's prayers have taken me this far. To all my friends, thank you.

Special thanks to my amazing, loving, and supportive wife, Patience Thango, who was patient enough with me during my studies. Thank you for listening to my coding challenges and for always believing in me. You have always been my number one supporter, and for that, I am grateful. Thank you to my daughters Zithelo and Zanothando for understanding when Daddy had to ask you to excuse him when he is working on his research.

ABSTRACT

Over the past decades, the investigation of masonry behaviour under in-plane and out-of-plane response has been an improving area of research. This thesis presents the findings from non-linear finite element analysis of masonry walls. The blast loading's effect on masonry structures has been investigated as part of this study using finite element analysis. Low-cost housing within the close proximity of mining operations have been heavily impacted by the effect of blast loading and this research intends at investigating the effect of blast loading on masonry walls.

Non-linear dynamic finite element analysis was used to create the structural model. Regarding the modelling approach that is adopted in this research, the masonry units are taken as continuum elements and the mortar joints as interface elements. The simplified micro modelling is used by defining the block-to-block interaction properties (mortar is not modelled). Through the use of friction interfaces and unilateral contact, zero tensile resistance between the joints is achieved. Utilizing the concrete damage plasticity model, the prediction of tensile and compressive failure of blocks was achieved. In terms of blast application, this research considered the surface blast and the different blast loading factors are considered which included the effect of standoff distance, explosive type and weight. The explicit dynamic solver is used in this research which adopts very small-time steps, that makes it appropriate for blast loading. Moreover, the small-time increments offered by the explicit solver are suitable for solving complex contact problems.

The first study investigated the behaviour of concrete brick walls under blast loading with varying standoff distance of 20m, 50m and 100m respectively. As part of the parametric investigating, the blast weight varied from 100kg TNT, 200kg TNT and 1150kg TNT for solid walls. For walls with opening, blast weights were increased to 2000kg TNT, and 3500kg TNT. According to the results, the effect of openings on walls proved to reduce the severity of damage on the walls.

The orientation of bricks in masonry wall construction is regarded as one of the aspects that architects consider vital for the aesthetics of the walls. However, the influence of brick patterns has not yet been thoroughly investigated. The second aspect of this research investigated the different bonding patterns which included the stacker bond, stretcher bond and English bond. It was observed that the failure modes under out-of-plane response among these different bonds

did not differ significantly, however, the different bonding pattern proved to have a significant influence on the response of the wall under horizontal loading (in-plane loading).

The introduction of machine learning methods for a fast-accurate prediction of the masonry wall response is achieved in this thesis as one of the innovations of this research. When compared to conventional numerical simulations, the machine learning methods offers a significantly reduced computational cost. Machine Learning (ML) approaches in the field of structural engineering is one aspect that is still being investigated by various researchers, however, the blast effect on masonry using these approaches is still not fully developed. As part of the deep learning technique, this study investigated the adoption of Artificial Neural Network (ANN). The dataset for ANN included the numerically generated results from commercial finite element software (ABAQUS) using varying blast weights and standoff distances. This process involved linking Python coding and MATLAB programming code to automatically generate these results without having to manually open the commercial finite element software. The accuracy levels that were obtained from the ANN models were in the acceptable range.

TABLE OF CONTENTS

List of Figures

Chapter 1

Chapter 2

Chapter 3

Chapter 5

List of Tables

Chapter 2

Chapter 5

Chapter 1 - Introduction

1.1 Background

Masonry is considered as the oldest building material that is still in use today for construction of structures. These structures comprise of residential houses, office, and commercial buildings. Most historical buildings are constructed using masonry units. The use of masonry has also been seen as the most affordable method to construct buildings. The construction method that is adopted includes the placement of stone or masonry units of each other and commonly bonded by means of mortar. In some cases, masonry walls are constructed as dry walls where the bricks are melded as interlocking bricks. Over the years, increasing research efforts have been developed, focusing on the evaluation of the structural behaviour of masonry walls. Masonry is described as a composite material, consisting of units and mortar arranged in a regular pattern forming joints, with the interface between the units and mortar joints acting as planes of weakness (Ahmad et al., 2014). Concrete masonry is also commonly used in low-cost houses. For these structural systems, the low tensile strength of masonry or mortar interfaces, may lead to an inadequate response when in and out of plane lateral forces reach high values.

The impact energy produced by blast casting in coal mining can break and cast rocks, yet the strong vibration effects at the same time affects the surrounding structures. Ground vibration originating from blasting operations can potentially lead to collapse of some structures. According to Nguyen et al (2019), complaints and litigation related to blast-induced vibrations are serious and can cause many open cast mines to stop production. The investigation of blasting forces on structures with specific reference to masonry structures is imperative. Other sources of blast loading include breaking of rock in construction activities. An increasing issue in contemporary society is the use of explosives by terrorist organizations throughout the world to attack civilian buildings and other facilities. Additionally, there are also accidental blast loads that masonry walls are subjected to, and those include gas explosions that take place in enclosed spaces. According to Devika et al (2021), blast loads are extreme, sudden, unpredictable impulses operating over milliseconds. This brings a serious challenge for structural engineers to accurately predict and model the effect of these loads on masonry structures.

The structural behaviour of masonry, especially in the context of blast loading, remains a captivating and challenging subject due to its heterogeneous composition. According to Shamim et al (2020), when the wall is exposed to blast, masonry walls break due to tensile and flexural failure, and any lateral stress is followed by the shearing of bed joints. The physics and thermochemistry of explosives, dynamic structural analysis, material behaviour, shock wave physics, and ballistics are all included in the interdisciplinary research on blast waves and how they interact with structures (Miller, 2004). Masonry is very stiff and brittle in-plane so that the forces transmitted by ground shaking or surface blast are high and failure is accompanied by a marked reduction in strength and stiffness (Sridhar et al., 1997). Damage normally comprises either collapse or diagonal cracking in both directions. Cracks, which will often be located between adjacent openings, will frequently follow the mortar joints. Recently, there has been various studies conducted by provided some insight on the response of unreinforced brick masonry walls when subjected to free-field explosions. The response of the wall to such loading is governed by the material and geometric nonlinearity (Macorini et al., 2014). The different brick patterns, size of bricks and their strength also plays a role in the structural response of masonry buildings. In the context of low-cost houses, poor workmanship has been observed in most developing countries and that can compromise the capacity of the walls.

In terms of analysing the masonry buildings, the finite element analysis (FEA) has gain popularity. FEA Software's such ANSYS, LS-DYNA, ABAQUS are commonly used in conducting numerical studies of masonry walls. This research work uses ABAQUS for modelling of walls subjected to blasting forces. One common requirement for all these FEA software packages is that the material properties must be properly defined and the definition of contact mechanisms. The definition of contact mechanisms depends on the complexity of the structure and the accuracy levels required from the analysis.

There are basically two numerical approaches that have been adopted by researchers to describe the mechanical behaviour of masonry: macro-modelling and micro-modelling (Lourenço et al., 1995). In macro-modelling, masonry is considered as a composite and homogeneous material while in case of micro-modelling masonry is considered as a discontinuous assembly of units connected by joints simulated by appropriate constitutive laws. Furthermore, in macro modelling technique, masonry units (concrete blocks, stone units), and the mortar between them are modelled as a single material. According to Kömürcü and Gedikli (2019), by using the macro modelling approach, the detailed failure mechanisms are generally not well reproduced. In most historical buildings, the macro approach is adopted.

The FEA however can be time consuming and computational expensive and, in most times, may be regarded impractical for simulations of large dataset. In that regard, data driven approaches have been regarded as an efficient approach in the sense that once offline training is complete, they can then predict fast and accurately the structural response, with reduced computational cost as compared to conventional numerical methods. Due to the reduced computational cost, data-driven approaches can also contribute towards the structural health monitoring of masonry walls under blast actions.

1.2 Motivation for the research

The South African coal mining sector produced 252.3 million tons of coal and contributed 2%, to the country's gross domestic product in 2017 (Minerals Council SA, 2018). Taking responsibility for public safety into account, this study takes cognisance that the coal production is essential in South Africa, at the same time the motivation to understand the impact of mining operations on public health and safety arose and hence the need to be able to able predict the masonry response to blasting forces. Around the globe, there are various minerals that are extracted by means of hard rock blasting and due to these activities, neighbouring structures has suffered. Figure1-1 below depicts some of the damages that have been linked to blast activities.

(a) (b) (c) (d)

Figure 1-1: a -b: Wall cracks after blasting in Glali Iron mine -Iran (Dehghani et al, 2021)

c: Wall cracks after blasting in Konkola Copper Mine- Zambia (ZNBC News, 2021)

d: Allegedly blast induced crack in Witbank- South Africa (Citizen news, 2018)

Terrorism and accidental explosions in recent years have become a threat to the safety of various existing structures. Failure of a masonry wall is likely to be sudden and severe that

poses significant debris hazard to building occupants when subjected to blast loads. Figure 1-2 below shows the catastrophic damage due to accidental damage and bombing attack.

(a) (b)

Figure 1-2: (a) Accidental explosion: Gas Explosion in Sunderland (Source: The Guardian-UK, 2017); Building damage due to bomb attack (Source: SABC News, 2021)

From the figure above, the importance of accurate analysis of buildings under blast loading and the provision of clarity of whether the alleged building cracks are caused by the blast action or not. Due to the apparent complexities and limitations associated with response prediction methods for blast loaded walls, it is worth noting that there is a need to investigate and develop methods for prediction of masonry failures under such loading conditions. This proposed study, through its model, will be able to provide a better understanding on the intensity or severity of blast action based on the explosive weight and the distance from the blast source to the targeted wall.

The simulation of the non-linear damage response of masonry walls comes with structural challenges that results from a wall being heterogeneous and anisotropic material due to mortar joints, with different tensile and compressive strength. Such challenges raise the need to adopt sophisticated constitutive descriptions, to capture failure due to opening-sliding in the interfaces plus compressive-tensile damage on the blocks. The simulation of blast load in this research is considered in the framework of non-linear time history (dynamic) analysis.

1.3 Research aims and objectives

This research aims at capturing the failure response of masonry walls using different blast properties (distance and charge weight), and to capture if the mode of failure is either in-plane or out-of-plane. This research presents the numerical investigation of the mechanical response

of masonry walls under blast actions, with and without openings. Non-linear finite element models are proposed to simulate all the joints between masonry units by introducing unilateral contact–friction interfaces. An empirical model is employed for the modelling of the blast action, and explicit dynamic analysis is used to construct this loading type. Different loading scenarios are examined, producing various failure mechanisms.

In addition, this research aims at introducing machine learning methods for a fast-accurate prediction of the masonry wall response. The investigation will focus on how neural networks can be used to predict the behaviour of masonry structures under blast loading considering the nonlinear constitutive relations of the corresponding material, with reduced computational cost than traditional methods of computation. The fast and accurate prediction of the wall's response leads to significant improvements in the field of structural engineering.

The objectives of the proposed study can be stated as follows:

- Propose a valid numerical model, which is able to predict the structural, ultimate response of masonry walls under blast actions generated from open cast mining activities.
- Investigate the behaviour of unreinforced masonry walls under blast loading using nonlinear finite element methods.
- Identify the detailed factors, such as in-plane or out-of-plane response and blast load properties, that govern the structural behaviour of masonry walls under blast actions.
- Investigate the effect of different brick bonding patterns on the in-plane and out-of-plane response of masonry walls.
- Investigate the suitability of neural networks for application in the structural analysis domain, particularly in simulating the behaviour patterns.
- Propose an automatic scheme, involving MATLAB, Python, and commercial finite element software, used to generate datasets describing the response of masonry walls under blast loads.
- Develop, train, and implement artificial neural networks to predict the structural response of masonry walls under blast action and compare the results of these neural networks with the results obtained from numerical simulations.

1.4 Research contributions

The aim of this study relies on the above considerations and is focused on the traditional and data driven approaches to provide an analysis of the possible failure mechanisms on the masonry structures that are subjected to blast loading, through FEA and machine learning methods. It is anticipated that this work will add valuable contribution to the field of structural engineering and computational mechanics. In this research, the main contributions are:

- Proposing a structural analysis scheme through numerical analysis that considers the non-linear response of masonry and can simulate all the joint interactions between masonry units by introducing unilateral contact–friction interfaces. Following the proposed approach, real failure modes due to blast actions, in the interface of masonry units or in the units, can be depicted.
- The influence of brick bonding patterns has been investigated by various research efforts under in plane loading. This study aimed at comparing the different bonding patterns under blast loading which cause out of plane deflections. The findings highlight the structural response when both in-plane loading (e.g. due to horizontal forces) and out of plane deflections due to blast, arise.
- Proposing numerical schemes using programming codes (MATLAB-Python) to automatically generate datasets providing the structural response of masonry walls under blast actions.
- Gaining insight and exploration the applicability of artificial neural networks as a fast-predicting tool for masonry walls subjected to blast loading.

1.5 Research approach and methodology

The general approach to achieving the objectives of this study was undertaken via numerical simulations and programming. Here are some highlights of the suggested technique (a) Nonlinear modelling of the walls using a commercial software and non-linear explicit dynamic finite element analysis adopting principles of contact mechanics and a concrete damage plasticity model to define the nonlinear properties of the wall (b) generation of a MATLAB and Python script to generate dataset via the commercial finite element software for training of neural networks, (c) using MATLAB R2019a to develop the neural network, train, and validation thereof.

It shall be noted that the scope of this study in terms of data collection is limited to numerically generated data, as experimental data for blast loading is expensive and unsafe, mainly for this

loading (blast actions). The cost aspect is associated with the construction of test walls, the procurement of explosives, hiring of measuring devices. Careful attention was paid to in ensuring that the numerical generated data can produce reliable results by comparing numerical results with existing experimental and numerical output.

1.6 Thesis structure

This thesis follows the structure of an "articles format thesis", which will consist of seven chapters. This thesis is therefore organized as follows:

Chapter One- Introduction

This chapter provides an introduction of the thesis, scientific or background information of the research and the rationale for the study. The aim and objectives of the research are outlined in this chapter.

Chapter Two- Literature review

This chapter discusses existing literature related modelling of masonry structures and machine learning applications. Related studies are reviewed, and a comparative discussion is made.

Chapter Three- Methodology

This chapter presents the methodology that was adopted for this study. The numerical approach is discussed here, involving the proposed finite element models and the methodological approach on the development of ANN models for the prediction masonry walls is discussed in detail.

Chapter Four (Paper 1)

A numerical investigation of masonry walls subjected to blast loads is presented in this chapter. A non-linear finite element model is proposed, to describe the structural response of the walls. This chapter is based on the published article with *MDPI -Computations.*

Chapter Five (Paper 2)

The Investigation of the effect of brickwork patterns on the response of masonry wall subjected to in-plane loading and blast loading is discussed in this chapter. This chapter is based on the article under review with *European Journal of Computational Mechanics.*

Chapter Six (Paper 3)

The prediction of masonry wall's response under blast loading using Artificial neural network (ANN) is presented in this paper. Feedforward Artificial Neural Network (FFANN) Application is adopted in this chapter. This chapter is based on the published article with *MDPI - Infrastructures.*

Chapter Seven -Conclusion and recommendations

This chapter provides a summary of the entire thesis. The main contributions and the final conclusions which can be derived from this study are listed in this chapter. Additionally, the future recommendations for future research in this field of study are also listed in this chapter.

1.7 References

ABAQUS v. 6.14.2 User's Manual. Available online: http://130.149.89.49:2080/v2016/index.html (accessed on 7 March 2022).

Ahmad, S., Elahi, A., Pervaiz, H., Rahman, A.G.A. and Barbhuiya, S. (2014). Experimental study of masonry wall exposed to blast loading, *Materiales de Construcción,* 64(313), http://dx.doi.org/10.3989/mc.2014.01513

CITIZEN NEWS (2018). available online, https://www.citizen.co.za/witbank-news/news-headlines/local-news/2018/12/17/problems-encountered-residents-vosman-emalahleni/, date accessed 25 September 2023

Dehghani, H., Jodeiri Shokri, B., Mohammadzadeh, H., Shamsi, S. and Salimi, N.A. (2021). Predicting and controlling the ground vibration using gene expression programming (GEP) and teaching–learning-based optimization (TLBO) algorithms. *Environ Earth Sci 80, 740 (2021).* https://doi.org/10.1007/s12665-021-10052-7

Devika, S., Jaleel, J., Mathews, M.T., Nayana, U.T. and Prabha, C. (2021). Prediction of blast loading and its effect on RCC structures, *International Research Journal of Engineering and Technology (IRJET)*, Volume: 08 Issue: 06 | June 2021, ISSN:2395-0056

Kömürcü, S. and Gedikli, A. (2019). Macro and Micro Modelling of the Unreinforced Masonry Shear Walls, *European Journal of Engineering and Natural Sciences*, 3(2): 116-123. https://dergipark.org.tr/en/pub/ejens/issue/49410/369461

Lourenço, P.B., Rots, J.G. and Blaauwendraad, J. (1995). Two Approaches for the Analysis of Masonry Structures: Micro and Macro-Modelling. *Heron,* 40, 313–338.

Macorini, L. and Izzuddin, B.A. (2014). Nonlinear Analysis of Unreinforced Masonry Walls under Blast Loading Using Mesoscale Partitioned Modelling, *American Society of Civil Engineers* (ASCE).

Miller, P. (2004). Towards the modelling of blast loads on structures, *Master of applied science thesis*, University of Toronto

Minerals Council South Africa (2018). Facts and Figures 2017, Retrieved from https://www.mineralscouncil.org.za%2Fdownloads%2Fsend%2F18-current%2F634-facts-and-figures-2017&usg=AOvVaw0KqG4yJaeqAqxJF15RqzFR, date accessed 12 April 2020

Nguyen, H., Moayedi, H., Jusoh, W.A.W. and Sharifi, A. (2019). Predicting Blast-Induced Ground Vibration in Open-Pit Mines Using Vibration Sensors and Support Vector Regression-Based Optimization Algorithms, pg 2-11

SABC News (2021). available online, https://www.sabcnews.com/sabcnews/israel-bombs-hamas-gaza-chiefs-home-as-fighting-enters-seventh-day/, date accessed 25 September 2023

Shamim, S., Shamd, S. and Khan, A. (2020). Numerical Modelling of Masonry Panel Subjected to Surface Blast Loading, *Journal of Xi'an University of Architecture and Technology*, ISSN No: 1006-7930

Sridhar, A., Steven R. and Brian W. (1997). Quantification and characterization of regional seismic signals from cast blasting in mines: a linear elastic model*, Earth and Environmental Sciences Division*, Los Alamos National Laboratory, University of California, Los Alamos, NM 87545, USA, pg 2-16

The guardian (2017). available online, https://www.theguardian.com/uk-news/2017/aug/11/sunderland-house-hit-by-gas-explosion, date accessed 25 September 2023

ZNBC News (2021). available online, https://www.znbc.co.zm/news/over-7-houses-develops-cracks/ , date accessed 25 September 2023

Chapter 2 – Literature Review

2.1 Description of Masonry

The most prevalent wall system used in the construction industry is the masonry wall system because it is strong and can be orientated in any direction. There are various types of masonry systems that exist, and the commonly used units are brick, concrete block, and stone. These masonry units are laid or jointed together by means of mortar. There are wall systems where the interlocking method is used and that does not require the use of mortar. The presence of individual units and mortar is what makes the masonry a heterogeneous material. The different loading systems that are imposed on masonry system results in both the units and mortar experiencing failure modes such as crushing and tensile crack failure. It has been highlighted by various researchers that mortar joints act as weakness planes under shear loads (Gajjar et al., 2021). Figure 2-1 below depicts the classification of stone masonry.

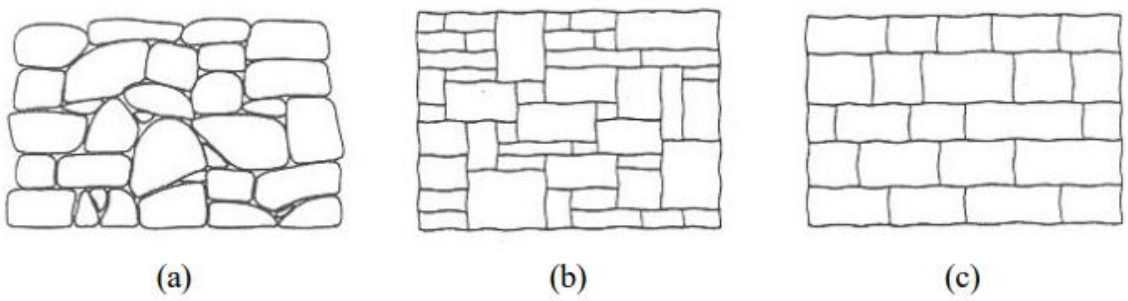

Figure 2-1:Different kinds of stone masonry: (a) rubble masonry; (b) ashlar masonry; (c) coursed ashlar masonry (Lourenco, 1998)

Most commonly, stone masonry is found in ancient buildings. The structural behaviour of rubble masonry in old structures is a fascinating phenomenon which has led to ongoing research due the heterogeneous nature of the material. The commonly used units in the past decades have been bricks. Figure 2-2 displays the typical bricks.

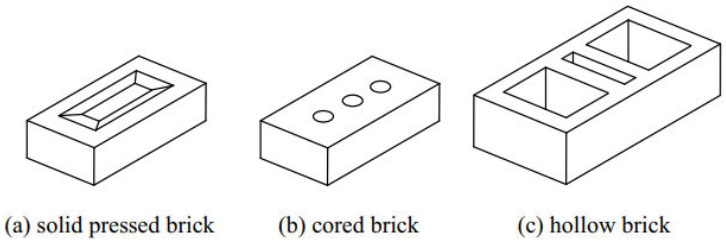

Figure 2-2:Contemporary clay bricks (Chaimoon, 2007)

Most buildings incorporate various architectural features and aesthetical finishing. Figure 2-3 shows the different types of brick bonding patterns that are commonly used in buildings. The stretcher bond, English bond and Flemish bond are the three main bond patterns commonly used in South Africa.

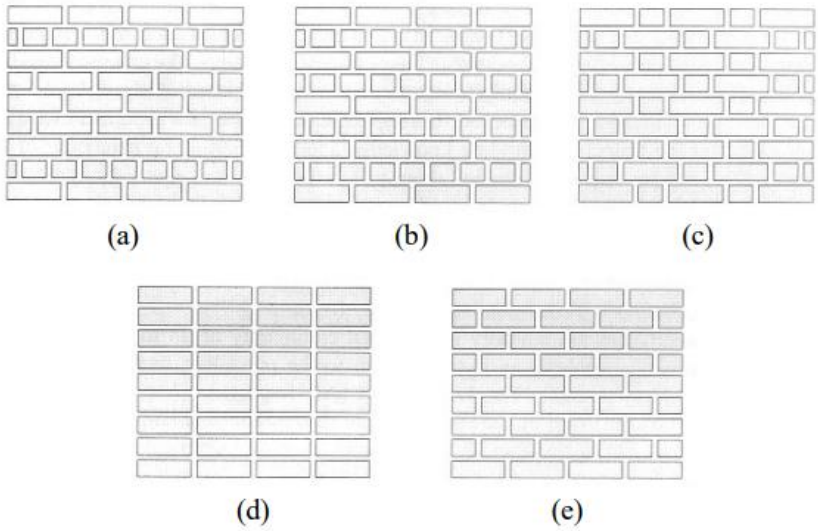

Figure 2-3:Different brick bonding patterns: (a) common bond; (b) English bond; (c) Flemish bond; (d) stack bond; (e) stretcher bond (Lourenco, 1998)

2.2 Mechanical behaviour of masonry

The mechanical behaviour is typically examined in relation to either the material or the structural components, where stiffness, strength, and ductility must be defined (D'Altri et al.,2020). These different types of masonry exhibit a common downfall which is the low tensile strength. However, experiment studies by various researchers have proven that masonry is strong in compression. According Thomoglou et al (2023), although bricks have a high compression strength, their poor tensile capacity causes them to fracture brittlely in tension and frictionally under shear loads. This mechanical behaviour is what makes the masonry an

anisotropic material which implies that the mechanical properties change based on the direction of loading. The unit-mortar interface is often regarded as the weakest component of masonry composite material due to the low tensile resistance of the mortar joins which leads to potential cracking. The mortar due to its lower Young's modulus tends to expand laterally but that is restricted by the bonding and frictional forces that are developed at the interface between masonry unit and mortar (Shrivastava,2022; Van der Pluijm et al., 2000). The differing compressive strengths and deformable characteristics of units and mortar are precursors of failure (Hilsdorf, 1969). Figure 2-4 below shows the mortar undergoing tri axial compression and the masonry unit undergoing biaxial tension coupled with vertical tension.

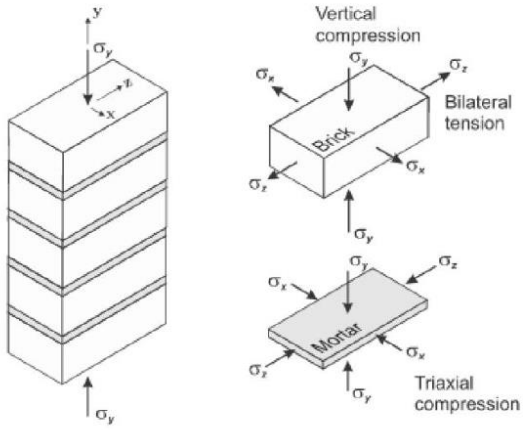

Figure 2-4:Stresses in brick-mortar composite (Canella, 2014)

According to Gatta (2019), when exposed to compressive stress, brick often responds in a brittle manner with high strengths, whereas mortar responds in a more ductile manner with lower resistance. Figure 2-5 (a) shows with reference to uni-axial compressive tests performed Binda et al. (1996). An experiment conducted by Kaushik et al. (2007) investigated the compressive behaviour of masonry prisms made of four brick types and three mortar grades. The results of the experiments highlighted that, contrary to the usually understood compressive behaviour of masonry, the stress-strain curves of masonry erected using bricks and mortar of equivalent strengths and stiffness were found to lie below the stress-strain curves of both bricks and mortar. This is shown in figure 2-5 (b).

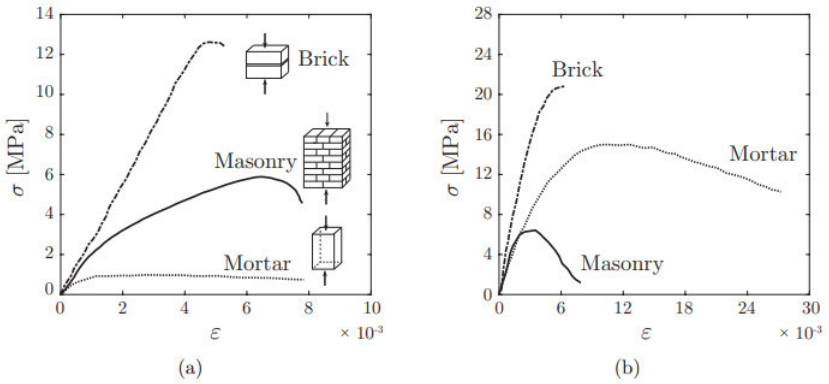

Figure 2-5:Stress-strain curves for bricks, mortar and masonry prims: (a) weak mortar (Binda et al., 1996) and (b) strong mortar (Kaushik et al., 2007)

Figure 2-6 below shows the behaviour of masonry under tension, compression and pure shear. According to Lourenco (1997) quasi-brittle material such as masonry often shows the softening behaviour which is due to material heterogeneity and material defects such flaws and voids. Strain-softening is a decline of uniaxial stress at increasing strain and further defined as the situation where the matrix of tangential elastic moduli ceases to be positive-definite (Bažant et al, 1984). Strain-softening does not only occur in tension but also in shear and compression. According to Bažant et al (1984), other mechanisms such as the rate effect can also be considered as the cause for strain-softening.

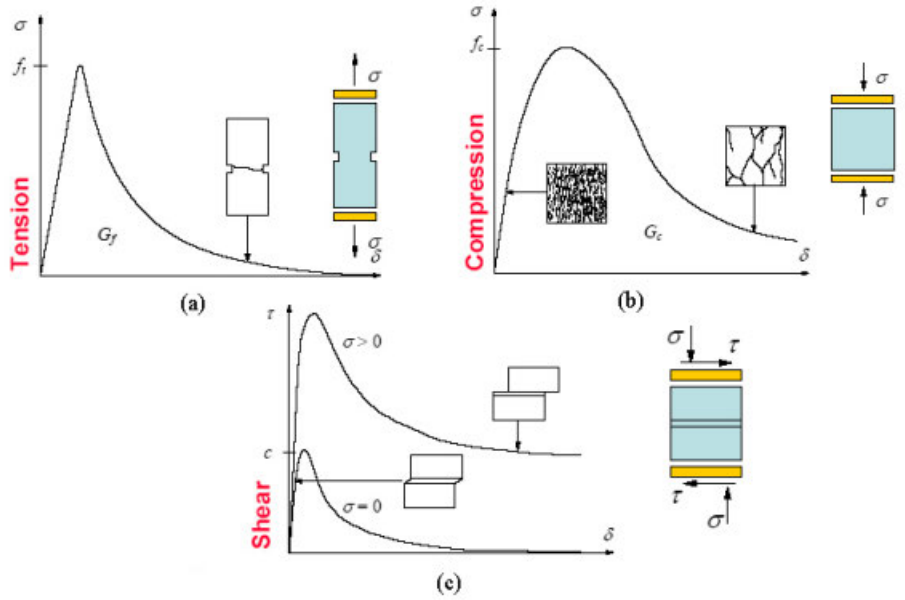

Figure 2-6:Typical behaviour of quasi-brittle materials and definition of fracture energy: uniaxial tensile loading (a); uniaxial compressive loading (b); pure shear (c). (Pelà ,2009)

The integral of the $\sigma-\delta$ diagram is the fracture energy, signified by G_f and G_c, for tension and compression, respectively. In case of slip of the unit-mortar interface under shear loading, the inelastic behaviour in shear can be described by the fracture energy $G_{II,f}$ which is defined by the integral of the $\tau-\delta$ diagram. The shear failure is a salient feature of masonry behaviour that must be taken into account in case of micro-modelling strategy. It is worth noting that this failure cannot be included in macro-modelling strategy as the unit-mortar properties are not discretized. According to Pelà (2009), shear failure is correlated with tension and compression modes in a principal stress space. The difference between micro and macro modelling strategy is later discussed in this chapter.

2.3 Masonry failure mechanism

The fundamental masonry failure mechanisms are depicted in figure 2-7 below. According to Lourenco, there are five failure mechanisms that can be observed from the assembly of two bricks and those include: joint tensile failure, joint shear failure, brick and mortar tensile failure, diagonal masonry failure, and masonry crushing. The joint mechanisms for tensile and shear failure of the mortar joint are depicted in Figs. 1(a) and 1(b), respectively. A combined brick and mortar failure mechanism that corresponds to brittle fracture of the brick assembly is shown in Fig. 2-7(c). The interaction between the bricks and the mortar joint is a key factor in the joint-brick failure processes seen in Figs. 2-7 (d) and 1(e).

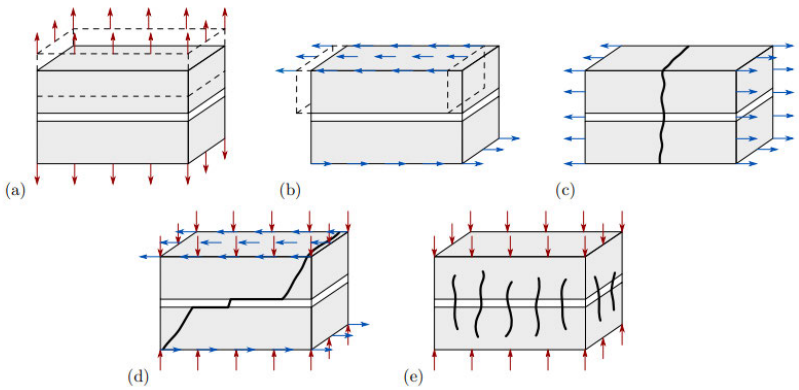

Figure 2-7:Masonry failure mechanisms: (a) joint tensile failure, (b) joint shear failure, (c) brick and mortar tensile failure, (d) diagonal masonry failure, and (e) masonry crushing. (Lourenco et al.,1997)

2.3.1 In-plane shear loading

Masonry systems presents some complexity in terms of the mechanical performance and the different failure patterns it presents under different loading conditions due to its heterogenous

behaviour. For this reason, it is essential to understand failure patterns for either the in-plane loading or out of plane loading. According to Page (1981), masonry walls are jointed together by mortar and the mortar joints act as plane of failure. As can be seen in figure 2-8 below, the majority of the failure patterns are along the joints with some failing under masonry crushing. It is worth mentioning that when the behaviour of masonry walls is investigated, the bond pattern of brick shall be carefully considered. When the principal tensile stresses within the wall supersede the in-plane capacity of the masonry units, the diagonal shear failure will form. According to Tomazevic (1999), the cracks in this failure mode will follow the mortar joints in a stair-case shape and in some cases go through the masonry units.

According to Ceroni et al (2021), shear failure is often observed by propagation of oriented cracks and these cracks can extend through the masonry unit or mortar. The common shear failure mechanics are sliding failure and diagonal shear failure. Mohr-coulomb criterion is commonly used to study the sliding mechanism (Ceroni et al., 2021). This can be described using eq. 2-1 below.

$$\tau = c + \tan \emptyset . \sigma \qquad (2\text{-}1)$$

where τ is the shear strength, based on cohesion, c, and the associated angle of friction, $\emptyset$, for the wall material and lastly, the level of normal compression, σ.

The typical in-plane failure mechanisms are depicted in figure 2-8 below.

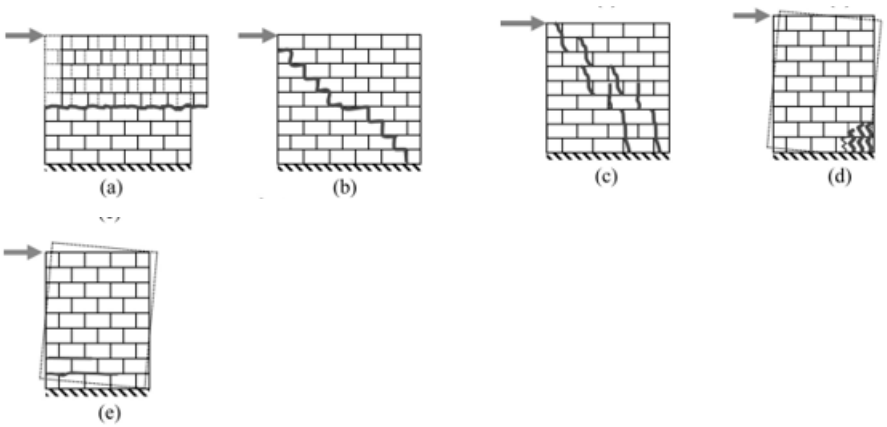

Figure 2-8:Masonry failure mechanisms: Shear failure (a, b, c); Compression failure (d); Tension failure (e) (Jovanoska & Churilov, 2009)

2.3.2 Out of plane failure mechanisms

For loading conditions such as blast loading, wind loading and seismic loading, their failure mechanisms are heavily reliant on the support conditions of the wall. The different support conditions mainly result in the behaviour of the wall being analysed as either one-way or two-way spanning, therefore uniaxial or biaxial bending is considered in this case. It is important to note that when walls are loaded laterally to their plane, such as with blast surface loading, the wall will develop bending actions and, when internal stresses exceed material strength, fracture patterns with directions rely on the boundary constraints definitions. An increase in shear capacity and high moment to shear ratio often results in flexural failure. Figure 2-9 shows the typical out-of-plane failure of masonry walls.

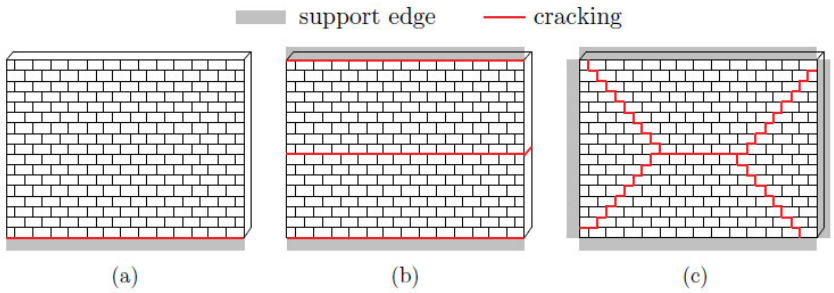

Figure 2-9:Typical out-of-plane failure cracking: (a) and (b) vertically spanning one-way walls and (c) two-way spanning walls. (Gatta ,2019)

According to Abrams et al (2017) highlighted that the out-of-plane response of walls is also dependent on other factors such as the level of the axial forces, the presence of openings and the quality of connections between the masonry units. The anisotropic nature of walls results in a much more complex structural behaviour when subjected to biaxial bending (Vaculik, 2012). Figure 2-10 below depicts internal joint stress distribution due to vertical bending, horizontal bending and bi-axial bending.

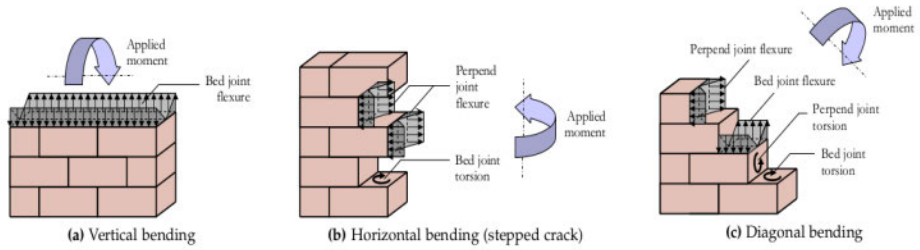

Figure 2-10:Internal stresses in the interfaces depending on the applied bending moment (Vaculik, 2012)

2.4 Masonry Modelling techniques

Due to the different characteristics of masonry unit and mortar, care is to be taken in modelling masonry walls. Modelling masonry walls aims at providing models that are close enough to the description and the behaviour of the real structure. According to Kömürcü and Gedikli (2019); Drosopoulos and Stavroulakis (2022), there are two commonly used modelling techniques, namely the heterogenous modelling and homogeneous modelling. This is demonstrated in figure 2-11 below. Under heterogenous modelling, there is micro modelling and simplified modelling. On the other hand, homogeneous modelling consists of macro modelling technique.

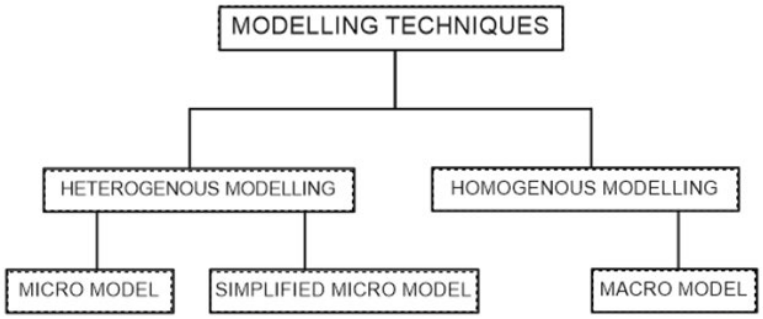

Figure 2-11:Modelling techniques for masonry walls (Kömürcü and Gedikli, 2019)

The modelling strategies for masonry structures are depicted in figure 2-12 below. Depending on the desired level of accuracy, masonry structures can be modelled using either the macro-modelling approach, in which masonry is simulated as a composite, or the micro-modelling approach, which accounts for all of the individual components of the masonry structures including the mortar and masonry units (Lourenco, 1995).

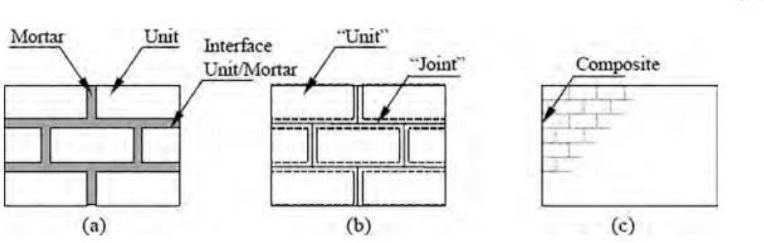

Figure 2-12:Modelling strategies for masonry structures: (a) detailed macro-modelling; (b) simplified micro-modelling; (c) macro-modelling (Lourenco, 1997)

The definition of these strategies is as follows:

- *Detailed micro-modelling*:

The masonry unit, mortar and interface are modelled as three different elements.

- *Simplified micro-modelling*:

Units are represented by continuum elements; introduction of normal and tangential contact surface definition to represent the mortar layer.

- *Macro-modelling:*

In this modelling approach, the mortar, and unit-mortar interfaces is treated as homogeneous. Due to the use of an anisotropic continuum model, units and joints are not represented, and the geometry of the components of masonry is lost (Zizi et al., 2017). This approach is common is analysing complex structures and historical buildings. The collapse mechanism is smeared out in the continuum using damage mechanics definitions. The homogenization approach requires special attention in correctly combining the masonry unit and the mortar, and that is mainly due to their differing properties.

2.5 Constitutive material model

The in-plane and out of plane response of masonry is analysed along with the available constitutive descriptions. FEM packages offer predefined material models that are suitable for the modelling of masonry behaviour. Traditional constitutive laws used to capture response of soils, concrete or masonry includes the Drucker-Prager and concrete damage plasticity. The Drucker-Prager plasticity model was originally created by Druker and Prager as a generalisation of the Mohr-Coulomb criterion in 1952. Initially, the criterion was introduced to deal with the plastic deformation of soils and has later been applied to rock, concrete, polymers, foams, and other pressure-dependent materials. On the other hand, the concrete damage plasticity model was originally developed for modelling concrete materials and other quasi-brittle materials.

2.5.1 Drucker-Prager model

The Drucker-Prager model is a popular model used for plasticity in materials such as masonry walls. According to Agüera *et al* (2016), it takes into account the effect of pressure on the yield stress of a material. The model considers the yield stress to be a function of the hydrostatic stress, which is the average stress acting on the material, and the deviatoric stress, which is the difference between the maximum and minimum stresses acting on the material. Drucker-Prager

is usually used to model frictional materials that have a greater compressive strength than tensile strength (Moonsamy, 2020). The equation for the yield surface of a linear Drucker-Prager model is given by:

$$t = d + \tan(\beta)(p) \quad (2.2)$$

Where t is the shear strength, $\tan(\beta)$ is the slope of failure, d is the cohesion, β is the angle of internal friction, and p is the normal stress.

The graphical presentation of the linear Drucker-Prager is show in figure 2-13 below.

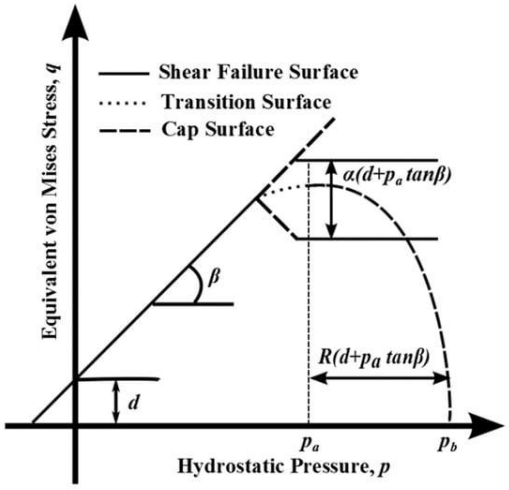

Figure 2-13:Illustration of the yield function and plastic potential for the DPC model (Buljak et al., 2021)

2.5.2 Concrete Damage Plasticity

Concrete Damaged Plasticity is a constitutive model used to simulate the behaviour of concrete structures under loading and unloading conditions. This model is commonly used for masonry walls and other structures that are prone to damage due to loading.

In the case of a masonry wall, the concrete damaged plasticity model may be used to predict the behaviour of the wall under various loading conditions, such as blast or seismic loads. This model takes into account the damage that may occur to the wall due to cracking or other forms of damage and can be used to determine the stability and safety of the wall in different scenarios. Concrete and masonry are ~~a~~ brittle material with very low tensile strength. Therefore, the concrete damage plasticity (CDP) model used to generate nonlinear properties of concrete and masonry (Daniel and Dubey, 2014).

The damage plasticity model incorporates the concept of material damage into the traditional framework that allows for a much more accurate representation of the progressive degradation and failure of material under loading. The plastic behaviour of the material and the evolution

of internal damage are the two key components that are identified by the damage plasticity model.

Several researchers have highlighted that when micromechanical approach is adopted, bricks and mortar are modelled separately. This approach assumes that nonlinear mechanisms are confined at mortar joints and for this reason, a linear elastic stress–strain relationship is assumed for blocks. The following equation depicts the linear elastic stress–strain relationship.

$$\sigma = E\varepsilon \tag{2.3}$$

Where σ is the stress related to elastic strain of the material ε, and E is the Young's modulus of material.

Additionally, the damage of a solid body can be defined as degradation phenomenon in material properties such as stiffness, strength, and anisotropy:

$$E = (1 - d)E_0 \tag{2.4}$$

Where E_0 represents the Young's elasticity modulus initial value and d denotes the degradation.

Lee et al (1998) developed an equation that defines the yield function of concrete damage plasticity model as the following.

$$\boldsymbol{F(\bar{\sigma}, k) = \frac{1}{1-\alpha}\left(\sigma\bar{I_1} + \sqrt{\frac{3}{2}}\,\|\bar{S}\| + \beta(k)\langle\overline{\sigma_{max}}\rangle\right) - c_c(k) \leq 0} \tag{2.5}$$

where:

$\boldsymbol{c_c(k)} = \boldsymbol{(\bar{\sigma}, k)}$ is the material cohesion,

$\boldsymbol{\bar{I_1}}$ is the first stress tensor invariant,

$\|\boldsymbol{\bar{S}}\| = \sqrt{\boldsymbol{\bar{S}} : \boldsymbol{\bar{S}}}$ is the stress tensor deviator norm,

$\boldsymbol{\bar{S} = \bar{\sigma} - \overline{\sigma_m}}$ I is the deviator of effective stress,

$\boldsymbol{\overline{\sigma_m} = \frac{1}{3}\, tr\bar{\sigma}}$ is the mean effective stress,

$\boldsymbol{\overline{\sigma_{max}}}$ is the algebraic maximum of eigenvalues of effective stress tensor,

From the above equation 2.5, the effective stress - total strain dependence for tension and compression is shown in figure 2-14 below.

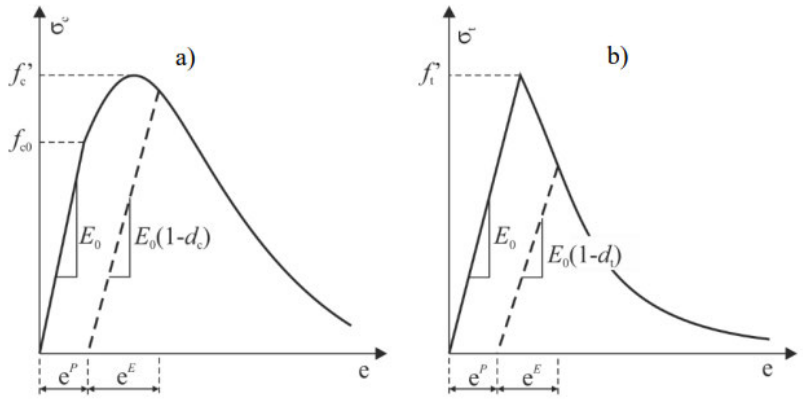

Figure 2-14:Dependence of stress on total strain for: a) compression and b) tension (ABAQUS, 2016).

2.6 Blast Phenomena

A blast wave is a particular kind of shockwave that is produced when a significant amount of energy is released suddenly, such in an explosion or detonation (Medici et al., 2014). Due to this rapid release of energy, the surrounding air is compressed by this outward flow of energy and moves ahead with a velocity front. Figure 2-15 shows the typical blast wave profile. As can be seen in figure 2-15, the ambient pressure rises nearly instantly following the explosion and starts to decline right away. Blast wave profile is illustrated by instant increase in pressure from ambient atmospheric pressure (P_0) to a peak incident overpressure (P_{S0}). According to Goel (2015), a positive phase duration is the time it takes for the peak incident overpressure to decline exponentially with time and revert to ambient air pressure at time t_0. The negative phase is more than double in terms of duration. It is worth mentioning that as the standoff distance increases, it can be noted that the duration/period of the positive blast wave phase increases, and that results in lower-amplitude, and significantly longer-duration shock pulse.

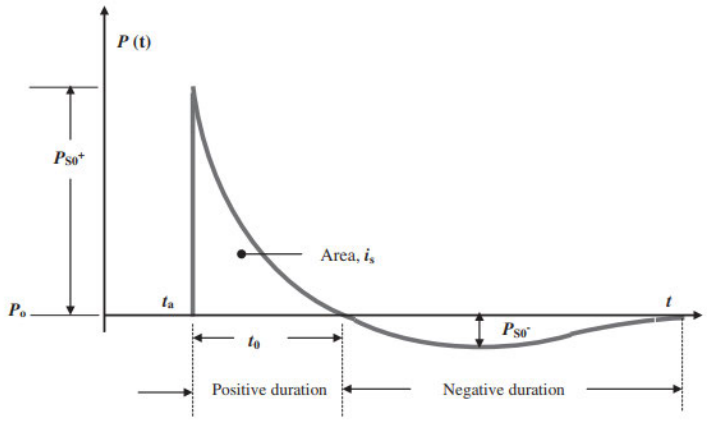

Figure 2-15:Blast wave pressure—time history from ideal explosion (Goel et al, 2012)

Using the Friedlander equation, the time evolution of the positive phase of the reflected pressure is analysed (Friedlander, 1946);

$$P(t) = P_{so}\left[1 - \frac{t}{t_0}\right]\exp\left[\frac{A\,X\,(t-t_a)}{t_0}\right] \quad (2.4)$$

where, *P(t)* is the pressure at time, P_{so} is the peak incident pressure, t_o is the positive phase duration and A is the wave decay coefficient.

The impulse of incident pressures is obtained by integrating the area under the pressure against time curve as per equation 2.5 below.

$$i = \int_{t_a}^{t_a+t_a} P(t)dt \quad (2.5)$$

Where i = impulse (MPa-ms), P= Pressure (MPa) and T = time (ms).

Figure 2-16 shows the variation of impulse and pressure with time from a characteristic explosion. The impulse is known as the level of the energy from an explosion that passes onto a building. The determination of impulse is vital for blast analysis especially in cases of shorter durations. In terms of response to peak pressure, brittle material such as glass are able to respond to peak incident pressure and are less affected by impulse while ductile materials respond more to impulse rather than peak incident pressure (FEMA, 2007). It can be highlighted that, a low order explosive with a prominent impulse that pushes for an elongated time will cause more damage to buildings and surrounding infrastructure.

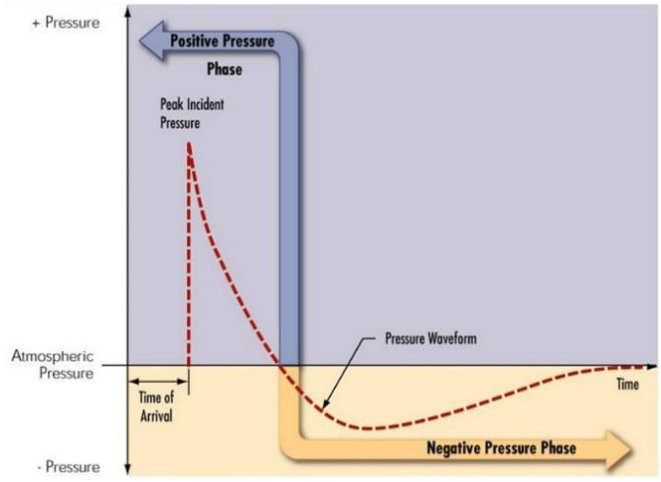

Figure 2-16:Typical Impulse Waveform (FEMA, 2007)

2.7 Types of explosions and classifications

Explosions are classified into two major categories, namely internal and external (TM5-1300 1990). Accidental explosions such gas explosions inside the building are regarded as internal explosions, whilst the external explosion refers to the blast in the open environment such as the blast activities in the mining sector. According to Yandzio et al (1999), explosions can be further classified as: Unconfined, Confined and explosive attached to a structure. Figure 2-17 depicts the types of unconfined explosions. Unconfined explosions have three types of bursts, namely free air burst, air burst and surface burst.

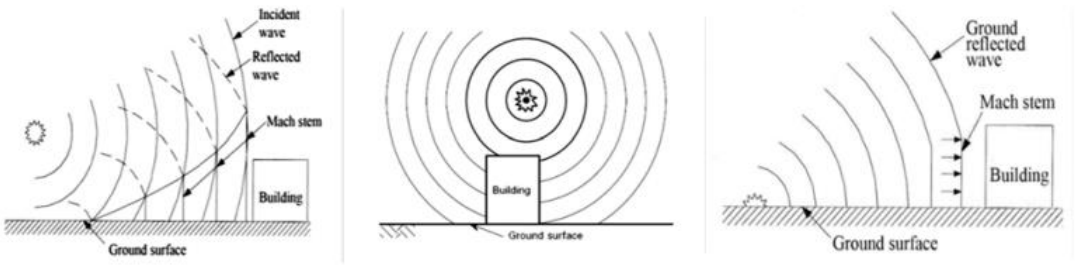

(a) (b) (c)

Figure 2-17:Classifications of external blast load: (a) Air burst with ground reflections, (b) Free-air burst explosion, (c) Surface burst (Jayasooriya, 2010)

Air Burst: The explosive explodes in the air such that the blast wave spreads spherically outward and strikes the structure after the first interaction with the ground; Mach wavefront is generated.

Free-air burst: The explosive explodes in the air such that the blast wave spreads spherically outward and strikes the structure directly without prior interaction with other obstacles or the ground.

Surface burst: The charge exploded just above the ground, the blast wave immediately interacted locally with the ground and then spread in a hemispherical shape outward and attacked the structure. In this type of explosion, the initial shock is amplified at the moment of detonation by reflections from the ground.

2.8 Blast Loading Factors

The effect of blast on structures is affected by various factors. According to Karlos and Solomos (2013), these factors include the stand-off distance, reflections and reflection angle.

Stand-off distance: The greater the distance between the explosive and the structure, the lower the incident and reflected pressure generated.

Reflections: When ground is considered as a reflection surface - the closer the explosive is to the ground, the smaller the addition of incident pressure, and the farther away it is, the greater the addition of incident pressure is.

Reflection angle: The reflection angle at which the blast wave strikes the structure affects the value of reflected pressure.

Explosive type and weight: The most commonly used explosive types is the TNT (Trinitrotoluene) and the weight of the explosive is usually estimated by taking into account the relevant attack or blast activity.

2.9 Recent studies on Structural analysis of Masonry walls under blast loading

Masonry walls, like any other structural element, requires proper analysis to withstand blast loading. The origination of these blast loading varies as some may be from mine activities, while some can be accidental explosions or deliberate attacks such as terrorist attacks. Several factors are considered when analysing masonry walls under such loading and that includes the material selection, structural configuration, wall thickness and joints definition.

Chen et al (2014) studied the out-of-plane behaviour of confined dry-stacked masonry walls against blast loading. Their walls consisted of an interlocking system which was laid in a stretcher bond pattern. This study conducted a numerical investigation using four cases using a charge weight of 4 kg, 8 kg, 12 kg, and 16 kg of Wabox explosive. From the non-linear

analysis carried out in this study, it was highlighted that numerical models are capable of correctly predict the pressure-time history and the results obtained in this study showed good agreement with the damage patterns from the experimental data.

Masi et al (2020) highlighted that masonry structures are characterized by non-planar and complex geometries. Their study adopted the Discrete Element Method for modelling the dynamic structural response to explosions. The proposed model was found to be able to accurately capture the dynamic response of the wall. The influence of micro-mechanical properties such as the tensile strength, dilatancy angle and the cohesion of masonry joints was investigated in this study. Furthermore, it was highlighted that the size of the building blocks and their shapes played a role in the overall strength of the masonry system.

Hao (2009) conducted numerical analysis of a 2880mm x 2820mm masonry wall subjected to blast load corresponding to TNT explosive weight W = 2000kg. In this study the four sides of the wall were modelled as fixed, with a mortar layer between the fixed boundary and the masonry units of the wall, which in turn is assigned homogenized material properties. It was demonstrated that the wall will collapse with larger explosives and a shorter standoff distance. The middle section of the wall collapses under out-of-plane loading, with one brick flying as a single piece. The wall was also seen to be damaged close to the boundary/edges. To estimate the masonry fragment size distributions, a novel method based on the combined facture mechanics and continuum damage mechanics theory was applied.

Anas et al (2022) assessed India's residential buildings and pointed out that most of the unreinforced masonry structures mainly constructed from clay bricks or concrete blocks or rubble masonry are capable of carrying some out-of-plane loads such as wind and earthquake. Under loading conditions such as high air-pressure that is generated by explosive-induced detonations, the walls were found to be more vulnerable. This study concluded that the maximum mid span deflection is less influenced by brick strength and mortar strength under peak reflected blast pressures that are greater than 2MPa. Additionally, the Young's modulus of masonry units plays a role in reducing the mid-span deflection. From this study, an important observation was made which highlighted the relationship between the failure mechanism and independent variables such as the peak overpressure, duration of the blast and boundary conditions.

In the study conducted by Wei et al (2021), the contact explosion load was considered. These contact explosion loads may arise from fireworks, gas stoves and high-pressure vessels. This

study highlighted the importance of carrying out this analysis as man-made explosions have resulted in causalities. In this study, the Riedel–Hiermaier–Thoma (RHT) strength and failure model is chosen to describe the behaviour of brick material, while MO-granular continuum model is used to describe the behaviour of mortar material. A similar study was carried out by Gu et al (2019) where masonry structures in the petrochemical industry were investigated. The three-dimensional solid element was adopted to discretize the geometrical model and to simulate brick and mortar material, the anisotropic material model in LS_DYNA was used. This study analysed the failure modes and the possibility of improving the blast resistance of masonry walls. The results obtained from this study indicate that the primary damage due to gas explosion was the flexural deformations and the complete collapse was latter observed from the full-scale field tests that were conducted. These two studies highlighted that a vast of studies have focused on far range explosions with less emphasis on the close range or contact explosion.

Ahmad et al (2021) conducted an experimental study of masonry wall exposed to blast loading. In this study, varying blast loads and standoff distances were considered. A total of 6 tests were performed and the results were comparable to the most published studies. Additionally, this study measured the pressure time history, and the acceleration history of the blast which was then compared to the one determined by the CONWEP function.

Ishfaq et al (2021) conducted a numerical study aimed at approximating blast loads on confined dry-stacked masonry wall. A nonlinear finite element method was developed using ANSYS-Autodyn to study the response of walls subjected to blast load. Explosive weights of 4kg, 8kg, 12kg and 16kg of Wabox were considered in their study and both air and explosive material were modelled using the Eulerian solver. It was further highlighted that the adequate understanding of the response of masonry walls against blast will assist designers in designing and constructing blast resistant buildings.

Chiquito et al (2018) studied the effects of blast and damage characterization on reinforced masonry walls at full-scale. A total of 16 walls which were 2.5m in length, 2.5m wide and 240mm thick were investigated via field experiments. In their study, Varying blast weights ranging from 18 to 38kg TNT at a constant standoff distance was considered. The effect of different types of masonry wall reinforcement was investigated which included using fibered mortar, recycled carbon fibre mesh and a polymer primed glass fibre. The results highlighted that the reinforcement influences the response of the wall significantly.

Urgessa (2009) adopted the finite analysis method to perform a dynamic analysis using an explicit time integration technique for modelling composite hardened walls subjected to blast loads. In this study, the finite element scheme was represented by a discrete system that only interact at nodal connectivity. The nodal displacements were obtained by solving equations of motions for the discrete system. One of the problem statements that this study highlighted was the unavailability of standard design guidelines for retrofitting masonry walls in order to withstand blast loading. A blast load of 0.5kg TNT was simulated at a distance of 1.83m. Furthermore, this study presented the uncertainties in the finite element analysis such as pressure distribution, the effect of mid height burst vs the one on the ground. It was concluded that the variation of modulus of elasticity displayed minimal significance on peak displacement which was then confirming the use of composites in retrofit designs as contributors in resistance deflection.

In the study conducted by Altunişik et al (2021), the response of brick walls subjected to blast loading was investigated numerically, experimentally and analytically. This study looked at terrorist attacks which results in structural damages. The explosive weights that were considered were 0.04kg, 0.150kg and 0.290kg which were placed at the centre of the walls. A nonlinear numerical investigation using macro-modelling approach was carried out using Ansys workbench and Autodyn software packages. In terms of the material properties and material models, the Riedel-Hiermaier-Thoma (RHT) model and P-alpha equation of state were chosen for brick elements. A direct relationship was observed between the increase of explosive weight and the displacement values. The higher explosive caused a collapse on the supporting joints of the wall.

Mollaei et al (2022) investigated the behaviour of masonry walls constructed with autoclaved aerated concrete blocks under blast loading. This study aimed addressing the issue of inadequate research being done on the lightweight walls when subjected to dynamic loading. Using ABAQUS/Explicit nonlinear method, the walls were investigated numerically under explosive weight of 5kg TNT and 7kg TNT at a standoff distance of 2, 5 and 10m. To define the nonlinear properties of concrete blocks, the concrete damage plasticity model was used. In this study, the simplified micro modelling approach was adopted. This research looked at three wall thicknesses being 15, 20 and 25cm. The conclusion from this study was that this type of masonry failed against explosion especially at shorter distances and also on walls with less thickness.

Zhang et al (2023) studied the dynamic behaviour of masonry walls under far-range explosions. In this study, numerical simulations were conducted on clay tile walls and masonry infill walls under far-range blast loads. The influence of boundary configuration and constraints was investigated. This study highlighted that far-range explosions can be considered as uniform load, and it was further highlighted that the boundary configuration had minimal influence of the wall's blast resistance while the boundary constraints played a role of the resistance or failure pattern of the wall.

Based on the above literature review, it can be highlighted that there is still space for more research investigating the collapse modes of masonry walls under blast actions. This research intends on providing further innovative insight into the way in-plane failure modes, such as diagonal cracking and out-of-plane damage, may appear in masonry walls subjected to blast actions.

2.10 Machine Learning Overview

2.10.1 General

Machine learning techniques have gained popularity in the field of structural engineering as valuable tools to improve design guidance and enhance current practices. Due to their flexibility, these data driven methods have been utilized in various areas, such as structural health monitoring, performance assessment of buildings, and prediction models of mechanical behaviour of structures. Artificial neural networks, support vector machines, and partial least squares are examples of supervised learning systems in machine learning (ML) that have shown effective in solving and optimising a wide range of engineering problems in the structural engineering domain. According to (Barkhordari et al., 2022), designing safe and dependable buildings requires the capacity to assess structural reaction and forecast the behaviour of structural elements, which these ML approaches offer. A graphical presentation of ML is depicted in Figure 2-18 below.

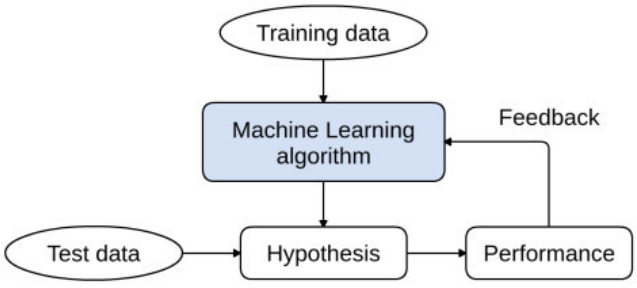

Figure 2-18:Machine learning process

Artificial Neural Network (ANN) is a machine learning technique composed of a system of interconnected neurons (Perez, 2022). According to Sildir et al., 2020, an artificial neural network is a computational mathematical modelling approach made up of several processing components that map and receive input data before producing outputs according to their predefined activation functions and algorithms. The concept of ANN emanates from the neural network or configuration in animals and human beings. ANNs are made up of several neurons that interpret information through connections.

2.10.2 Feedforward artificial neural network (FFANN) structure

According to Mtsweni (2021), the information in a feedforward artificial neural network (ANN) moves from the input layer via the hidden layers and out to the output layer exclusively. The reason it is termed "feedforward" is that the data flows over the network without going backward. Feedforward tasks are generally divided into two groups: function approximation and pattern classification. This research focuses on the approximation group/class. Figure 2-19 illustrates the design architecture of ANN consisting of three forms of layers, namely input, hidden and output layers. The network consists of neurons that are connected by synapse and each node translates values from the incoming connections. According to Kokossalakis (2000), each connection represents a channel where the neurons interchange information.

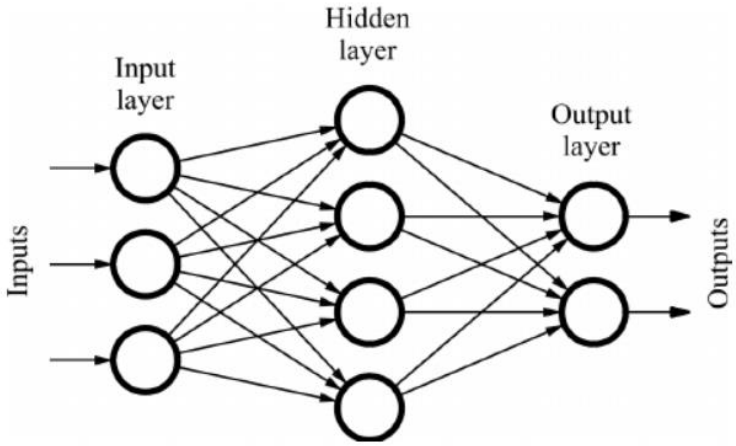

Figure 2-19:Feedforward ANN design architecture

The operation of each neuron from figure 2-19 is further illustrated in figure 2-20. There are calculations that are performed in the activation of neurons as they receive the signals from other neurons. This involves summing up the weighted incoming signals plus the bias terms, and there after feed the results to a transfer function (Kokossalakis ,2000).

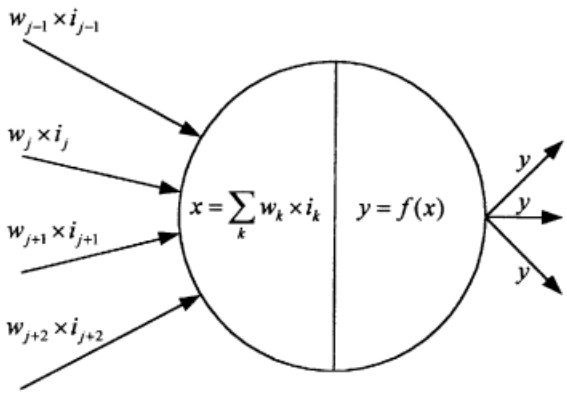

Figure 2-20:Simple Neuron

As illustrated in figure 2-20, the input from the j'th connection to the neuron is represented as i_j. The result of the operation at the left-hand side of the neuron can be explained with eq 2-6:

$$x = \sum_k (w_k \text{ x } i_k + b_k) \quad (2.6)$$

Where *k* is the number of the connections that are feeding the neuron. X represents the input to the neuron, w represents the weight, and b represents a bias term. The obtained results are then fed in a transfer function $f(x)$. The output with activation function is explained using eq 2-7.

$$y = f(x) = f\ (\sum_k (w_k \text{ x } i_k + b_k)) \quad (2.7)$$

A neural network's learning (training) process is an iterative one that involves doing computations both forward and backward through each network layer until the loss function is as small as possible. With this iteration process, the new ANN values become the new inputs that will feed the next layer in the network. According to Alom et al (2019), in the event that the total of the signals is greater than a certain threshold, the iteration will continue, and a signal will be continuously received.

2.10.3 Supervised learning

Supervised learning is a type of machine learning where an algorithm learns from a dataset containing input-output pairs (Liu and Wu ,2012). In this form of machine learning, during the training process, the ANN input variables are defined as the input vector on the network which then predicts the output vector. Once the output is generated, a comparison is made between the actual target vs the generated output and the error signal is generated based on this difference. According to Yang et al (2019), the input weights are then adjusted until error margins are reduced and that is the real output matching the desired output.

2.10.4 Unsupervised learning

Unsupervised learning is a method of learning in which the model gathers information on its own without any kind of supervision (Rojas, 2019). Unsupervised learning is often adopted for identifying patterns and trends in raw datasets. It can also be used in the exploratory phase to provide a better understanding of the datasets (Van Engelen et al., 2019). When compared with supervised learning, less human interaction is required. This type of learning is able to use raw and unlabelled training data.

2.10.5 Network build up

The components of the ANN are input layer, hidden layer, and output layer. These layers are discussed below:

-*Input layer*: The input layer is the first layer of neurons in a neural network which is aimed at receiving the input data which then communicates with one or more hidden layers.

-*Hidden layer*: This layer is known as the second layer of contact in ANN architecture. The hidden layer acts as an intermediate layer between the input and output layer and it processes the data by using complex non-linear functions. When defining the network parameters, the user can decide on the number of hidden layers/neurons. According to Jayasinghe et al (2022), the number of chosen hidden layers may result in some instabilities of the networks such as the issue of too many hidden neurons which causes over-fitting which has low bias and high variance. Minimal hidden layers on the other hand will not be able to capture the function's underlying trend of the data.

A neural network uses activation functions to calculate the weighted total of inputs and biases, which is then used to determine whether or not a neuron may be activated. According to Haykin (2009), the output of a neural network is influenced by the nature of the activation function ($\varphi(v)$) in the network, in terms of the induced local field v.

The section below discusses the widely used activation functions in developing neural networks.

- Sigmoid function: This a commonly used activation function in ANN, particularly feedforward neural networks. It is a mathematical function with a characteristic “S”-shaped curve. This activation function exists between 0 to 1 and it is regarded as the suitable function to predict the probability of the output. The sigmoid function is defined by equation 2-8 below.

$$\varphi(v) = \frac{1}{e^{(-\alpha v)}+1} \tag{2-8}$$

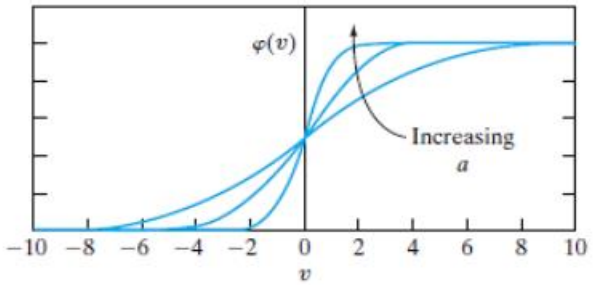

Figure 2-21:Sigmoid function for varying slope parameter a (Haykin, 2009)

- The threshold function: As shown in figure 2-22, this function gives 1 as the output of the input is either 0 or positive. This function can be expressed mathematically as:

$$\varphi(v) = \begin{cases} 1 \; if \; v \geq 0 \\ 0 \; if \; v < 0 \end{cases}$$

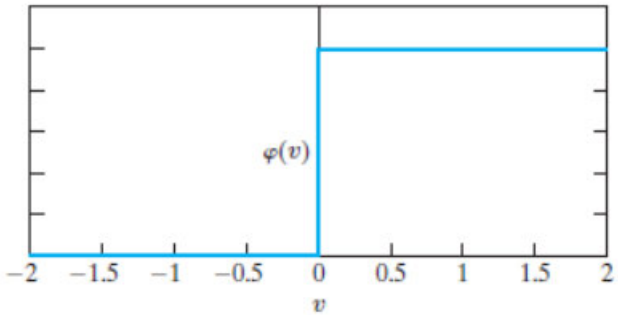

Figure 2-22:Threshold function (Haykin, 2009)

- Purelin activation function; This function does not affect the complicated character of the data collection and has an endless number of points inside its range (Wriggers, 2021). This function can be represented mathematically as

$$f(x) = x; \; f^1(x) = 1$$

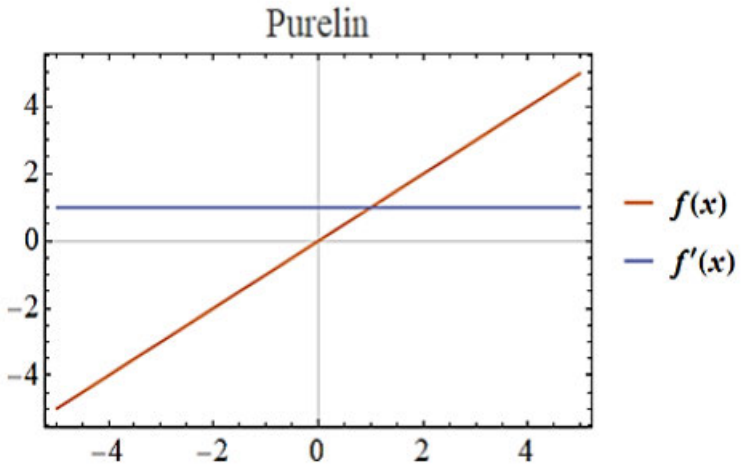

Figure 2-23:The Graph of Purlin Activation Function (Aldakheel et al., 2021)

-*Output layer*: The input goes through an arrangement of changes utilizing the hidden layer, which at last comes about in yield that's passed on utilizing this layer.

2.10.6 Performance criteria

The performance of the ANN is often measured using the criteria listed in table 2-1 below. The first performance measure is the coefficient of determination which measures how well the model explains and predicts the output. The Root mean squared error measures the error of a model in predicting quantitative data. The variance between the major values in the dataset and the predicted values is represented by the mean absolute error.

Table 2-1:Expressions to calculate the performance measures for ANN.

Name of the measure	**Symbolisation**	**Expression**
Coefficient of determination	R^2	$\boldsymbol{R} = \frac{[\sum_{i=1}^{n}(\boldsymbol{y}-\bar{y})(\boldsymbol{y'}-\bar{y})]^2}{\sum_{i=1}^{n}(y-\bar{y})^2 \sum_{i=1}^{n}(\boldsymbol{y'}-\bar{y})^2}$ Where y'= predicted value, y =actual value and n= number of samples
Root mean squared error	RMSE	$MSE = \frac{1}{n}\sum_{i=1}^{n}(y-y')^2$
Mean absolute error	MAE	$MAE = \frac{1}{n}\sum_{j=1}^{n}\lvert y-y'\rvert$

Root relative squared error	RRSE	$RRSE = \sqrt{\sum_{j=1}^{n}(y - y')^2 / \sum_{i-1}^{n}(y - \bar{y})^2} \times 100$

2.10.7 Related Machine Learning studies

Aguilar et al (2016) developed an ANN to predict the in-plane shear strength of reinforced masonry walls. The experimental database that included the specimens built using ceramic bricks and concrete bricks were tested. This dataset from the experiments was used to develop and train the network. In this study, the wall aspect ratio, the axial pre-compression on the wall, compressive strength of the masonry and the spacing of reinforcement were all taken into account during the testing of walls. It was concluded that the ANN was able to give good predictions and comparable to the results obtained from the experiments.

Khaleghi et al (2021) investigated the response of unreinforced masonry walls using ANN. This study looked at the reduction of the wall's load bearing capacity that can cause structural damage. The masonry wall was subjected to in-plane loading with 49 different configurations considered which included perforated masonry walls and solid walls. This study concluded the ANN'S ability to accurately predict the reduction of load capacity and the initial stiffness due to perforation of unreinforced masonry wall.

Argyropoulos et al (2019) used ANN to predict the masonry compressive strength. In this study, the nonlinear relation between the compressive strength of masonry and the geometry as well as the compressive strength of masonry was investigated. The network was trained using experimental data available in the literature. This study highlighted the ability of the ANN to approximate the compressive strength of masonry walls.

Bewick et al (2011) investigated the effectiveness of blast barrier walls in reducing blast loads on structures. This study raised the vital point of the difficulty in obtaining large datasets experimentally as blast experiments are time intensive and costly. The dataset for this study was generated numerically. Their approach was able to estimate the peak pressure, impulse, time of arrival and time duration of blast for buildings that are protected by barrier walls. The neural network-based simulation was able to provide efficient solution for prediction of blast loads effects on structures. Also, in Remennikov et al (2007), ANN was used to predict the effectiveness of blast wall barriers. A total of 285 measurements were used in their study and the cross-validation techniques were adopted in which the training set was employed to decide

the connection weight, whereas the validation set was used to evaluate the performance of the model.

Pitchaipillai et al (2019) used deep neural network to investigate the mechanical behaviour of various masonry infill walls with hybrid fibre mortar. A total of 60 specimens were used which were constructed using clay bricks and fly ash bricks. Shear tests and flexural tests were performed on the walls to develop the dataset. Their proposed modelling technique was evaluated by comparing it with the existing techniques.

In Motsa et al (2023), artificial neural networks were used to predict the response of masonry arch bridges. A dataset was numerically created, with input variables the geometric characteristics of masonry arches and output the ultimate, failure load and the collapse mechanism. To create the dataset, non-linear finite element simulations were conducted, introducing unilateral contact interfaces between masonry stones, as potential failure planes.

According to the given literature review, limited efforts are found on machine learning on masonry structures and even less on machine learning on masonry under blast action. This raises the need for development of machine learning models for masonry wall that are subjected to blast loading.

2.11 References

ABAQUS v. 6.14.2 User's Manual. Available online: http://130.149.89.49:2080/v2016/index.html (accessed on 13 March 2022).

Aguilar, V., Sandoval, C., Adam, J., Garzón-Roca, J., and Valdebenito, G. (2016). Prediction of the shear strength of reinforced masonry walls using a large experimental database and artificial neural networks. *Structure and Infrastructure Engineering*, 12(12), 1661-1674. https://doi.org/10.1080/15732479.2016.1157824

Ahmad, S., Elahi, A., Pervaiz, H., Rahman, F. and Barbhuiya, S. (2014). Experimental study of masonry wall exposed to blast loading. *Materiales De Construcción*, 64(313), e007. https://doi.org/10.3989/mc.2014.01513

Aldakheel, F., Satari, R. and Wriggers, P. (2021). Feed-Forward Neural Networks for Failure Mechanics Problems. (C. M. A., Ed.) *Applied Sciences*. DOI: https://doi.org/10.3390/app11146483

Alom, M.Z., Taha, T.M., Yakopcic, C., Westberg, S., Sidike, P., Nasrin, M.S., Hasan, M., Van Essen, B.C., Awwal, A.A.S. and Asari, V.K. (2019). A State-of-the-Art Survey on Deep Learning Theory and Architectures. *Electronics*, 8(3), 1-66.

Altunişik, A., Önalan, F. and Sunca, F. (2021). Experimental, numerical and analytical investigation on blast response of brick walls subjected to tnt explosive. Journal of Structural Engineering & Applied Mechanics,4(1), 28-45. https://doi.org/10.31462/jseam.2021.01028045

Anas, S., Alam, M. and Umair, M. (2022). Experimental studies on blast performance of unreinforced masonry walls: a state-of-the-art review. Asps Conference Proceedings, 1(1), 1791-1802. https://doi.org/10.38208/acp.v1.720

Argyropoulos, I., Cavaleri, L., Rodrigues, H., Varum, H., Thomas, J. and Lourenço, P. (2019). masonry compressive strength prediction using artificial neural networks., 200-224. https://doi.org/10.1007/978-3-030-12960-6_14

Bažant, Z.P, Belytschko, T.B. and Chang, T.P. (1984). Continuum Theory for Strain-Softening, Journal of Engineering Mechanics, Volume 110, Issue 12, ASCE, https://doi.org/10.1061/(ASCE)0733-9399(1984)110:12(1666)

Bewick, B., Flood, I. and Chen, Z. (2011). A neural-network model-based engineering tool for blast wall protection of structures. International Journal of Protective Structures, 2(2), 159-176. https://doi.org/10.1260/2041-4196.2.2.159

Binda, L., Mirabella Roberti, G. and Tiraboschi, C. (1996). Problemi di misura dei parametri meccanici della muratura e dei suoi componenti, in: La meccanica della muratura tra teoria e progetto, Messina, pp. 45–54

Buljak, V., Baivier-Romero, S. and Kallel, A. (2021). Calibration of Drucker–Prager Cap Constitutive Model for Ceramic Powder Compaction through Inverse Analysis. *Materials 2021*, 14, 4044. https://doi.org/10.3390/ma14144044

Canella, E. (2014). Experimental characterization of the compressive behaviour of brick-lime mortar masonry. *Barcelona: UPC*.

Celano, T., Argiento, L.U., Ceroni, F. and Casapulla, C. (2021). Literature Review of the In-Plane Behavior of Masonry Walls: Theoretical vs. Experimental Results. *Materials*, 14, 3063. https://doi.org/10.3390/ ma14113063

Chen, L., Fang, Q., Fan, J., Zhang, Y., Hao, H. and Liu, J. (2014). Responses of masonry infill walls retrofitted with cfrp, steel wire mesh and laminated bars to blast loadings. Advances in Structural Engineering, 17(6), 817-836. https://doi.org/10.1260/1369-4332.17.6.817

Chiquito, M., López, L., Castedo, R., Santos, A. and Pérez-Caldentey, A. (2018). blast effects and damage characterization on reinforced masonry walls at full-scale. https://doi.org/10.2495/susi180111

D'Altri,M., Messali,F., Rots,J., Castellazzi,G. and De Miranda,S. (2019). A damaging block-based model for the analysis of the cyclic behaviour of full-scale masonry structures. *Engineering Fracture Mechanics*,209, pp. 423–448. https://doi.org/10.1016/j.engfracmech.2018.11.046.

Drosopoulos, G.A., and Stavroulakis, G.E. (2022). Non-linear mechanics for composite heterogeneous structures, CRC Press, Taylor & Francis

Federal Emergency Management Agency (FEMA) 426. (2007). Manual to mitigate potential terrorist attacks against buildings, Chapter 4, Explosive Blast.

Gajjar, P. N., Gabrielli, E., Martin-Alarcon, D. C., Pereira, J.M., Lourenco, P. B. and Colla, C. (2021). An experimental and numerical contribution for understanding the in-situ shear behaviour of unreinforced masonry, *Journal of Building Engineering*, V. 44, p. 103389

Gatta, C. (2019). Masonry nonlinear response modelling and analysis of the effects of damaging mechanisms, *PhD Thesis in Structural Engineering,* Faculty of Civil and Industrial Engineering Department of Structural and Geotechnical Engineering, Sapienza Universita di Roma

Goel, M.D., Matsagar, V.A., Gupta, A.K. and Marburg, S. (2012). An abridged review of blast wave parameters. *Def Sci J 62(5):300–306.*

Goel, M.D. (2015). Blast: Characteristics, Loading and Computation—An Overview, Springer India, *Advances in Structural Engineering*, DOI 10.1007/978-81-322-2190-6_3

Gu, M., Ling, X., Wang, H., Yu, A. and Chen, G. (2019). Experimental and numerical study of polymer-retrofitted masonry walls under gas explosions. Processes, 7(12), 863. https://doi.org/10.3390/pr7120863

Haykin, S. (2009). Neural networks and learning machines. Third edition 2009 ISBN-13: 978-0-13- 147139-9.

Hilsdorf, H.K. (1969). Investigation into the failure mechanism of brick masonry loaded in axial compression. Designing engineering and constructing with masonry products, 34{41}.

Hao, D. (2009). Numerical Modelling of Masonry Wall Response to Blast Loads," Australian Journal of Structural Engineering. 10(1):37-52. https://doi: 10.1080/13287982.2009.1146503

Ishfaq, M., Ullah, A., Ahmed, A., Ali, S., Ali, S., Uddin, M. and Shahzada, K. (2021). Numerical approximation of blast loads on confined dry-stacked masonry wall. Mathematical Problems in Engineering, 2021, 1-13. https://doi.org/10.1155/2021/2394931

Jayasinge, T., Gunawardena, T. and Mendis, P. (2022). Assessment of shear strength of reinforced concrete beams without shear reinforcement: A comparative study between codes of practice and artificial neural network. *Case studies in construction materials*. Vol. 16. 01102. DOI: https://doi.org/10.1016/j.cscm.2022.e01102

Jayasooriya, R. (2010). Vulnerability and Damage analysis of reinforced concrete framed buildings subjected to near field blast events. *Ph.D. thesis*, Faculty of Built Environment and Engineering, Queensland University of Technology

Jovanoska, D.E. and Churilov, S. (2009). Calibration of a numerical model for masonry with application to experimental results, *Protection of Historical Buildings*, PROHITECH 09 – Mazzolani (ed), Taylor & Francis Group, London, ISBN 978-0-415-55803-7

Karlos, V. and Solomos, G. (2013). Calculation of blast loads for application to structural components. *European Commission*. Joint Research Centre. Institute for the Protection and the Security of the Citizen.

Kaushik, H.B., Rai, D.C. and Jain, S.K. (2007). Stress-strain characteristics of clay brick masonry under uniaxial compression. *Journal of Materials in Civil Engineering*, 19, 728–739.

Khaleghi, M., Salimi, J., Farhangi, V., Moradi, M. and Karakouzian, M. (2021). Application of artificial neural network to predict load bearing capacity and stiffness of perforated masonry walls. *Civil Eng*, 2(1), 48-67. https://doi.org/10.3390/civileng2010004.

Lee, J. and Fenves, G.L. (1998). Plastic-Damage Model for Cyclic Loading of Concrete Structures. *Journal of Engineering Mechanics*, 1998, 124 (8): 892–900, DOI: 1008 https://doi.org/10.1061/(ASCE)0733-9399(1998)124:8(892)

Liu, Q. and Wu, Y. (2012). Supervised Learning. In Encyclopaedia of the Sciences of Learning (pp. 3243–3245). *Springer US.* https://doi.org/10.1007/978-1-4419-1428-6_451.

Lourenco, P. B. and Rots, J. G. (1997). Multi-surface interface model for analysis of masonry structures. *Journal of Engineering Mechanics*, 123(7), 660-668.

Lourenço, P.B., Rots, J.G. and Blaauwendraad, J. (1995). Two approaches for the analysis of masonry structures: micro and macro-modelling. *HERON* 1995;40(4).

Lourenço, P.B. (1996). Computational Strategies for Masonry Structures. *Ph.D. Thesis*, Delft University of Technology, Delft, The Netherlands.

Masi, F., Stefanou, I., Maffi-Berthier, V. and Vannucci, P. (2020). A discrete element method based-approach for arched masonry structures under blast loads. *Engineering Structures*, 216, 110721. https://doi.org/10.1016/j.engstruct.2020.110721.

Medici, E. F., Allen, J. S. and Waite, G. P. (2014), Modelling shock waves generated by explosive volcanic eruptions, *Geophys.* Res. Lett.,41, 414–421, doi:10.1002/2013GL058340

Mollaei, S., Ghazijahani, R., Farsangi, E. and Jahani, D. (2022). Investigation of behaviour of masonry walls constructed with autoclaved aerated concrete blocks under blast loading. *Applied Sciences*, 12(17), 8725. https://doi.org/10.3390/app12178725.

Motsa, S. M., Stavroulakis, G. E., and Drosopoulos, G. A. (2023). A data-driven, machine learning scheme used to predict the structural response of masonry arches. In Engineering Structures (Vol. 296, p. 116912). Elsevier BV. https://doi.org/10.1016/j.engstruct.2023.116912

Mtsweni, S. (2021). Performance optimization modelling of a horizontal roughing filter for the treatment of mixed greywater, *Doctor of Engineering thesis*, Durban University of Technology.

Page, A. (1981). The Biaxial Compressive Strength of Brick Masonry. University of Newcastle, New South Wales, s.n., pp. 893-906.

Pelà, L. (2009). Continuum Damage Model for Nonlinear Analysis of Masonry Structures, *Phd thesis*, Universitat Politècnica de Catalunya.

Pitchaipillai, N. and Kumar, P. (2019). Deep neural network-based mechanical behaviour analysis for various masonry infill walls with hybrid fiber mortar. Structural Concrete, 20(6), 1974-1985. https://doi.org/10.1002/suco.201900064.

Remennikov, A. M. and Rose, T. A. (2007). Predicting the effectiveness of blast wall barriers using neural networks, *International Journal of Impact Engineering*, V. 34, No. 12, pp. 1907–23.

Rojas, R. (1996). Unsupervised Learning and Clustering Algorithms. In: *Neural Networks*, *Springer, Berlin, Heidelberg*, 99-121.

Sildir, H., Aydin, E. and Kavzoglu, T. (2020). Design of Feedforward Neural Networks in the Classification of Hyperspectral Imagery Using Super Structural Optimization. *Remote Sensing*, 12(6), 956.

Solís-Pérez, J. E., Hernández, J. A., Parrales, A., Gómez-Aguilar, J. F. and Huicochea, A. (2022). Artificial neural networks with conformable transfer function for improving the performance in thermal and environmental processes. *Neural Networks*. Elsevier BV. https://doi.org/10.1016/j.neunet.2022.04.016.

Thomoglou, A.K., Karabini, M.A., Achillopoulou, D.V., Rousakis, T.C. and Chalioris, C.E. (2023). Failure Mode Prediction of Unreinforced Masonry (URM) Walls Retrofitted with Cementitious Textile Reinforced Mortar (TRM). *Fibers 2023*, 11, 53. https://doi.org/10.3390/fib11060053.

Urgessa, G. (2009). Finite element analysis of composite hardened walls subjected to blast loads. American Journal of Engineering and Applied Sciences, 2(4), 804-811. https://doi.org/10.3844/ajeassp.2009.804.811.

Vaculik, J. (2012). Unreinforced Masonry Walls Subjected to Out-of-Plane Seismic Actions, Adelaide: *PhD Thesis,* University of Adelaide, School of Civil, Environmental and Mining Engineering.

Van der Pluijm, R., Rutten, H. and Ceelen, M. (2000). Shear behaviour of bed joints ,12th international brick, in: Block Masonry Conference.

Van Engelen, J.E. and Hoos, H.H. (2019). A survey on semi-supervised learning. *Machine Learning*, 109, 373-440.

Wei, J., Zhixin, D., Zheng, Y. and Ounhueane, O. (2021). Research on damage characteristics of brick masonry under explosion load. Shock and Vibration, 2021, 1-11. https://doi.org/10.1155/2021/5519231.

Wriggers, P. (2006). Computational Contact Mechanics (2nd ed.). Berlin, Heidelberg, New York: Springer-Verlag.

Yandzio, E. and Gough, M. (1999). Protection of Buildings against Explosions, Steel Construction Institute.

Yang, R.Y. and Rai, R. (2019). Machine auscultation: enabling machine diagnostics using convolutional neural networks and large-scale machine audio data. *Advances in Manufacturing*, 7(2), 174-187.

Zhang, Y., Hu, J., Zhao, W., Hu, F. and Yu, X. (2023). Numerical study on the dynamic behaviours of masonry wall under far-range explosions. *Buildings,* 13(2), 443. https://doi.org/10.3390/buildings13020443.

Zizi, M., Campitiello, F. and De matteis, G. (2017). Non-linear FE model for cyclic response of brick-cement mortar masonry shear-walls. XV forum internazionale, world heritage and disaster, le vie dei. Mercanti, Naples 15- Capri 16, 17 June 2017.

Chapter 3 - Methodology

3.1 Introduction

The finite element method is adopted to develop the numerical models for this study. The first and second part of this study involved analysing masonry walls under blast actions taking into account their nonlinear properties. The main aim of this chapter is to outline the methodology that was followed to create the FEA models. This study also investigated the use of machine learning methods for prompt prediction of a masonry wall's response under blast loading. The methodology of creating the ML methods is discussed in this chapter. The first part of the study entails the investigating the response of masonry under blast action using nonlinear methods, followed by investigating the effect of different brick bonding patterns, and lastly using deep learning techniques to predict the response of masonry walls.

The proposed numerical method is capable of analysing static and dynamic engineering problems. The finite element modelling process is depicted in figure 3-1 below. The steps are applicable to both static and dynamic analysis. Once the model is analysed, the user is able to optimize the model based on the results obtained.

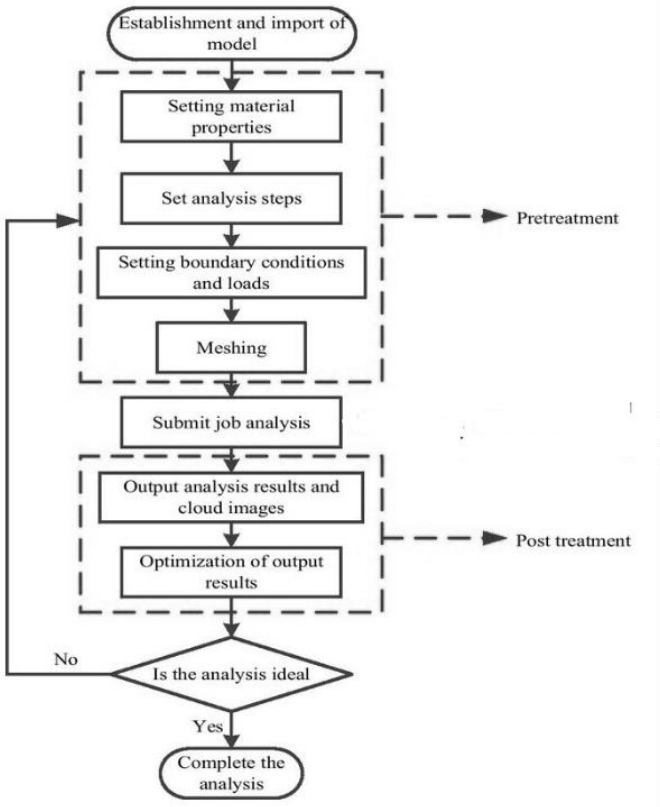

Figure 3-1: Finite element modelling process

3.2 Definition of geometry and assigning of material properties

The initial part of modelling involves defining some general data. In this study, the model was defined to be a 3D model.

The dimensions of each masonry unit considered in the study are equal to 390mm x 140mm x 190mm as shown in figure 3-2. The size of each unit used is as per the Concrete Manufactures Association (2011). The primary conventional masonry units adopted in South Africa for low-income housing include concrete masonry units and red clay bricks. This research focuses on the adoption of concrete blocks and the following wall specification was adopted:

– Single leaf, single storey, external, unreinforced walls

– Category 1 buildings (SANS 10400-A, 2010)

– H3 and H4 (residential) occupancy classes (SANS 10400-A, 2010)

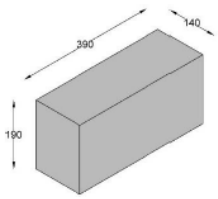

Figure 3-2:Dimensions of masonry unit (CMA, 2011)

Two walls were considered for the results presented in chapter 4 and that investigated the effect of an opening such as a window on the response of walls under blast loading. Figure 3-3 displays the two geometries considered in chapter 4.

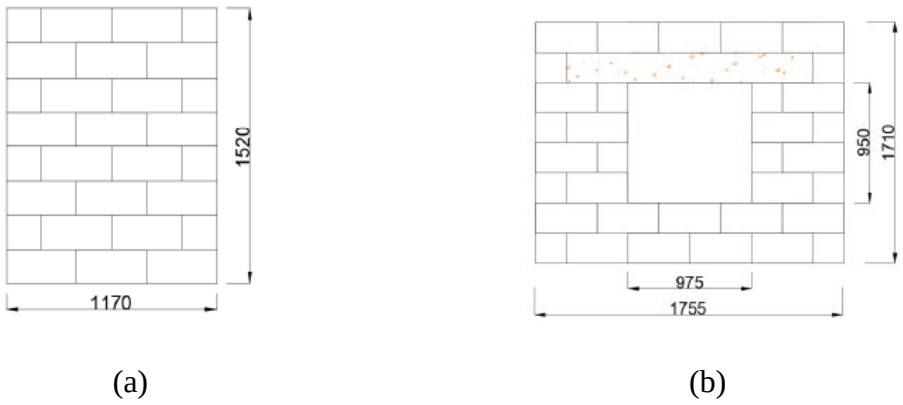

Figure 3-3:(a) Geometry 1 (wall with no opening); (b) geometry 2 (wall with an opening)

The above models were used for results presented in chapter 4 and chapter 6. In chapter 4, a nonlinear FEA was performed to investigate the response of masonry walls under blast loading. The FEA models that were used in chapter 5 were also utilized in chapter 6 for the machine learning study. As for chapter 5, bricks were used to investigate the effect of different bonding patterns on the response of walls against blast loading. A brick size of 222mm long x 106mm wide x 73mm high was adopted. In terms of wall configurations, figure 3-4 shows the different patterns that were considered for chapter 5. The modelled wall is 1110mm wide and 1268mm high including a beam of 100mm deep.

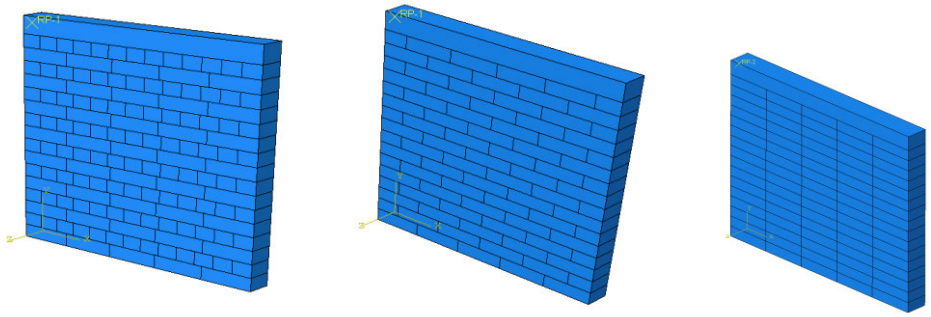

(a) **(b)** **(c)**

Figure 3-4:Numerical Model of Masonry wall in ABAQUS: (a) English bond; (b) Stretcher bond; (c) Stack bond

In terms of meshing of walls. Three-dimensional, eight-node linear brick elements were used, with element side equal to 40mm for both walls in chapter 4 and 20mm for walls in chapter 5.

3.3 Contact interfaces

Non-linear finite element models that were used to simulate all the joints between the masonry units, by introducing unilateral contact-friction interfaces are discussed in this section. The proper definition of contact mechanics is vital for such modelling approach in order to obtain realistic results. In the modelling approach, which is proposed in this research, the masonry units are taken as continuum elements and the mortar joints as interface elements. Through the use of friction interfaces and unilateral contact, zero tensile resistance between the joints is achieved. Equations 1-4 provides a mathematical expression of the contact-friction laws as per the work conducted by Drosopoulos et al (2006). These contact laws were introduced in the interfaces between the masonry units.

Equation (1) represents the non-penetration relation, while equation (2) defines that only compressive stresses (t^n) can be developed in the interfaces and equation (3) shows the complementarity relation, stating that either contact takes place ($u-g=0$, with u being the single degree of freedom and g an initial gap) or separation in the interface occurs ($t^n=0$).

$$h = u - g \leq 0 \Rightarrow h \leq 0 \quad (1)$$

$$-t^n \geq 0 \quad (2)$$

$$t^n (u - g) = 0 \quad (3)$$

A static form of Coulomb's friction law is taken into consideration for the reaction in the tangential direction of the interfaces. Thus, sliding in the interfaces is initiated when the shear stress t^t reaches the critical value τ_{cr}, according to equation (4):

$$t^t = \tau_{cr} = \pm\mu|t^n| \quad (4)$$

where μ is the friction coefficient and t^n the normal stress (contact pressure) in the interfaces. Using these contact mechanics principles, Figure 3-5 shows the interfaces between the blocks that was introduced using the surface-to-surface contact option in ABAQUS. The same was applied for the wall with different bonding patterns.

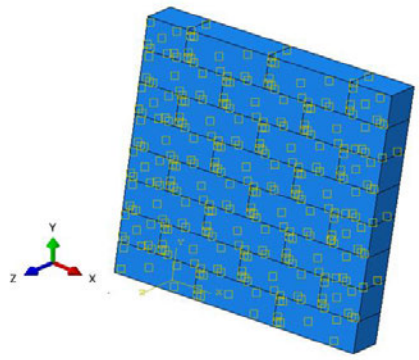

Figure 3-5:Interfaces between the blocks

3.4 Continuum damage law for the masonry units

In this research, the concrete damage plasticity (CDP) model was used to generate nonlinear properties of masonry units, in order to capture compressive and tensile failure on the masonry blocks. Figure 3-6 displays uniaxial stress-strain plots typical of plasticity, damage, and damage-plasticity models; loading branches are represented with solid thick lines and unloading / reloading branches are plotted with dashed thin lines. E_0 is the initial (undamaged)

elastic stiffness (deformation modulus), while ε^{el} and ε^{pl} are the elastic (recoverable) and plastic (irrecoverable) strain, respectively.

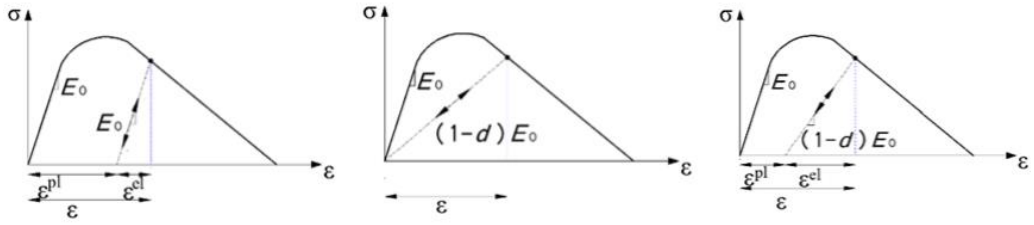

a) Plasticity Model b) Damage Model c) Plastic Damage Model

Figure 3-6:Uniaxial stress-strain plots: plasticity, damage and damage-plasticity models (Oller ,2014)

According to Oller (2014), the above graphs shows that damage generates stiffness degradation since the slope of unloading / reloading branch is (1- *d*) E_0 where d is a damage variable ranging between 0 (no damage) and 1 (destruction).

The corresponding uniaxial stress-strain relations, representing tension and compression, are provided below:

$$\sigma_t = (1 - d_t)E_0\,(\varepsilon^t - \varepsilon_{pl}^t) \quad (5)$$

$$\sigma_c = (1 - d_c)E_0\,(\varepsilon^c - \varepsilon_{pl}^c) \quad (6)$$

In the above equations, d_t and d_c are the tensile and compressive damage variables.

3.5 Material Properties

The material properties of the masonry units are detailed in table 3-1 below. These were used as part of the concrete damage plasticity law that was adopted for this research.

Table 3-1:Mechanical properties of masonry unit and mortar (Dauda and Iuorio, 2018)

Plasticity parameter	**Value**
Dilation angle	30
Eccentricity parameter	0.1
Bi and unidirectional compressive strength ratio	1.16

Stress ratio in tensile meridian	0.67
Viscosity parameter	0.001

The figures below show the related damage variable diagrams and the compressive and tensile stress-strain curves used in this study to characterise the compressive and tensile failure response of the masonry units using the numerical models. As seen in figure 3-7 below, the uniaxial stress-strain behaviour of concrete is modelled using the Hognestad type parabola (Hognestad, 1951).

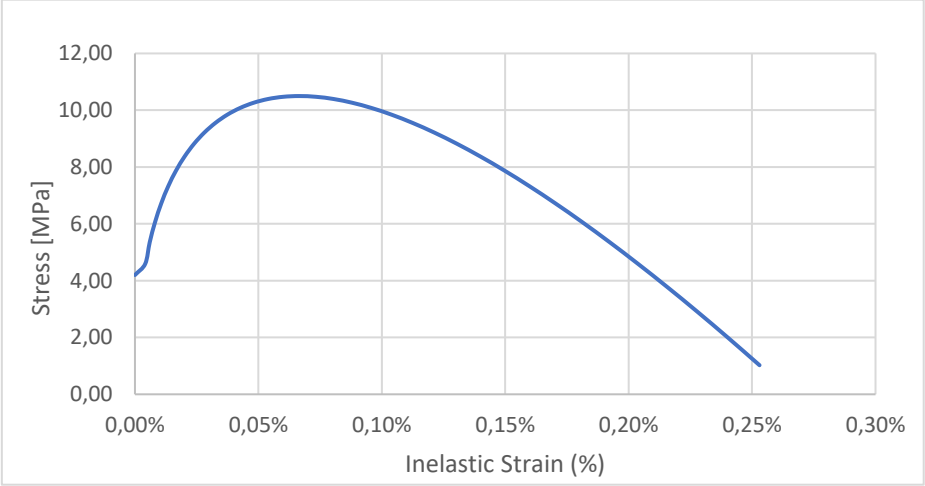

Figure 3-7:Compressive stress vs strain diagram

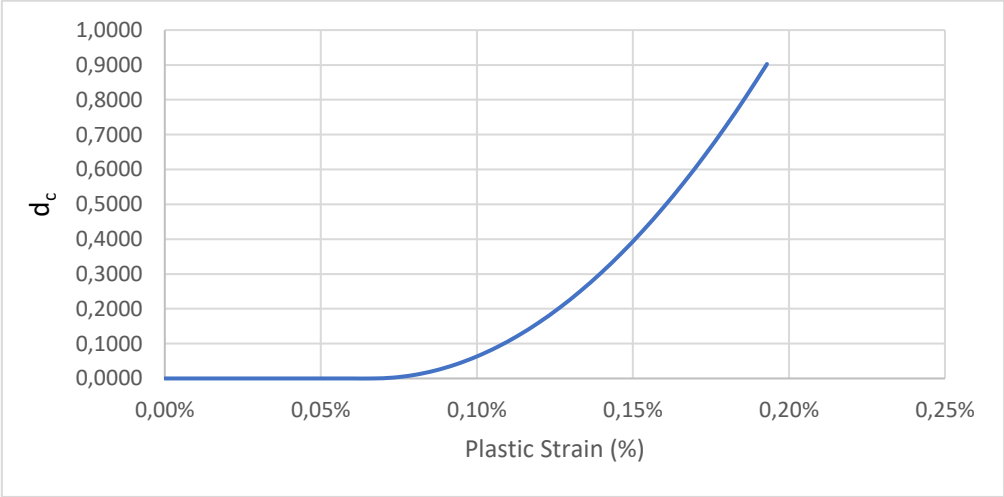

Figure 3-8:Compressive damage variable vs plastic strain diagram

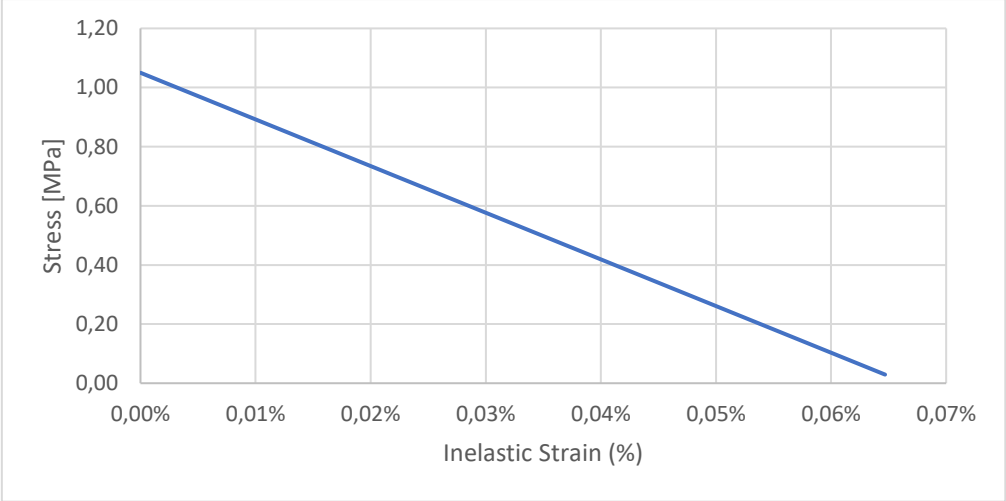

Figure 3-9:Tensile stress vs strain diagram

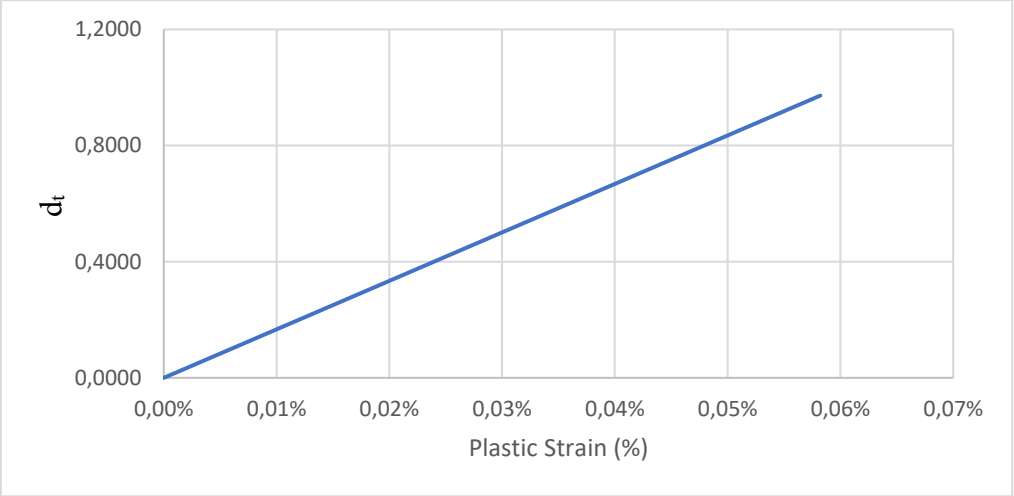

Figure 3-10:Tensile damage variable vs plastic strain diagram

The Young's modulus, Poisson's ratio as well as the tensile and compressive strength which are used in the developed models, are given in Table 3-2.

Table 3-2:Material properties (Dauda and Iuorio, 2018).

Material	**Modulus of Elasticity [MPa]**	**Poisson's Ratio**	**Tensile Strength [MPa]**	**Compressive Strength [MPa]**
Masonry Unit	15500	0.15	1.050	10.5

3.6 Boundary conditions and loading

The boundary conditions were defined for each model. The first model presented in chapter 4, the wall was fixed on all sides in three translational degrees of freedom. The model that investigated the effect of bonding patterns considered both fixed sides when out of plane loading was applied, whereas the in-plane capacity of wall was investigated with only the bottom side fixed. It is worth highlighting that in the case where all sides are fixed, it was assumed that an upper slab or roof will supply the restriction in that direction, which explains why the top side of the walls are restrained in the Z direction.

The loading of walls was divided into two categories:

- Static loading
- Dynamic loading (Blast loading)

Under static loading, a vertical pressure of 0.25MPa acting downward and normal to the top surface of the wall was applied. A horizontal displacement load of 20mm was applied to act from left to right along the top row of masonry units. The static loading was similar for both chapter 4 and chapter 5.

The investigated topic involves dynamic loading (blast) which occurs over a very short duration. ABAQUS has the ability to analysis such loads using the CONWEP model. The model allows the user to impose pressure loading due to an explosion in air. The blast wave types in this FEA package are air blast (spherical) and surface blast (hemispherical).In terms of the blast loading, different blast weights were considered at varying standoff distances. Using CONWEP model, the blast load was applied perpendicular to the surface of the wall. This programme determines the distribution of blast pressure on the contact surface automatically by entering the explosive charge weight and the stand-off distance. Additionally, the model provides the values of maximum overpressure, time of arrival, positive phase duration and the exponential decay coefficient of the blast load. In this study, the explicit dynamic solver was adopted which is an analysis type used to simulate the dynamic response adopting very small time steps, which makes it appropriate for blast loading. Additionally, the small time increments offered by the explicit solver are suitable for solving complex contact problems and it is able to solve nonlinear problems.

3.7 Output/Results

The main outputs for chapter 4 and 5 were the total deformation (X and Z direction), Von mises stress also known as equivalent stresses, compression damage and tension damage of the blocks. The concrete damage properties assisted in the development of tension and compression damage of the wall. The precision of the output is greatly dependent on the output request. The deformation results provided an insight into understanding the dominating mode of failure of the wall. Scaling of results was done to better display the findings from the numerical simulations.

3.8 Machine Learning

Chapter 6 of this thesis presents the novel approach of fast prediction of masonry wall response to blast loading. The use of machine learning methods for prediction for structural response is represented in chapter 6. A feed forward artificial neural network is used to predict the response with the variations being made on the distance and the blast explosive weight.

In this case, the finite element software is used to perform parametric numerical simulations of masonry walls. In order to automate the generation of dataset, a python script was generated. The blast weight and the standoff distance varied automatically. Appendix A provides the code that was used to generate these models. All the nonlinear definitions and loading are included in the script, namely, the boundary conditions of the wall, the applied loads including self-weight, meshing, and the interaction properties between the masonry units. A batch file was created to run the jobs simultaneously. The batch file was used to run the *inp* files which then generate the *odb* files.

A node group was defined in the numerical model in order to call out the required deformations from the four vertices of the masonry unit. A python script was created to extract the deformations after the end of each finite element analysis. The deformation values with the corresponding inputs (blast weight and standoff distance) were arranged in a table format in preparation for dataset to be used for training purposes of the neural network.

The details of the proposed data-driven scheme are shown in figure 3-11 below.

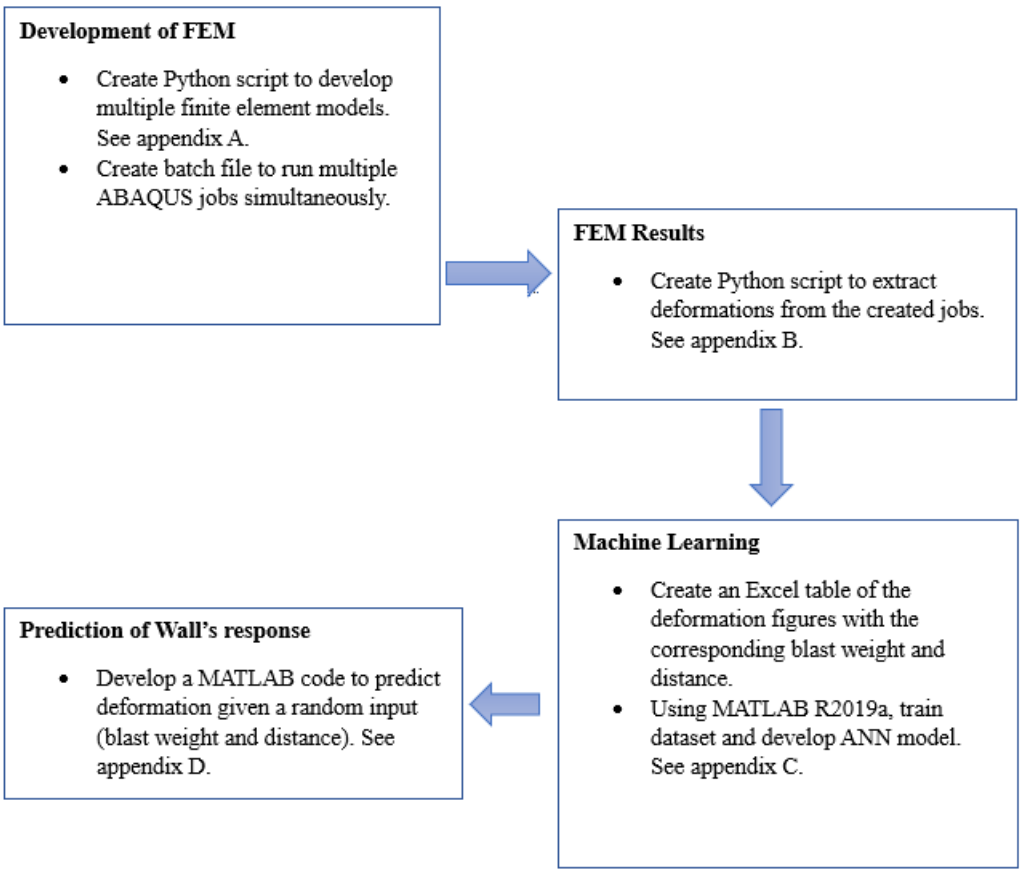

Figure 3-11:Flowchart of proposed data-driven scheme

3.8.1 Dataset

Machine learning methods require a reasonable number for dataset for training, validation and testing. The commonly used explosive is TNT. A wall size of 1170 mm (width) vs 1520mm (high) was used to generate the dataset using FEM . The commercial finite element software enables the modelling of blast wave parameters and wave propagation (Ma et al,1998). The equations applied in the software is founded on the Kingery-Bulmash procedure. CONWEP law was used to model the blast loads. The blast weight explosive were changed, also the standoff distance in increments of 5m.

3.8.2 Development of ANN and model accuracy

The dataset consisted of 95 non-linear time history analysis simulations that were generated by using MATLAB and Python scripts. This study used MATLAB R2019a which is a widely used tool for ANN modelling. As shown in figure 3-12, the network's inputs were blast weight and standoff distance. The 80/10/10 rule was used during the training process, which stipulates that 80% of the dataset is utilised for training, 10% is used for validating the neural network and the remaining 10% is set aside for testing the neural network.

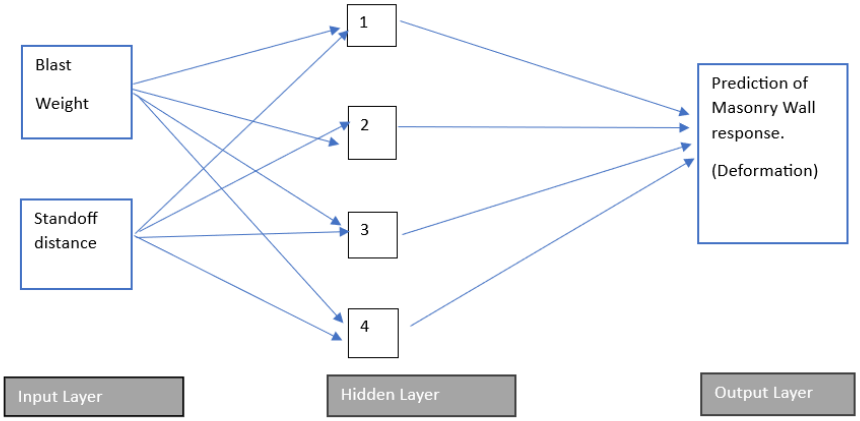

Figure 3-12:Network 1 (Deformation/displacement predictions)

As shown in figure 3-13, the Levenberg-Marquardt algorithm was adopted for this study due to its significantly higher convergence speed. The optimum network consisted of one hidden layer with 10 neurons. The choice of hidden layers considered issues of overfitting and underfitting of ANN networks.

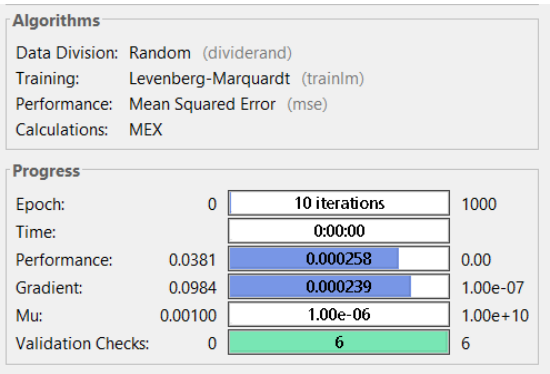

Figure 3-13: ANN Model training

3.8.3 ANN Performance and accuracy

Statistical parameters were adopted to measure the performance and accuracy of the ANN. The mean squared error (MSE) and R correlation coefficient for the training, testing, validation, and all data sets was evaluated. The R correlation close to one was regarded as an indicator of the model's ability to predict the outputs based on the trained data. This study also consisted randomly selecting blast weights and distances which were investigated using MATLAB script based on the trained and validated model. The investigation entailed comparing the MATLAB output and those from ABAQUS. These weights and distances were not part of the 95 datasets.

3.9 References

ABAQUS v. 6.14.2 User's Manual. Available online: http://130.149.89.49:2080/v2016/index.html (accessed on 13 March 2022).

Concrete Manufactures Association (CMA). (2011) Concrete Masonry Manual, 9th ed.; Concrete Manufactures Association: Menlo Park, CA, USA. Available online: https://www.cma.org.za/Portals/0/Docs/brickasandblocks (accessed on 22 April 2022).

Drosopoulos, G., Stavroulakis, G. and Massalas, C. (2006). Limit analysis of a single span masonry bridge with unilateral frictional contact interfaces. *Engineering Structures,* 28**,** 1864-1873.

Hognestad, E. (1951). A study of combined bending and axial load in reinforced concrete members, University of Illinois, engineering experiment station, bulletin series No.399. 32-54

Ma, G.W., Hao, H. and Zhou, Y.X. (1998). Modelling of wave propagation induced by underground explosion, *Computers and Geotechnics*, Volume 22, Issues 3–4, Pages 283-303, ISSN 0266-352X, https://doi.org/10.1016/S0266-352X(98)00011-1.

Oller S. (2014). Nonlinear Dynamics, International Centre for Numerical Methods in Engineering, Technical University of Catalonia.

Chapter 4 -Investigation of the failure response of masonry walls subjected to blast loading using nonlinear finite element analysis.

This chapter presents the research paper that investigated the failure response of masonry walls using nonlinear finite element method. The enclosed article proposed a modelling technique, adopting non-linear constitutive descriptions, incorporating opening-sliding failure modes using contact mechanics, as well as compressive/tensile damage, using continuum damage laws, all within finite element analysis.

This chapter is presented in the format of the published article.

To cite this article:

Thango, S.G., Stavroulakis, G.E and Drosopoulos, G.A. (2023). Investigation of the Failure Response of Masonry Walls Subjected to Blast Loading Using Nonlinear Finite Element Analysis. *Computation,* 11, 165. https://doi.org/10.3390/computation11080165

computation

MDPI

Article

Investigation of the Failure Response of Masonry Walls Subjected to Blast Loading Using Nonlinear Finite Element Analysis

Sipho G. Thango [1], Georgios E. Stavroulakis [2,*] and Georgios A. Drosopoulos [1,3]

[1] Discipline of Civil Engineering, University of Kwazulu-Natal, Durban 4041, South Africa; 209523102@stu.ukzn.ac.za (S.G.T.); gdrosopoulos@uclan.ac.uk (G.A.D.)
[2] Department of Production Engineering and Management, Technical University of Crete, 73100 Chania, Greece
[3] Discipline of Civil Engineering, University of Central Lancashire, Preston PR1 2HE, UK
* Correspondence: gestavroulakis@tuc.gr; Tel.: +30-2821037418

Abstract: A numerical investigation of masonry walls subjected to blast loads is presented in this article. A non-linear finite element model is proposed to describe the structural response of the walls. A unilateral contact–friction law is used in the interfaces of the masonry blocks to provide the discrete failure between the blocks. A continuum damage plasticity model is also used to account for the compressive and tensile failure of the blocks. The main goal of this article is to investigate the different collapse mechanisms that arise as an effect of the blast load parameters and the static load of the wall. Parametric studies are conducted to evaluate the effect of the blast source–wall (standoff) distance and the blast weight on the structural response of the system. It is shown that the traditional in-plane diagonal cracking failure mode may still dominate when a blast action is present, depending on the considered standoff distance and the blast weight when in-plane static loading is also applied to the wall. It is also highlighted that the presence of an opening in the wall may significantly reduce the effect of the blasting action.

Keywords: masonry; collapse mechanism; blast actions; unilateral contact; dynamic analysis; finite element analysis

Citation: Thango, S.G.; Stavroulakis, G.E.; Drosopoulos, G.A. Investigation of the Failure Response of Masonry Walls Subjected to Blast Loading Using Nonlinear Finite Element Analysis. *Computation* **2023**, *11*, 165. https://doi.org/10.3390/computation11080165

Academic Editors: Manolis Georgioudakis, Vagelis Plevris, Mahdi Kioumarsi and Demos T. Tsahalis

Received: 17 July 2023
Revised: 16 August 2023
Accepted: 18 August 2023
Published: 21 August 2023

1. Introduction

Over the years, increasing research efforts have been developed focusing on analyzing the structural behavior of masonry walls. Masonry is defined as a set of stone units that are connected using mortar joints that are organized to form a regular pattern [1]. Masonry is commonly used in monuments, masonry arches, and also in low-cost houses. For these structural systems, the low tensile resistance of masonry or mortar interfaces may lead to a compromised response when in- and out-of-plane lateral forces reach high values.

Among several loading conditions, ongoing research aims to investigate the impact of blasting forces on masonry structures. In particular, research on this type of loading focuses on mining activities using blasting operations, which comprise the first phase of the production cycle in most of the mining processes. Blasting is used to fragment the rock overlying the coal seams in most mines. When the explosives are detonated, most of the energy is consumed in rock fragmentation [2]. According to [3], energy not used to break rock radiates out from the blast site in the form of ground vibrations and air blasts. Additionally, when explosives are ignited in rock, a shock wave is produced that breaks the rock and then a force in the form of gas pressure is formed [4]. An explosion or blast activity is defined as the release of a significant amount of energy that takes place in a short time period.

Computer advancement in the past decades has enabled researchers to model masonry with its complexities using finite element analysis. The finite element (FE) method is one of

the advanced numerical techniques that is commonly applied to analyze complex structural engineering problems. Research work presented in [5–9] and others indicate that by using the FE method, the failure modes that occur in masonry due to blast loading can be successfully analyzed.

According to [10], the collapse modes of masonry walls that are exposed to blast actions may include flexural failure, direct shear failure, and flexural–shear failure. Collapse modes are further discussed in this section and elaborated in the analysis section of this article. It is noted that these collapse modes were used for the validation of the proposed numerical model.

D'Altri et al. [11] considered a masonry wall with dimensions of 1190 mm × 795 mm with a brick size of 112 mm × 53 mm × 36 mm. The boundary conditions were taken as fixed on all four sizes of the wall. The wall was loaded with a 20 KN/m^2 out-of-plane load. Their research aimed to assess the effectiveness of the micro-modeling approach and assess the out-of-plane response of the masonry walls. As defined by Lourenço [12], micro-modeling is where "masonry units and mortar joints are represented by continuum elements, where the unit-mortar interface is represented by a discontinuous constitutive description". A quasi-static (transient dynamic) procedure was used for the numerical study. Furthermore, the brick–mortar bond failures were accounted for using brick–mortar nonlinear cohesive interfaces. The failure pattern in the wall indicated that the maximum displacement often occurs at the center of the wall.

The discrete element method was used in [13] to investigate the behavior of masonry structures under blast actions. A 2400 mm × 2400 mm wall, fixed on all sides, was simulated, and typical modes of failure, including out-of-plane failure, were observed. Furthermore, the study depicted the complete failure of the wall under a load of 810 kg TNT explosive weight at a standoff distance of 37 m. According to Masi et al. [13], the geometry of the blocks and the interfaces may be directly modeled using the discrete element method. Their study was conducted using 3DEC software and the empirical model CONWEP to simulate the blast action. They used a soft-contact technique to simulate joint interactions between adjacent blocks. It is worth mentioning that the magnitude of the wall failure is dependent on various factors such as standoff distance, wall dimensions/properties, and boundary conditions.

Hao [5] conducted a numerical analysis of a 2880 mm × 2820 mm masonry wall subject to blast load corresponding to a TNT explosive weight W = 2000 kg using AUTODYN software. In that study, the four sides of the wall were modeled as fixed, with a mortar layer between the fixed boundary and the masonry units of the wall, which, in turn, was assigned homogenized material properties. It was shown that for higher explosive weight and shorter standoff distances, the wall would collapse, and the center portion of the wall failed out-of-plane as one brick flew out as a single piece. The wall was also observed to be damaged near the boundary.

Shamim et al. [14] conducted a numerical study investigating the effect of a blast on a 3000 mm × 3000 mm × 230 mm masonry wall, which had a reinforced concrete frame of 230 mm × 235 mm cross-section dimensions. In their macro-approach, masonry units, mortar joints, and the brick–mortar interface were modeled as a single material. They investigated the effect of 100 kg TNT explosive weight over 20 m, 30 m, and 40 m distances from the wall. Furthermore, their study considered a wall without an opening as well as a wall with a window opening at its center. The boundary conditions were defined such that the top of the wall was restrained in the direction parallel to the blast, simulating the restrain obtained from a slab due to its high in-plane stiffness. The results for the wall without the window showed that the peak values of displacements are found at mid-span. The peak displacement values were equal to 267.8 mm, 95.1 mm, and 59.9 mm for the three mentioned standoff distances between the blast source and the wall, respectively. For the wall with the window, the values of peak displacement at the top of the opening when out-of-plane failure arose were equal to 353.6 mm, 121.9 mm, and 73.2 mm, respectively. Overall, they observed that peak values on the wall with the window were higher than

those of the wall without the window; however, the standoff distances were not the same when the opening was considered.

In a similar investigation presented in [15], it was shown that a wall subjected to blast actions developed the highest displacement in the midsection of the masonry infill panel, while the reinforced concrete frame remained undamaged. It was shown that when the blasting source was close to the wall, the masonry panel collapsed completely, depicting displacements greater than the thickness of the wall (>230 mm). Their study also looked at the effect of changing blast load sizes, considering a TNT equivalent weight of charge equal to W1 = 25 kg, W2 = 50 kg, W3 = 75 kg, and W4 = 100 kg for a constant standoff distance of 20 m. It was observed that peak displacement increases with increasing weight of charge (at constant standoff distance of 20 m) and decreases with increasing distance.

In [16], a numerical study was conducted on a masonry wall with dimensions of 1700 mm × 1550 mm × 100 mm. The model was constructed with 23 courses of solid clay bricks and analyzed using a simplified micro-modeling approach within finite element analysis. The simulation was implemented in steps, involving vertical displacements and cyclic out-of-plane actions. The failure mode was due to the formation of diagonal cracks caused by in-plane loading. As derived from the mentioned literature, the type of failure modes of masonry walls under in-plane and blasting, out-of-plane loading, are influenced by various characteristics—such as the load application, geometry, boundary conditions, and the quality of materials.

Some recent efforts aim at investigating the response of different types of reinforced masonry walls under blast actions. In [17], a masonry wall connected with two transverse walls, one at each end, was numerically tested using the micro-modeling technique within non-linear finite element analysis. The work proposed numerical models to reinforce the wall using CFRP wrapping and a steel angle-strip system. In [18], the behavior of unreinforced masonry walls with CFRP wrapping and mild welded steel wire mesh, under blast with low standoff distance, was investigated using non-linear finite element analysis. In [19], a fragility analysis of masonry walls was proposed, illustrating the vulnerability of the structures against blast load, focusing on different types of unreinforced masonry walls and reinforced walls, using finite element analysis. In [20], for masonry walls made of autoclaved aerated concrete and polymer-reinforced concrete that are subjected to heavy TNT explosive loads, both experimental and numerical testing were provided. In the numerical models, non-linear finite element analysis was used with cohesive zone models to depict damage to the wall.

Based on this short review of recent results, it seems that there is still space for more research investigating the collapse modes of masonry walls under blast actions. In particular, one of the goals of this article, which also highlights its innovative points, is to provide further insight into the way in-plane failure modes, such as diagonal cracking and out-of-plane damage, may appear in masonry walls subjected to blast actions. From another point of view, this article proposes a modeling technique using non-linear constitutive descriptions, incorporating opening-sliding failure modes adopting contact mechanics, as well as compressive/tensile damage, using continuum damage laws, all within finite element analysis. The proposed models can be implemented in commercial software.

Within the given framework, a numerical investigation of the mechanical response of masonry walls under blast actions, with and without openings, is presented. Non-linear finite element models are proposed to simulate all the joints between masonry units by introducing unilateral contact–friction interfaces. For the simulation of the blast action, an empirical model is used, and explicit dynamic analysis is adopted implementing this loading type. Various loading cases are tested, resulting in different failure modes.

In Section 2 of this article, failure modes of masonry walls are provided and modeling approaches that can be used to capture these modes are briefly discussed. In Section 3, all the details of the numerical model that is proposed in this article are presented. Among others, the details of the blast load simulation, the material constitutive description, and the geometry of the walls are given in this section. In Section 4, a validation of the proposed

model is conducted using a comparison of some results with published output. In Section 5, results and discussions derived from the suggested approach are provided, and in Section 6, the conclusions of this investigation are presented.

2. Failure Modes and Modeling Approaches of Masonry Walls

In this section, a preliminary discussion of failure modes for masonry walls that occur under various loading scenarios is provided. Both in-plane and out-of-plane damage patterns are recognized. In the next sections, it will be shown that some of these modes arise also under blast actions, depending on the load combination.

In addition, general concepts elaborating modeling approaches, which are used to capture the mentioned failure modes, are discussed. Within this framework, the proposed model will be identified.

2.1. In-Plane Response of Masonry Walls

Three types of failure modes of masonry walls under static loading are discussed below, and these are sliding shear, flexural failure, and diagonal shear. These failure modes are illustrated in Figure 1.

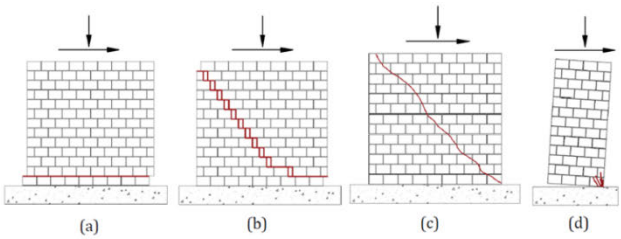

Figure 1. Typical Failure modes of masonry walls subjected to a vertical load and a horizontal (shear) load. These two loads will result in (**a**) sliding shear failure, (**b**) shear failure (staircase-shaped cracks), (**c**) diagonal shear, and (**d**) crushing, which is mainly compressive cracks [21].

According to [21], the in-plane failure of a wall is generally shear failure, as can be seen by the diagonal cracking, and this is often ruled by the tensile resistance or capacity of the masonry unit or mortar joints. Additionally, a wall's failure can be observed as the crushing of units under compression. The capacity for large displacement and average energy dissipation is related to unit crushing [22], contrary to failure involving sliding shear, which is more ductile as a higher amount of energy is dissipated. This energy dissipation is more common under seismic/blast loading actions. The above modes of failure have been proven by many researchers to be the common failure modes when horizontal displacement and vertical pressure loading are applied to walls.

2.2. Out-of-Plane Response of Masonry Walls

Subject to blast loadings, the failure mode of masonry walls is often out-of-plane flexural failure. This may be accompanied by a flexural cracking pattern, which consists of horizontal cracks arising at halfway of the wall and stepped diagonal cracks toward all corners of the wall, as can be seen in Figure 2, where a typical out-of-plane response of a masonry wall under blast loading is shown. It is noted that these descriptions of the failure modes will be used later in this article to verify the results that are obtained from the proposed numerical scheme.

Figure 2. Out-of-plane failure pattern of a wall subjected to blast loading.

2.3. General Modeling Approaches for Masonry Structures

The mechanical behavior of masonry buildings has been described using two broad numerical approaches: macro-modeling and micro-modeling [12]. In the macro-modeling method, masonry is analyzed as a uniform material that obtains its average (effective) material properties by a homogenization scheme. Thus, in the macro-modeling technique, masonry units (concrete blocks, stone units) and the mortar joints are modeled as solitary materials using homogenization concepts. According to [23], when using the macro-modeling approach, the detailed failure mechanisms may generally not be reproduced well.

According to micro-modeling, masonry consists of joints connecting individual units, and using appropriate constitutive laws, simulation of such walls is conducted. Due to the different compression or tensile strength of brick vs. mortar, it is worth noting that mortar joints become the weakest link in masonry walls. According to [12], the unit–mortar interface controls the nonlinear response of the joints, and this is one of the most pertinent features of masonry wall behavior. Different modeling techniques used to simulate the response of masonry structures are depicted schematically in Figure 3.

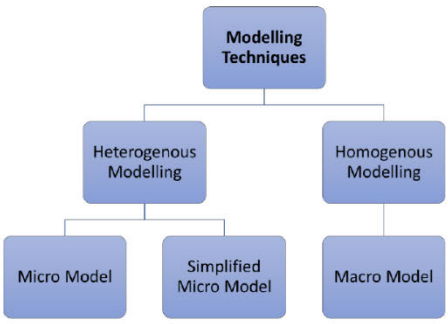

Figure 3. Modeling techniques for masonry walls.

The masonry units are modeled as continuum elements, while the mortar joints are modeled as interface elements in this article. Zero tensile resistance between the joints is introduced, using unilateral contact and friction interfaces. More details about the model used in this article are provided in the following sections.

3. The Numerical Model Proposed in the Present Article

A non-linear finite element model is proposed for this study to simulate the response of masonry walls to blasts. For the evaluation of the failure response that is derived from

the masonry unit interfaces, a unilateral contact and friction constitutive description is assigned to these interfaces. Thus, both in-plane and out-of-plane opening and/or sliding between the masonry units can be depicted with the proposed model. Since all the contact conditions between the blocks in the wall are simulated using principles taken from contact mechanics, it can be stated that the micro-modeling approach is used.

The unilateral contact law, provided in Equations (1)–(3) for a single degree of freedom system, is assigned in the interfaces between masonry blocks. Equation (1) is the non-penetration relation, Equation (2) states that only compressive stresses (t^n) can be developed in the interfaces, and Equation (3) is the complementarity relation, stating that either contact takes place ($u - g = 0$, where u is a single degree of freedom and g is an initial gap) or separation in the interface occurs ($t^n = 0$).

$$h = u - g \leq 0 \Rightarrow h \leq 0 \tag{1}$$

$$-t^n \geq 0 \tag{2}$$

$$t^n (u - g) = 0 \tag{3}$$

For the response in the tangential direction of the interfaces, a static version of Coulomb's friction law is considered. Thus, sliding in the interfaces is initiated when the shear stress t^t reaches the critical value τ_{cr}, according to Equation (4):

$$t^t = \tau_{cr} = \pm\mu|t^n| \tag{4}$$

where μ is the friction coefficient and t^n the normal stress (contact pressure) in the interfaces.

To represent the failure response of the masonry units, a continuum concrete damage plasticity model is used. Compressive and tensile failure modes developed at the masonry blocks are then depicted. In the following sections, the details related to the implementation of the blast loading, the material properties, and the dimensions of the walls that are studied in this article are provided.

3.1. Blast Shock Wave Modeling

An explosion loading wave is defined by three parameters, namely, the shape of a wave, the maximum pressure (P_{ro}), and the positive wave duration (t_o), which is the time that pressure reaches zero [24]. Various research efforts have shown that depending on the source of the explosion, the generated waves are divided into shock and pressure waves. In a shock wave, the pressure of gasses from the explosion or blasting is developed by emission from the source of the explosion [24,25]. The pressure increases to the maximum value P_{ro} and decreases to the environmental pressure, as shown in Figure 4. Mining activities involving blasting generate blast pressures on neighboring structures. The pressure distribution from a blasting source at a particular distance is considered nearly consistent over a normal reflecting surface. According to [26], a close-in explosion produces a pressure distribution that changes significantly in magnitude over the reflecting surface. This creates more complexity due to the non-uniform of pressure.

To determine the magnitude of peak overpressure, two major parameters are used: the charge weight and the distance between the blast source and the structure. By observing the pressure–time diagram depicted in Figure 4, two main phases can be identified. The positive part of the diagram is called the positive phase and has a duration t_o, as shown in Figure 4, while the negative part is called the negative phase and has a duration t_{o-}, also shown in Figure 4. According to [13], when a primary shock strikes a target, the reflected overpressure P_r instigates. The negative phase exists for a longer duration with lower intensity pressure than the positive phase. As the standoff distance increases, it can be noted that the duration/period of the positive blast wave phase increases, and that results in lower amplitude and a significantly longer-duration shock pulse.

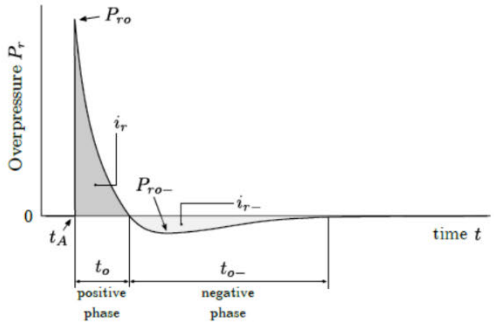

Figure 4. Shock wave distribution [27].

Using the Friedlander equation, the time evolution of the positive phase of the reflected pressure is analyzed (Friedlander, 1946):

$$P_r(t) = P_{ro}\left(1 - \frac{t^*}{t_o}\right) H[t^*](1 - H[t^* - t_o]\, H[t^*])\exp\left(-d\frac{t^*}{t_o}\right) \quad (5)$$

where *H[t*]* represents the step function, d is the exponential decay coefficient, and $t^* = t - t_A$, where t_A is depicted in Figure 4. According to Rigby et al. [28], the impulse i_{ro} or i_r associated with the positive phase, which symbolizes the area under the pressure curve, can be formulated as:

$$i_{ro} = \int_{t_A}^{t_A + t_0} P_r dt = \left[e^{-d} + d - 1\right] \frac{P_{ro}\, t_o}{d^2} \quad (6)$$

One of the most effective means of representing a blast impact is the use of the CONWEP model. According to [29], CONWEP is a model used to simulate the effects of a collection of conventional weapons, including air blast routines, breach, cratering, ground shock, and fragment and projectile penetration. The CONWEP charge property parameter is used in this study to simulate an air-based explosion using empirical data [30]. Furthermore, according to this consideration, a time history diagram of the pressure loading is built. In order to utilize this empirical model, one would need to define the equivalent TNT (trinitrotoluene) mass of the explosive as well as the source point (i.e., where the explosive is located). The initial process in calculating the explosive wave from a blast source other than TNT is to convert the charge mass to TNT equivalent mass [31].

Therefore, the CONWEP charge property is used in this study within commercial finite element software to simulate an air-based explosion by developing a time history pressure loading, similar to the one shown in Figure 4. The data, which were entered to define the blast charge properties, include the equivalent mass of TNT, a multiplication factor to convert from that mass unit into kilograms, and multiplication factors to convert from the standoff distance, time, or pressure to meter, second, or pressure in Pascals, respectively.

3.2. Continuum Damage Law for the Masonry Units

A concrete damaged plasticity law is used to represent damage on masonry units. Rate independence is claimed for this law, which is based on incremental plasticity theory. According to Lubliner et al. [32], Lee and Fenves [33], Tapkın et al. [34], and Daniel and Dubey [35], this constitutive description is appropriate for the analysis of quasi-brittle materials such as concrete and masonry. It relies on the concept of isotropic damaged elasticity for the representation of the irretrievable damage or failure that occurs during the cracking process for materials under fairly low pressure. The concrete damage plasticity

law uses a non-associated potential plastic flow, which is in turn the implementation of the Drucker–Prager hyperbolic function for flow potential [36].

The common failure mechanisms that can be illustrated with this law are, namely, tensile cracking and compressive crushing. When unloading takes place, the elastic stiffness of the material is deemed damaged. This damage is implemented by introducing two damage variables as functions of the plastic strain, one for tension and the other for compression. A zero value of the damage variable indicates undamaged material, while a value equal to one indicates a total loss of strength. The corresponding uniaxial stress–strain relations, representing tension and compression, are provided below:

$$\sigma_t = (1 - d_t)E_0\,(\varepsilon^t - \varepsilon^t_{pl}) \tag{7}$$

$$\sigma_c = (1 - d_c)E_0\,(\varepsilon^c - \varepsilon^c_{pl}) \tag{8}$$

In the above equations, E_0 is the preliminary elastic stiffness of the material and d_t and d_c are the tensile and compressive damage variables, respectively.

The compressive and tensile stress–strain curves used in this work to define the compressive and tensile failure response of the masonry units on the numerical models, as well as the corresponding damage variables diagrams, are provided in the figures below. The uniaxial stress–strain behavior of concrete is modeled utilizing a Hognestad-type parabola [37], as per Figure 5 below. Figures 6–8 provide the compressive damage parameter as well as the tensile stress–strain law and the tensile damage parameter used for this model [37].

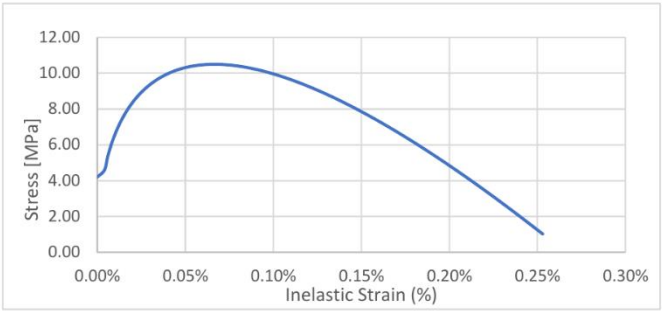

Figure 5. Compressive stress vs. strain diagram [37].

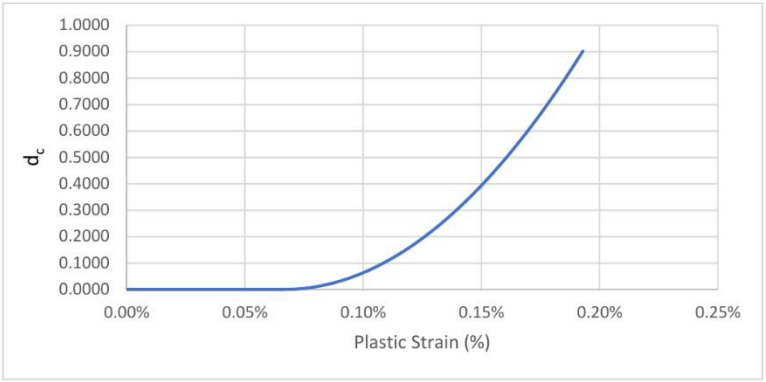

Figure 6. Compressive damage variable vs. plastic strain diagram [37].

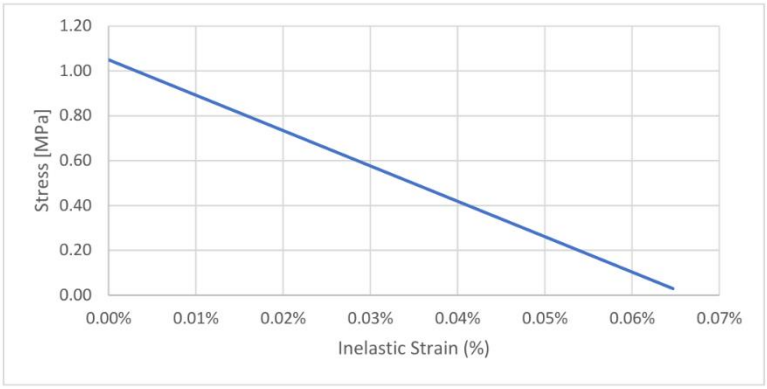

Figure 7. Tensile stress vs. strain diagram [37].

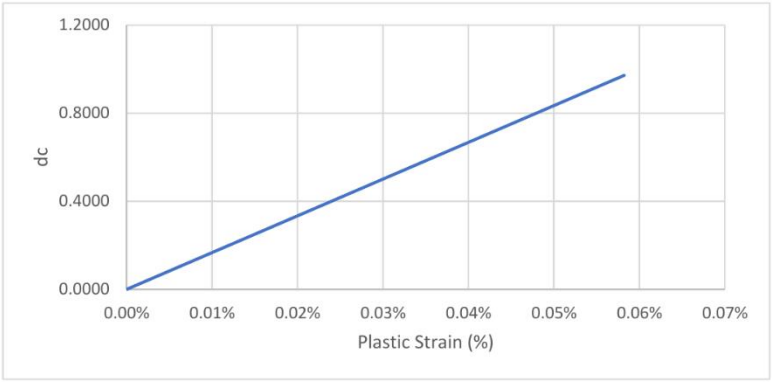

Figure 8. Tensile damage variable vs. plastic strain diagram [37].

The uniaxial tensile damage and uniaxial compressive damage parameters were developed using the post-failure stress as a function of cracking strain. The cracking strain is equal to the total strain minus the elastic strain of the undamaged material [32].

Some additional material properties used within the concrete damage plasticity law are provided in Table 1. The material properties for each masonry unit are provided in Table 2.

Table 1. Mechanical properties of the masonry unit and mortar [38].

Plasticity Parameter	Value
Dilation angle	30
Eccentricity parameter	0.1
Bi- and uni-directional compressive strength ratio	1.16
Stress ratio in tensile meridian	0.67
Viscosity parameter	0.001

Table 2. Material properties [38].

Material	Modulus of Elasticity (MPa)	Poisson's Ratio	Tensile Strength (MPa)	Compressive Strength (MPa)
Masonry Unit	15,500	0.15	1.05	10.5

3.3. The Geometry of the Masonry Walls

The dimensions of each masonry unit considered in this study are equal to 430 mm × 140 mm × 190 mm. The size of each unit is as per the Concrete Manufactures Association [39]. Low-cost housing in South Africa often uses concrete masonry blocks and clay bricks. This paper focuses on the use of concrete blocks, and the following limitations are noted:

- A single-leaf wall is considered, and the wall is unreinforced.
- Category 1 buildings [40].

Two geometries are used in this study for the walls, as shown in Figures 9 and 10. The first is a solid wall and the second represents a wall with an opening.

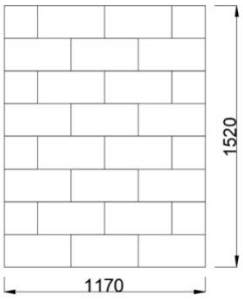

Figure 9. Geometry 1 (wall with no opening (mm)).

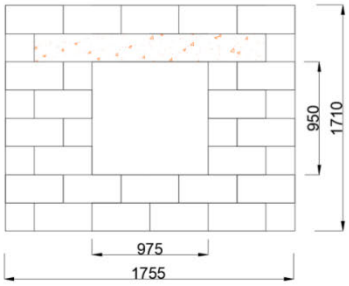

Figure 10. Geometry 2 (wall with an opening (mm)).

3.4. Details of the Finite Element Model

Figure 11 shows the mesh that is adopted in this study for the models without and with an opening. Three-dimensional, eight-node linear brick elements are used, with the element side equal to 40 mm for both walls. A total number of 4800 elements for the model without the opening and 5600 elements for the model with the opening are used, as shown in Figure 11.

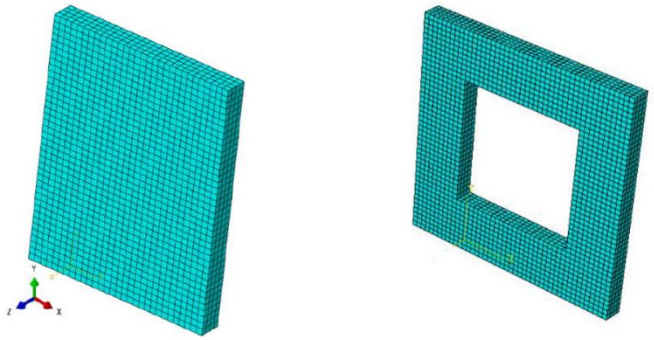

(**a**) (**b**)

Figure 11. Mesh of the considered masonry walls: (**a**) with no opening and (**b**) with a window opening.

All four sides on the perimeter of each of the two walls are considered as fixed in three translational degrees of freedom, according to the coordinate system shown in Figure 11. It is noted that the restraining of the top side of the walls in the Z-direction is attributed to the assumption that an upper slab or roof will provide restraint in that direction.

Concerning the loading of the models, two load steps are used. In an initial, pre-existing step, a vertical pressure of 0.25 MPa is applied to the top side of the structure. In the first load step, a horizontal shear (in-plane) displacement of 10 mm is applied to the top side of the walls. Alternatively, the wall with no horizontal in-plane displacement is also considered. In the second load step, the blast loading is applied.

The simulation is conducted using explicit dynamic analysis. This type of analysis is appropriate since it is able to capture the very short duration of the blast action. It is noted that the explicit dynamic analysis was originally developed to simulate high-speed dynamic events that would otherwise require significant computational resources within implicit codes. For the implementation of this analysis, an automatic time incrementation is used.

For the application of the contact–friction conditions between the masonry blocks, the method of Lagrange multipliers is used. A friction coefficient equal to 0.45 is assigned to the interfaces.

It is noted that for the implementation of the blast load, a charge weight expressed in TNT at the standoff distances of 100 m, 50 m, and 20 m is used. In addition, the effect of the blast weight, as well as the effect of changing the blast charge while keeping the distance constant and changing the standoff distance while keeping the blast charge weight constant, are also investigated. Only the front surface of the walls is loaded (incident surface). In the following sections, results obtained from various parametric investigations, emphasizing the corresponding failure mechanisms, are provided.

4. Validation of the Proposed Model

Before presenting the results from the simulations, a validation of the proposed model is conducted by comparing the output with published numerical studies. Then, the results of the investigation are elaborated, emphasizing collapse mechanisms for the used load cases.

A comparison between results derived from the proposed model and existing numerical solutions is provided. As depicted in the figures below, similar collapse mechanisms were obtained when a blast load or in-plane, vertical pressure, and shear displacement loads are applied to the wall.

- Masi et al. [13] depicted complete failure, indicating that after a wall is damaged close to the boundary, it comes out in one piece in the middle portion. The explosive

weight was 810 kg at 37 m standoff distances (Figure (a)). Out-of-plane experiments conducted by Du et al. [41] depicted complete failure in the middle of a real wall (Figure (b)).

(**a**) (**b**) (**c**)

The proposed model depicted complete failure of the middle section of the wall, under a blast load with an explosive weight of 810 kg at a standoff distance of 37 m. This is shown in Figure (c).

- Salmanpour [21] predicted sliding failure along staircase-shaped cracks as mode of failure for a wall subjected to vertical pressure and shear displacement loading. The damage to buildings during the 2002 Molise earthquake in Italy, as reported in [42], resembles the crack pattern shown below in Figure (d).

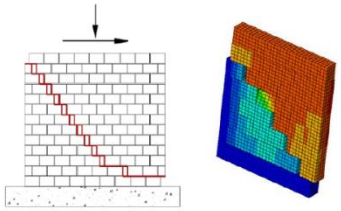

(**d**) (**e**)

The proposed model depicted staircase-shaped cracks when subjected to vertical pressure and shear displacement loading. This is shown in Figure (e).

5. Results Obtained from the Proposed Numerical Scheme

In the next sections, results depicting the structural response of two masonry walls, one without an opening and one with an opening, are provided. Within this investigation, parametric studies depicting the influence of the variation in the weight of charge and the blast source–structure distance on the response of the walls, were conducted. Relevant discussions emphasize the collapse modes, which arise in the provided framework. In total, the cases listed in Table 3 are considered for the walls without and with an opening.

Table 3. Cases considered in the framework of this investigation.

Case Description	Blast Load	Standoff Distance
Case 1 (solid wall loaded with vertical pressure, horizontal shear displacement, and blast load).	100 kg TNT	20 m, 50 m
	200 kg TNT	20 m, 50 m
	1150 kg TNT	20 m, 50 m, 100 m
Case 2 (wall with an opening loaded with vertical pressure, horizontal shear displacement, and blast load).	1150 kg TNT	50 m
	2000 kg TNT	5 m
	3500 kg TNT	10 m
Case 3 (solid wall loaded with vertical pressure and blast load). No horizontal shear displacement is considered.	100 kg TNT	50 m
	200 kg TNT	100 m
	1150 kg TNT	100 m

5.1. Case 1: Solid Masonry Wall Loaded with Vertical Pressure, Shear Displacement, and Blast Load

This section provides results obtained from simulations on a solid wall loaded at its top boundary surface with a vertical downward pressure and a horizontal shear displacement load. A blasting action is also applied to the wall.

Figure 12 depicts the displacement and the failure mechanism, which are obtained from an explosive weight of 100 kg at a standoff distance of 20 m. According to this figure, in-plane diagonal cracking in the form of opening/sliding between the blocks is accompanied by some out-of-plane flexural displacement, attributed to the blast load. It can be observed that though the wall does not collapse totally, significant displacements are developed. In addition, according to Figure 12b,c, significant compressive and tensile failure is developed on the masonry blocks. This is attributed to the out-of-plane flexural displacement of the fixed (in its perimeter) wall. As expected, tensile failure is more expanded in the wall than compressive failure.

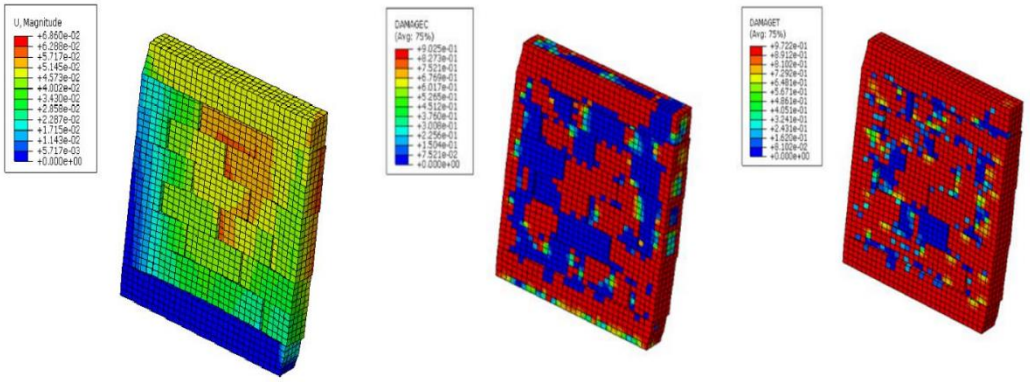

(**a**) (**b**) (**c**)

Figure 12. Solid wall loaded with a charge weight of 100 kg at a distance of 20 m: (**a**) displacement of the wall at the end of the simulation (m), (**b**) compressive damage variable, and (**c**) tensile damage variable distribution.

Next, the weight of the explosive is gradually increased to 200 kg (Figure 13) and 1150 kg (Figure 14) while the standoff distance is kept constant and equal to 20 m. As observed in Figure 13a, the out-of-plane deflection becomes higher compared with Figure 12a,

due to the increase in the blast weight. In addition, Figure 13b,c shows that extensive compressive and tensile failure is developed in the masonry blocks. Figure 14 shows that for the maximum quantity of explosive weight, out-of-plane deflection dominates the in-plane cracking. In addition, the wall fails completely for this maximum explosive weight when it is considered at the same distance of 20 m, as above.

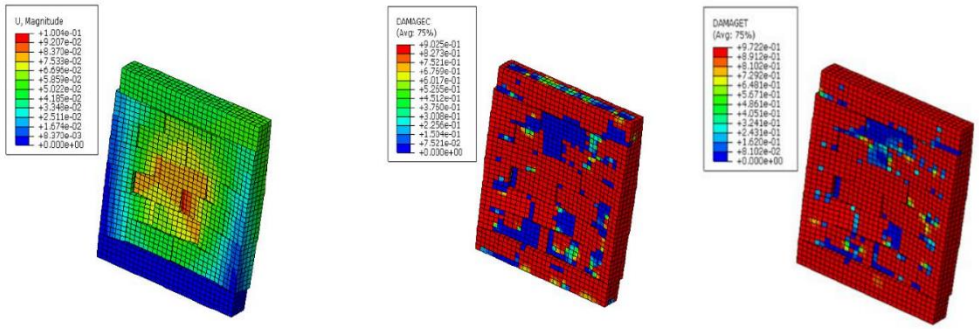

(**a**) (**b**) (**c**)

Figure 13. Solid wall loaded with a charge weight of 200 kg at a distance of 20 m: (**a**) displacement of the wall at the end of the simulation (m), (**b**) compressive damage variable, and (**c**) tensile damage variable distribution.

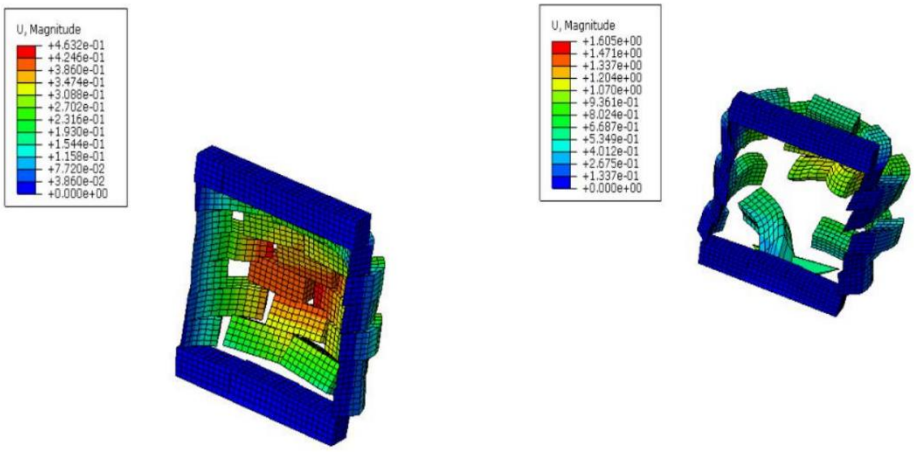

(**a**) (**b**)

Figure 14. Displacement of the solid wall loaded with a charge weight of 1150 kg at a distance of 20 m: (**a**) depicted in a previous time step prior to complete damage of the wall and (**b**) depicted at the final time step.

Next, an investigation using an increased standoff distance of 50 m is conducted, using explosive weights of 100 kg, 200 kg, and 1150 kg, respectively. From the first case of 100 kg explosive weight, it is determined that the in-plane failure mode is dominant, as shown in Figure 15. A diagonal cracking appears, in this case, at the top part of the wall. On the

contrary, for the lower distance of 20 m shown in Figure 12, both in-plane and out-of-plane flexural deflection are observed.

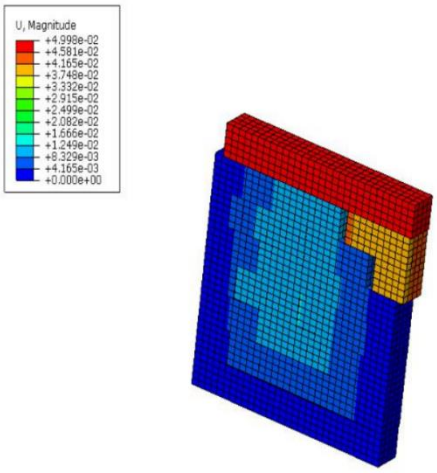

Figure 15. Displacement of the solid wall loaded with a charge weight of 100 kg at a distance of 50 m.

For the case of 200 kg explosive weight, the failure mechanism which arises is a stair-case diagonal cracking along the wall, as shown in Figure 16. This indicates that the failure mode changes compared with Figure 13, where mainly an out-of-plane response is observed for the same explosive weight and lower standoff distance (20 m). It is noted that the damage pattern depicted in Figure 16 is observed in masonry walls that are loaded with in-plane actions. Some limited out-of-plane flexural displacement also arises in this case.

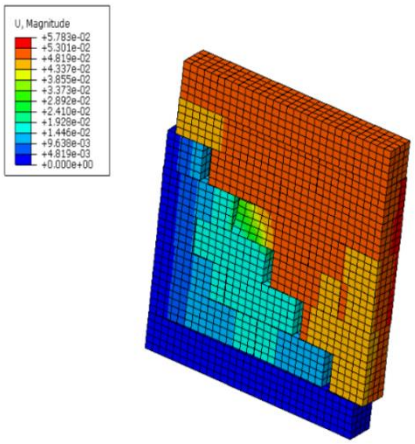

Figure 16. Displacement of the solid wall loaded with a charge weight of 200 kg at a distance of 50 m.

For the case of the highest explosive weight of 1150 kg (standoff distance 50 m), it is determined that out-of-plane flexural deflection is the dominant response, leading to a corresponding failure mode. Moreover, as can be observed in Figure 17b,c, both tensile and compressive failure are developed in the whole mass of the wall. By comparing this with the case of the same explosive weight and lower standoff distance (20 m) shown

in Figure 14, it is noticed that although both walls fail due to the out-of-plane response attributed to the blast action, the model with the lower standoff distance leads to a total out-of-plane collapse.

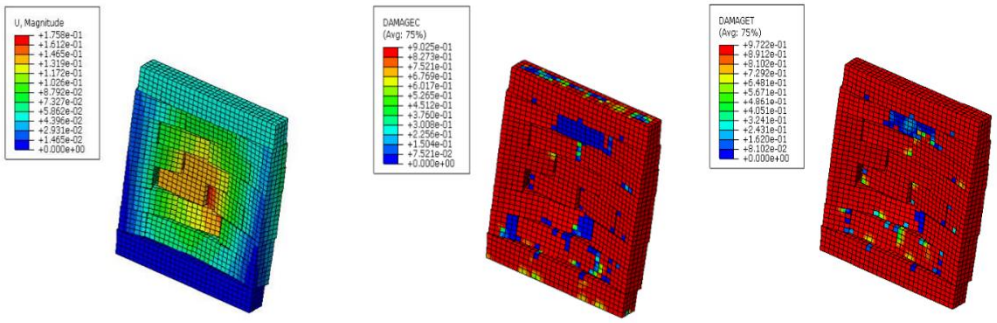

(**a**) (**b**) (**c**)

Figure 17. Solid wall loaded with a charge weight of 1150 kg at a distance of 50 m: (**a**) displacement of the wall at the end of the simulation (m), (**b**) compressive damage variable, and (**c**) tensile damage variable distribution.

When an increase in the standoff distance from 50 m to 100 m is considered for the case of the maximum explosive weight of 1150 kg, the failure mode changes and diagonal in-plane cracking becomes dominant, as shown in Figure 18, contrary to the out-of-plane flexural deflection observed at a distance of 50 m (Figure 17). Some out-of-plane flexural deflection, accompanied by tensile failure at the perimeter and at the central part of the wall, is also obtained, as shown in Figure 18. Compressive failure is more limited and is mainly developed at the wall's bottom corner.

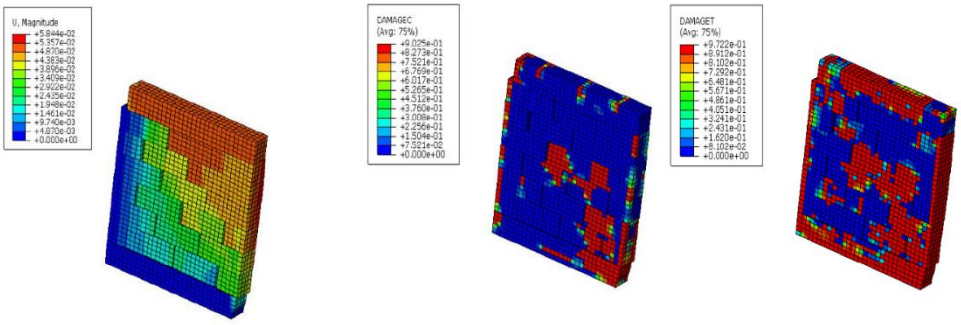

(**a**) (**b**) (**c**)

Figure 18. Solid wall loaded with a charge weight of 1150 kg at a distance of 100 m: (**a**) displacement of the wall at the end of the simulation (m), (**b**) compressive damage variable, and (**c**) tensile damage variable distribution.

To summarize the effect of varying standoff distances for each explosive weight, the diagrams shown in Figure 19 are used. It is observed that for bigger explosive weights and lower standoff distances, higher deflections of the wall are obtained. When the standoff distance is increased, the impact of the blast loading on the structural system is reduced since the maximum displacements are also reduced. It is noted that for the case of out-

of-plane response for the maximum explosive weight and minimum distance, a large deflection is obtained, as depicted with point X in the graph shown in Figure 19a. This value is only indicative, highlighting a total collapse of the central part of the wall.

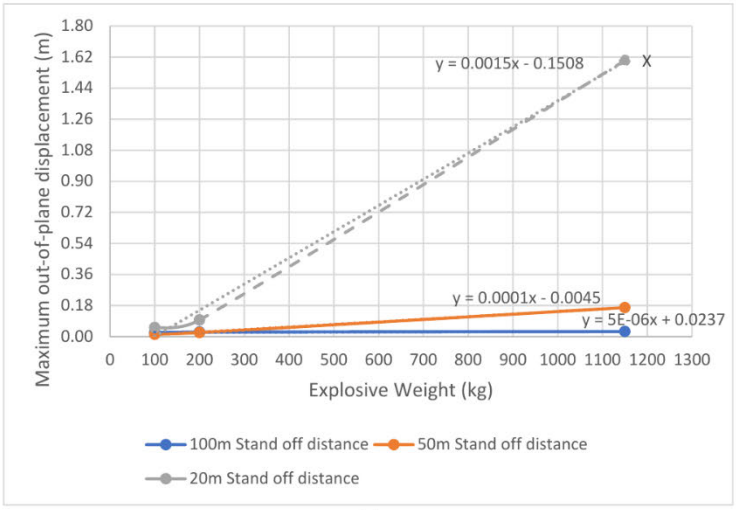

(**a**)

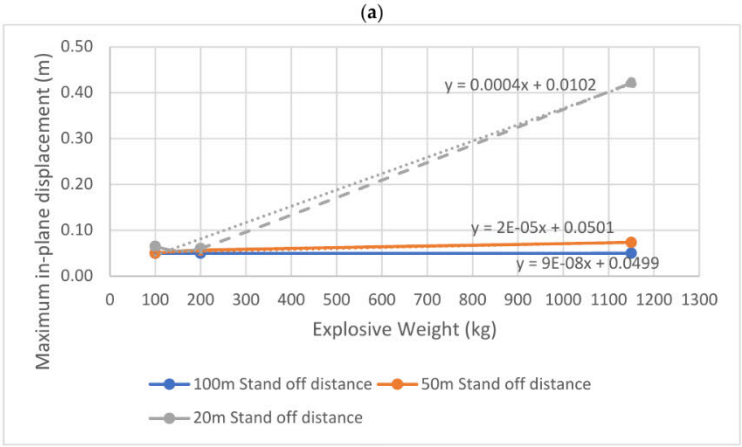

(**b**)

Figure 19. Displacement–explosive weight diagrams depicting the (**a**) out-of-plane and (**b**) in-plane response.

In Figure 19a,b, linear regression formulas are determined, providing approximate mathematical expressions that can be used to calculate the deflection of the walls for different explosive weight values and standoff distances. In particular, for standoff distances of 20 m, 50 m, and 100 m, the correlation coefficients are found to be equal to $R^2 = 0.9962$, $R^2 = 0.9993$, and $R^2 = 0.85$, respectively, for the out-of-plane response. In terms of the in-plane response, standoff distances 20 m, 50 m, and 100 m provide correlation coefficients of 0.9906, 0.9618, and 0.9926, respectively. It is noted that an R^2 close to 1 indicates that the regression prediction is of satisfactory accuracy. Equations on the graphs were tested by inserting a random independent variable "x" (explosive weight) to estimate the displacement "y" (deflection of the wall).

5.2. Case 2: Masonry Wall with an Opening Loaded with Vertical Pressure, Shear Displacement, and Blast Load

To capture the influence of openings (windows) on the structural response of masonry walls under blast actions, a new model is developed, introducing a window in the middle of the wall, as shown in Figure 10. Similar to Section 5.1, a vertical downward pressure and a shear in-plane loading applied at the top surface of the wall are considered together with the blast action. To simulate the influence of the lintel, which is a concrete beam usually built just above the opening and in contact with the masonry above, the vertical displacements for the elements above the window are restricted.

In Figure 20, the displacement contour plot, which was obtained when an explosive weight of 1150 kg at a standoff distance of 50 m is applied to the wall, is shown. It is observed that relatively low max displacements arise at the final load step, with an in-plane diagonal cracking above the window on the left-hand side of the wall just emerging. By comparing this with Figure 17, which depicts the response of the solid wall under the same blast loading and standoff distance, it appears that the wall with the opening develops significantly lower deflection with no obvious out-of-plane deformation, contrary to the solid wall. This is attributed to the fact that the blast load is modeled as a surface force under the incident wave (CONWEP), and the damage or effect of the blast is directly proportional to the exposed surface. In addition, the window is inserted at the middle part of the wall, where the out-of-plane response due to the blast load would become maximum in the case of a solid wall.

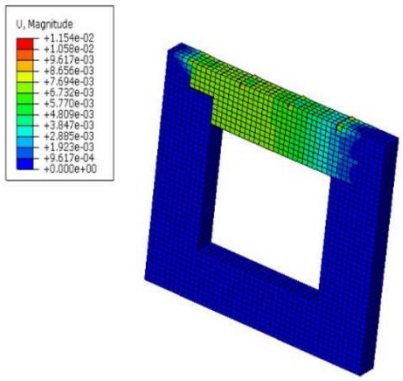

Figure 20. Displacement contour plot at the end of the simulation for a wall with an opening subjected to 1150 kg TNT at a standoff distance of 50 m.

Next, to depict the failure of the wall with the opening, the weight of the explosive is increased and the standoff distance is reduced. In particular, the displacement plots for the wall obtained from explosive weights of 2000 kg and 3500 kg at standoff distances of 5 m and 10 m are provided in Figure 21. For both cases, out-of-plane failure is obtained as depicted in Figure 21a,b with the case of 2000 kg explosive weight at a distance of 5 m being the most severe.

In an effort to provide a qualitative comparison of the response of the walls with and without a window, it is observed that the most severe collapse of the wall with the window occurs for 2000 kg explosive weight positioned at 5 m (Figure 21a). The corresponding most severe collapse of the solid wall occurs for 1150 kg explosive weight positioned at 20 m (Figure 14). Thus, it seems that the opening in the middle of the wall significantly reduces the effects of the blast action. This observation is in agreement with the findings provided in [43], where the area of an opening in a masonry building is shown to have a significant impact on both the normal and shear stresses produced by blast.

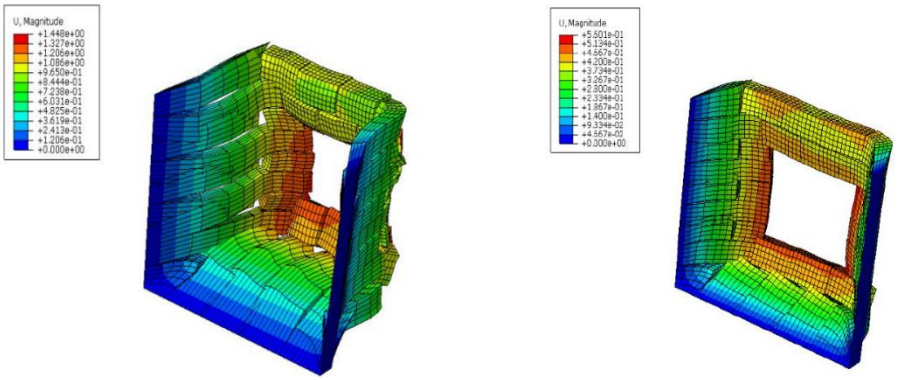

(**a**) (**b**)

Figure 21. Displacement contour plot at the end of the simulation for a wall with an opening subjected to (**a**) 2000 kg TNT at a standoff distance of 5 m and (**b**) 3500 kg TNT at a standoff distance of 10 m.

5.3. Case 3: Solid Masonry Wall Loaded with Vertical Pressure and Blast Load

In this section, the response of the wall without an opening loaded with a vertical downward pressure at the top surface and the blast action is investigated. Thus, contrary to Section 5.1 (and Section 5.2), no shear horizontal displacement is applied at the top of the wall. In Figure 22, the response of the wall subjected to 100 kg and 200 kg TNT at standoff distances of 50 m and 100 m, respectively, is provided. In Figure 23, the response of the wall subjected to 1150 kg TNT and 100 m standoff distance is shown.

In both Figures 22 and 23, the out-of-plane deflection characterizes the response of the wall. Contrary to this behavior, the model of the wall loaded with shear horizontal displacement, 100 kg explosive weight, and 50 m standoff distance, resulted in diagonal in-plane cracking (Figure 15) with significantly higher maximum deflection, compared with the wall shown in Figure 22a.

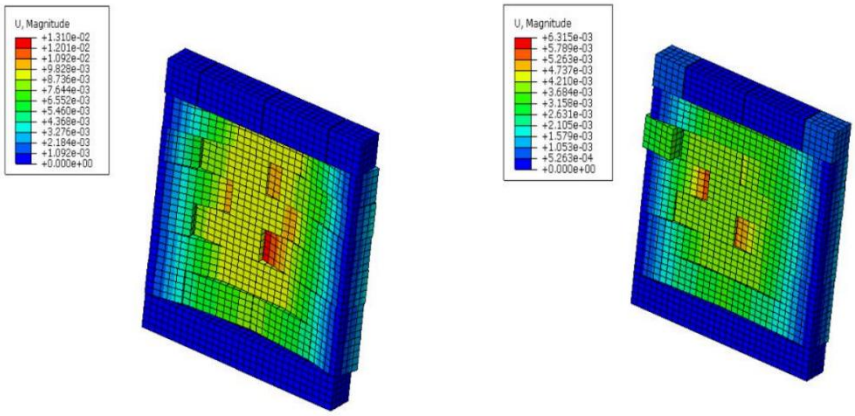

(**a**) (**b**)

Figure 22. Solid wall subjected to (**a**) 100 kg TNT at a standoff distance of 50 m and (**b**) 200 kg TNT at a standoff distance of 100 m when no horizontal displacement loading is applied to the top surface of the wall (a scale factor equal to 10 is used to magnify the displacement contour plots).

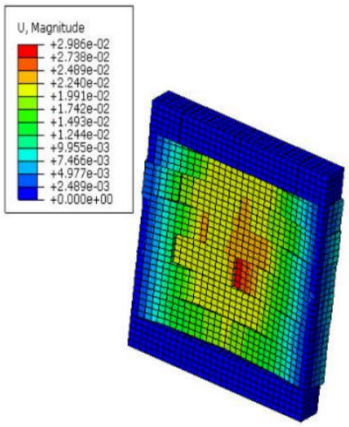

Figure 23. Solid wall subjected to 1150 kg TNT at a standoff distance of 100 m when no horizontal displacement loading is applied to the top surface of the wall (a scale factor equal to 10 is used to magnify the displacement contour plots).

A similar comparison can be made between Figures 18 and 23, representing the displacement contour plot of the wall under the same blast load and standoff distance (1150 kg, 100 m) with and without the shear displacement load, respectively. As shown in Figure 18, a significantly higher maximum deflection is obtained when the shear displacement load is applied to the wall, compared with Figure 23. In addition, the in-plane diagonal cracking is dominant in Figure 18.

6. Conclusions

In this article, the response of masonry walls under static in-plane and blast loads is investigated using non-linear finite element analysis software [44]. For the simulation of damage in the interfaces between the stone blocks, unilateral contact–friction interfaces are applied to depict opening and sliding failure. In addition, a concrete damage plasticity model is used to describe tensile and compressive damage in the blocks. The proposed scheme is applied to a solid masonry wall and to a wall with an opening (window).

This investigation aims in highlighting potential collapse mechanisms by testing different blast load parameters, namely, the weight of the explosive and the standoff distance between the source of the explosion and the structure. The influence of a horizontal shear displacement in-plane loading at the top of the wall is also investigated.

According to the findings of this study, the failure mode of the wall loaded with both shear in-plane displacement and the blast action can be either in-plane diagonal cracking or out-of-plane flexural failure. The first mode arises when the shear in-plane displacement is the dominant loading, compared with the blasting action, while the second arises when the blast is the dominant loading. For the same material properties and wall dimensions, the weight of the explosive and the standoff distance are the critical parameters, which determine which of the two loading types dominates. In the results section, case studies highlighting both failure modes are discussed for various values of the explosive weight and the standoff distance. A combination of both failure modes can also arise, depending on the values of these parameters.

Another outcome of this work is the fact that the presence of an opening (window) in the wall may reduce the effect of the blast action by decreasing the out-of-plane response of the structure. The reason for this is that due to the opening being located in the middle of the wall, the blast load is not applied to this critical (for out-of-plane flexure) middle part of the surface of the wall. Thus, this study shows that the blast action must occur at a closer

standoff distance compared with the solid wall, in order to cause significant damage to the structure.

When no shear displacement in-plane loading is applied, the response is dominated by the out-of-plane flexural deflection, attributed to the blasting action. In this case, lower maximum displacements are obtained compared with the wall loaded with shear displacement and blast actions.

Several future investigations could be used to extend the present work. A potential concept is to study the influence of the area, position, and number of windows on the response of the walls under blast actions. The usage of different initial static loading could modify the results, as was shown in the conducted numerical investigation. Design or re-design based on these findings could also form an interesting research topic. Another concept is related to the implementation of data-driven structural dynamics, introducing machine learning tools, to evaluate the influence of several parameters such as the dimensions of the walls and the blast load parameters on their structural response.

Author Contributions: Conceptualization, G.A.D.; methodology, G.A.D.; formal analysis, S.G.T.; investigation, S.G.T. and G.A.D.; resources, G.A.D.; data curation, S.G.T.; writing—original draft preparation, S.G.T.; writing—review and editing, S.G.T., G.A.D. and G.E.S.; visualization, S.G.T.; supervision, G.A.D. and G.E.S.; project administration, G.A.D. All authors have read and agreed to the published version of the manuscript.

Funding: This research received no external funding.

Data Availability Statement: Not applicable.

Conflicts of Interest: The authors declare no conflict of interest.

References

1. Ahmad, S.; Elahi, A.; Pervaiz, H.; Rahman, A.G.A.; Barbhuiya, S. Experimental study of masonry wall exposed to blast loading. *Mater. Constr.* **2014**, *64*, 2–6. [CrossRef]
2. Gertsch, L.; Baird, J. *A Phased Array Approach to Rock Blasting*; University of North Texas, UNT Digital Library: Denton, TX, USA, 2006; pp. 13–40. Available online: https://digital.library.unt.edu (accessed on 22 March 2022).
3. Aloui, M.; Bleuzen, Y.; Essefi, E.; Abbes, C. Ground Vibrations and Air Blast Effects Induced by Blasting in Open Pit Mines: Case of Metlaoui Mining Basin, Southwestern Tunisia. *J. Geol. Geophys.* **2016**, *5*, 5–7. [CrossRef]
4. Ipmawati, M.R.; Nainggolan, D.R.; Wiyono, B.; Sunary, R. Effect double-primer placement for improving the fragmentation on harder material in stemming column: A case study. *IOP Conf. Ser. Earth Environ. Sci.* **2018**, *212*, 012064. [CrossRef]
5. Hao, D. Numerical Modelling of Masonry Wall Response to Blast Loads. *Aust. J. Struct. Eng.* **2009**, *10*, 37–52. [CrossRef]
6. Wang, W.; Zhang, D.; Fangyun, L.; Wang, S.C.; Tang, T. Experimental study and numerical simulation of the damage mode of a square reinforced concrete slab under close-in explosion. *Eng. Fail. Anal.* **2013**, *27*, 41–51. [CrossRef]
7. Zhao, C.F.; Chen, J.Y. Damage mechanism and mode of square reinforced concrete slab subjected to blast loading. *Theor. Appl. Fract. Mech.* **2013**, *63–64*, 54–62. [CrossRef]
8. Macorini, L.; Izzuddin, B.A. Nonlinear Analysis of Unreinforced Masonry Walls under Blast Loading Using Mesoscale Partitioned Modeling. *J. Struct. Eng.* **2014**, *140*, A4014002. [CrossRef]
9. Kernicky, T.P.; Whelan, M.J.; Weggel, D.C.; Rice, C.D. Structural Identification and Damage Characterization of a Masonry Infill Wall in a Full-Scale Building Subjected to Internal Blast Load. *J. Struct. Eng.* **2015**, *141*, D4014013. [CrossRef]
10. Jia, H.; Yu, L.; Wu, G. Damage Assessment of Two-Way Bending RC Slabs Subjected to Blast Loadings. *Publ. Corp. Sci. World J.* **2014**, *2014*, 718702. [CrossRef]
11. D'Altri, A.M.; Miranda, S.; Castellazzi, G.; Sarhosis, V. A 3D Detailed Micro-Modelling Approach for the In-Plane and Out-Of-Plane Analysis of Masonry Structures. *Comput. Struct.* **2018**, *206*, 18–30. [CrossRef]
12. Lourenço, P.B.; Rots, J.G.; Blaauwendraad, J. Two Approaches for the Analysis of Masonry Structures: Micro and Macro-Modeling. *Heron* **1995**, *40*, 313–338.
13. Masi, F.; Stafanou, I.; Maffi-Berthier, V.; Vannucci, P. A Discrete Element Method based-approach for arched masonry structures under blast loads. *Eng. Struct.* **2020**, *216*, 110721. [CrossRef]
14. Shamim, S.; Shamd, S.; Khan, A. Finite element analysis of masonry wall subjected to blast loading. *Int. J. Adv. Mech. Civ. Eng.* **2019**, *6*, 50–53.
15. Shamim, S.; Shamd, S.; Khan, A. Numerical Modelling of Masonry Panel Subjected to Surface Blast Loading. *J. Xi'an Univ. Archit. Technol.* **2020**, *12*, 846–856.
16. Abdulla, K.; Cunningham, L.; Gillie, M. Non-linear simulation of masonry behaviour under cyclic loads. In Proceedings of the 2017 MACE PGR Conference, Manchester, UK, 3 April 2017; pp. 20–22.

17. Anas, S.M.; Alam, M.; Umair, M. Strengthening of braced unreinforced brick masonry wall with (i) C-FRP wrapping, and (ii) steel angle-strip system under blast loading. *Mater. Today Proc.* **2022**, *58*, 1181–1198. [CrossRef]
18. Shariq, M.; Alam, M.; Husain, A.; Islam, N. Response of strengthened unreinforced brick masonry wall with (1) mild steel wire mesh and (2) CFRP wrapping, under close-in blast. *Mater. Today Proc.* **2022**, *64*, 643–654. [CrossRef]
19. Shamim, S.; Khan, R.A.; Ahmad, S. Fragility analysis of masonry wall subjected to blast loading. *Structures* **2022**, *39*, 1016–1030. [CrossRef]
20. Yu, Q.; Zeng, D.; Xu, X.; Li, S.; Dong, W.; Dai, L. Experimental and numerical investigation of polymer-reinforced and normal autoclaved aerated concrete masonry walls under large TNT explosive loads. *Int. J. Impact Eng.* **2022**, *164*, 104188. [CrossRef]
21. Salmanpour, A.H. Displacement Capacity of Structural Masonry. Ph.D. Thesis, ETH Zurich, Zurich, Switzerland, 2017.
22. De Villiers, W.I. Computational and Experimental Modelling of Masonry Walling towards Performance-Based Standardisation of Alternative Masonry Units for Low-Income Housing. Ph.D. Thesis, Stellenbosch University, Stellenbosch, South Africa, 2019.
23. Kömürcü, S.; Gedikli, A. Macro and Micro Modeling of the Unreinforced Masonry Shear Walls. *Eur. J. Eng. Nat. Sci.* **2019**, *3*, 116–123.
24. Ranji, A.R.; Esmaeli, A. Blast load response of one-way reinforced concrete slabs retrofitted with Fiber reinforced plastic. *Proc. Odessa Polytech. Univ.* **2018**, *2*, 49–58. [CrossRef]
25. Tan, W.A.; Tingatinga, E.A.; Alvarez, V. Blast load analysis and simulation of unreinforced concrete masonry. *J. Phys. Conf. Ser.* **2019**, *1264*, 012008. [CrossRef]
26. Weggel, D.C. Blast threats and blast loading. In *Blast Protection of Civil Infrastructures and Vehicles Using Composites*; Series in Civil and Structural Engineering; Woodhead Publishing: Swaston, UK, 2010; pp. 3–43. [CrossRef]
27. Botez, M.D.; Bredean, L.A. Numerical Study of a RC Slab Subjected to Blast: A Coupled Eulerian-Lagrangian Approach. *IOP Conf. Ser. Mater. Sci. Eng.* **2019**, *471*, 2–5. [CrossRef]
28. Rigby, S.E.; Tyas, A.; Bennett, T.; Clarke, S.D.; Fay, S.D. The Negative Phase of the Blast Load. *Int. J. Prot. Struct.* **2014**, *5*, 1–19. [CrossRef]
29. Alsayed, S.H.; Elsanadedy, H.M.; Al-Zaheri, Z.M.; Salloum, Y.A.; Abbas, H. Blast response of GFRP strengthened, infill masonry walls. *Constr. Build. Mater.* **2016**, *115*, 438–451. [CrossRef]
30. Bolhassani, M.; Hamid, A.A.; Lau, A.C.W.; Moon, F. Simplified micro modelling of partially grouted masonry assemblages. *Constr. Build. Mater.* **2015**, *83*, 159–173. [CrossRef]
31. Draganić, H.; Sigmund, V. Blast Loading On Structures. *Tech. Gaz.* **2012**, *19*, 643–652.
32. Lubliner, J.; Oliver, J.; Oller, S.; Oñate, E. A plastic-damage model for concrete. *Int. J. Solids Struct.* **1989**, *25*, 299–329. [CrossRef]
33. Lee, J.; Fenves, G.L. Plastic-Damage Model for Cyclic Loading of Concrete Structures. *J. Eng. Mech.* **1998**, *124*, 892–900. [CrossRef]
34. Tapkin, S.; Tercan, E.; Motsa, S.; Drosopoulos, G.; Stavroulaki, M.; Maravelakis, E.; Stavroulakis, G. Structural Investigation of Masonry Arch Bridges Using Various Nonlinear Finite-Element Models. *J. Bridge Eng.* **2022**, *27*, 04022053. [CrossRef]
35. Daniel, J.; Dubey, R. Finite Element Simulation of Earthquake Resistant Brick Masonry Building Under Shock Loading. *Adv. Struct. Eng.* **2014**, *81*, 1027–1038. [CrossRef]
36. Dogu, M.; Menkulasi, F. A flexural design methodology for UHPC beams posttensioned with unbonded tendons. *Eng. Struct.* **2020**, *207*, 110193. [CrossRef]
37. Hognestad, E. *A Study of Combined Bending and Axial Load in Reinforced Concrete Members*; Bulletin Series No.399; University of Illinois, Engineering Experiment Station: Chicago, IL, USA, 1951; pp. 32–54.
38. Iuorio, O.; Dauda, J.A. Retrofitting Masonry Walls against Out-Of-Plane Loading with Timber Based Panels. *Appl. Sci.* **2021**, *11*, 5443. [CrossRef]
39. Concrete Manufactures Association. *Concrete Masonry Manual*, 9th ed.; Concrete Manufactures Association: Menlo Park, CA, USA, 2011. Available online: https://www.cma.org.za/Portals/0/Docs/brickasandblocks (accessed on 22 April 2022).
40. *SANS 10400-A 2010*; The Application of the National Building Regulations Part A: General Principles and Requirements, 3rd ed. SABS Standards Division: Pretoria, South Africa, 2010; ISBN 978-0-626-25157-4.
41. Wei, J.; Du, Z.; Zheng, Y.; Ounhueane, O. Research on Damage Characteristics of Brick Masonry under Explosion Load. *Shock Vib.* **2021**, *2021*, 5519231. [CrossRef]
42. Decanini, L.; De Sortis, A.; Goretti, A.; Langenbach, R.; Mollaioli, F.; Rasulo, A. Performance of masonry buildings during the 2002 Molise, Italy, earthquake. *Earthq. Spectra* **2004**, *20* (Suppl. S1), 191–220. [CrossRef]
43. Raza, I.; Shamim, S.; Ahmad, S.; Khan, R.A. Analysis of two-storey masonry structure under blast loading. *Mater. Today Proc.* **2023**, *80*, 1605–1610. [CrossRef]
44. ABAQUS v. 6.14.2 Users Manual. Available online: http://130.149.89.49:2080/v2016/index.html (accessed on 13 March 2022).

Chapter 5 - Investigating the effect of brickwork patterns on response of masonry walls under blast load

This chapter presents the research paper that investigated the effect of brickwork patterns on the response of walls against blast loads. Three bonding patterns were considered in this study, namely, English bond, stretcher bond and stack bond. Following the previous chapter where one bonding pattern was considered. This chapter aims at providing a comparison between different bonding patterns that are commonly used in the building industry.

(This article is currently under review with the European Journal of Computational Mechanics)

This chapter is presented in the format of the submitted manuscript.

Investigating the effect of brickwork patterns on response of masonry walls under blast load

Sipho Gcinangaye Thango[a, *], Siphesihle Mpho Motsa[a], Georgios E. Stavroulakis[b], Georgios A. Drosopoulos[c, a]

[a] University of KwaZulu Natal, Department of Civil Engineering, Durban 4041, South Africa.

[b] Technical University of Crete, School of Production Engineering & Management, 73100 Chania, Crete, Greece

[c] University of Central Lancashire, Division of Civil Engineering, Preston PR1 2HE, UK

[*] Corresponding author.

E-mail address: 209523102@stu.ukzn.ac.za / thangosiphog@gmail.com

Abstract

Architects consider the brickwork patterns vital for the aesthetics of the walls. The different brick bonding patterns can influence the resistance of masonry walls when subject to in-plane and out-of-plane loading. This study investigates the effect of different bonding patterns under a blast load of 50kg TNT at a standoff distance of 20m. The adoption of a simplified micro-modelling approach provided meaningful results on the behaviour of the wall. The in-plane and out-of-plane response of walls with different bonding patterns was investigated and comparisons were made. This study concluded that the stack bond has a weaker binding pattern than other widely used bonds like English bond and Stretcher bond due to the lack of interlocking between the masonry units. Shear failure and vertical cracking were seen as the typical failures in all the three walls, with the stack bond depicting higher deflections under both in-plane and blast loading.

Keywords: Blast; Masonry; Mortar; In plane; Out of plane; Brick Patterns

1. Introduction

The orientation of bricks in masonry wall construction is regarded as one of the aspects that architects consider vital for the aesthetics of the walls. In Debnath et al [1], it was investigated how unreinforced masonry (URM) wall components function under lateral or typical seismic loads with each of the four types of brick bonds: Header bond, Stretcher bond, English bond, and Flemish link. In Shrestha et al [2], it was concluded that the URM walls made with English and Flemish bonds show almost 1.2 times the load-carrying capacity exhibited by the walls made by Header and Stretcher bonds. The study presented in Bacigalupo et al [3] assessed the in-plane behaviour of Header, Stretcher, and English bonds using parametric micro-modelling. The conclusions from this study were that the header bond portrayed higher lateral capacity together with equal shear capacity as that of English bond. In Shah et al [4], tensile-compressive loads were applied to masonry walls leading to the following fundamental distinctions: the herringbone pattern's tensile strength attributes seem to be significantly higher than the comparable strength of its constituent parts.

Thango et al [5] studied the failure response of masonry walls subjected to blast loading using nonlinear finite element analysis. This study considered the stretcher bond pattern. Explosive

weights of 100kg TNT, 200kg TNT and 1150kg TNT were considered with the varying standoff distances which included distances such as 20m, 50m, and 100m. This study highlighted the effect of the standoff distances and blast weight on the damage intensity, the closer the explosive, the higher the damage intensity.

According to Elmenshawi et al [6] it is necessary to characterize the mechanical properties of masonry, such as strength and stiffness, to comprehend how it behaves as a structural material. The stress-strain relationship is often defined or expressed by the material constitutive law that is defined over the range of applicability of the material being considered. In the modelling approach herein proposed, the masonry units are taken as continuum elements and mortar joints as interface elements. Zero tensile resistance between the joints was introduced (Mortar properties were not introduced or defined).

According to D'Altr et al [7], Pasquantoniog et al [8] and Stankowski et al [9] each mortar layer is continuously linked to a brick and separated by an interface from other bricks. Weyler et al [10] highlights that the in the zero-thickness interfaces between the Representative Elements, the contact penalty approach is used. Conventional point-against-surface contact method is considered. In such modelling, the penalty stiffness is assumed to keep insignificant the penetration of the elements and to pledge good convergence rates of simulations. For the 3D model, a rigid infinitely resistant behaviour for bricks was assumed, whereas for joints a Mohr-Coulomb failure criterion with the same tensile strength and friction angle used in the homogenized approach for joints was adopted. Eight-noded (hexahedron) brick elements were utilized both for joints and bricks, with a double row of elements along wall thickness.

However, the influence of brick patterns has not yet been thoroughly investigated. In the present paper, the dynamic behaviour of masonry wall with different types of brick bonding is investigated computationally. The wall is analysed using both in-plane and out of plane loading, and one of the out of plane loading considered in this case is blast loading. Blasting can arise from various activities including mining activities that involves breaking of rocks. Blasting is a crucial aspect of mining operations that involves the use of explosives to break down hard rock formations and access valuable minerals. Explosions and bombing scenes also put residential houses at risk of damage. Finite element analysis was adopted in this study to model different brick bonding patterns and boundary conditions. Non-uniform blast loads were considered. Changes in displacement time histories and plastic hinge formations resulting from varying the axial load were examined. The breakdown of brick-mortar bonding, which functions as planes of weakness, is typically a major factor in the mechanical behaviour of masonry buildings that are on the verge of collapsing [11]. Accordingly, in this paper nonlinear numerical analyses were performed for progressive collapse assessment. The walls with different bonding patterns were compared. Prior to conducting the numerical assessment, literature review was conducted to ascertain the available knowledge on this topic and address the research gap. This paper is organized as follows; in Section 2 of this article, materials and methods adopted for this study are briefly discussed. In Section 3, the finite element modelling approach and failure modes are discussed. Section 4 provides the validation of the model while Section 5 details the proposed Finite element model. In Section 6, results and discussions are provided. Lastly, Section 7, the conclusions of this investigation are presented.

2. Materials and Methods

2.1 Explosions and blast phenomenon

Explosion is defined as a large-scale, quick, and unexpected discharge of energy. Depending on their nature, explosions can be classified as physical, nuclear, or chemical phenomena [12]. A general rule of explosives is that the detonation of the explosives results in a high-velocity shock wave and a great release of gas. This high-velocity shock and gas release has over the years been causing damages to neighbouring structures and even fatalities. With specific reference to buildings, the air-blast shock wave is the main mode that explosions cause damage.

Blast loads are produced by detonation of explosion materials. Detonation is a chemical reaction that proceeds through the explosive material at supersonic speed and converts the material into pressure gas. Due to this, a pressure wave is developed which travels in all the directions and has got push-pull action on air. This gas pressure, also known as detonation pressure, propagates like shock wave, and affects the surrounding structures. The demonstration of the blast loading on structures is shown in figure 1 below.

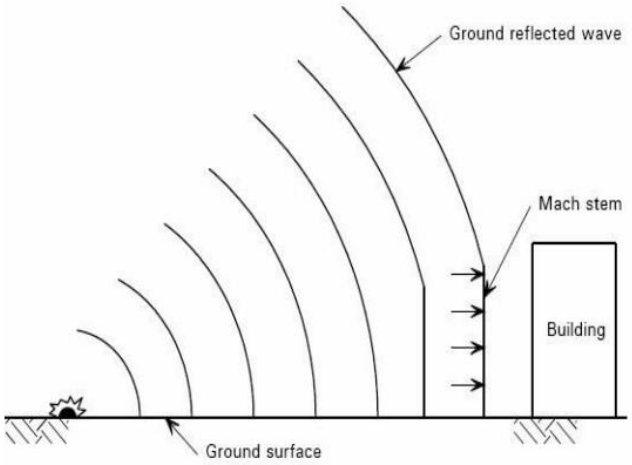

Figure 1: Blast pressure and loads on a structure [13]

2.2 Model description

The section below looks at the different brick bonding patterns that were investigated in this paper.

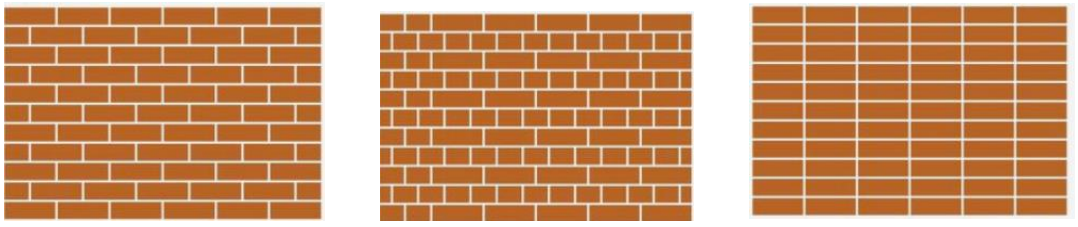

(a) (b) (c)

Figure 2: Different brick bond patterns: a stretcher bond; b English bond; c stack bond

A simplified representation of the mortar joint as a zero-thickness interface was adopted for this study. The assumption of a mortar joint as a zero-thickness interface is a simplification useful in modelling the behaviour of masonry structures [14]. In reality, mortar joints have a measurable thickness, typically on the order of a few millimetres. However, when analysing

the response of a masonry wall to external loads or other stresses, modelling the mortar joints as zero-thickness interfaces can simplify the analysis and provide reasonable results. This is because the mortar joint has a significantly lower strength compared to the masonry units it is bonding together, and so the joint's thickness is often negligible in terms of the structural response of the masonry structure.

3. Finite element modelling

3.1 Modelling approach

Finite element method of analysis is an advanced method which is commonly applied recently to solve complex structural analysis problems including blast problems. According to Lourenco [15], modelling masonry structures can be grouped into two classes: Micro-modelling and macro-modelling. As can be seen in figure 3, in micro-modelling (detailed), continuum components are used to represent the brick unit and mortar, while interface elements are used to depict the unit-mortar interface. In the simplified micro-modelling, brick units are modelled as continuum elements and the unit-mortar interfaces are grouped and modelled with the interface elements.

According to Lourenco et al. [16], the macro-modelling distinction between brick/stone units and mortar joints is treated as one unit. The consideration of brick and mortar as one homogeneous material tends to make the macro-modelling techniques more suitable for practical use as the computer resource required is less when compared with micro-modelling techniques. As discussed by Braimah [17], the macro-modelling technique is not able to offer information on failure mechanism, which most often is not needed in the analysis. This is further stated by Kömürcü and Gedikli [18], by using the macro modelling approach, the detailed failure mechanisms are generally not well reproduced. Recent advances in homogenization that incorporates XFEM could enhance the effectiveness of macro-modelling in this respect, see Drosopoulos and Stavroulakis [19].

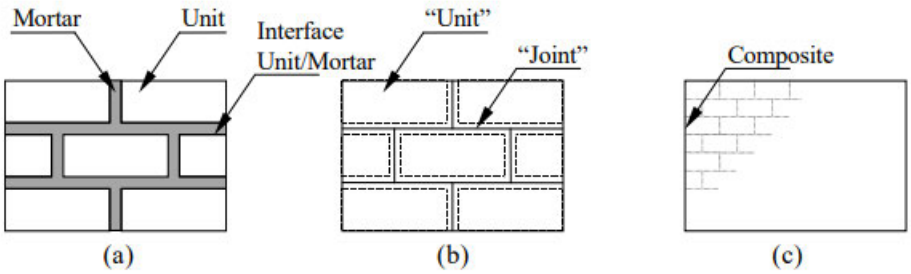

Figure 3: Modelling techniques for masonry structures (a) detailed micro-modelling, (b) simplified micro-modelling, (c) macro-modelling [15]

3.2 Contact mechanics and material properties

To develop informative numerical models, to investigate the structural behaviour of the masonry wall, material properties obtained from published literature have been used. A continuum model is adopted to define the damage mechanics laws, which is used to simulate the nonlinear material behaviour of the masonry and mortar, focusing on tensile and compressive damage. The interfaces between the masonry units are given a unilateral contact and friction constitutive description for the evaluation of the failure reaction that results from these interfaces. Assuming u to be the single degree of freedom in the system, while g

represents the initial opening and t^n as the equivalent contact pressure during the contact of the units. Equation (1) represents the non-penetration relation, equation (2) specifies that only compressive stresses ($\boldsymbol{t^n}$) can develop in the interfaces, and equation (3) represents the complementarity relation, which states that either contact occurs (u-g=0).

$$\boldsymbol{h = u - g \leq 0 \Rightarrow h \leq 0} \quad (1)$$

$$\boldsymbol{-t^n \geq 0} \quad (2)$$

$$\boldsymbol{t^n\,(u - g) = 0} \quad (3)$$

A static form of Coulomb's friction law is taken into consideration for the reaction in the tangential direction of the interfaces. According to equation (4), sliding in the interfaces begins when the shear stress t^t reaches the critical value $\boldsymbol{\tau_{cr}}$.

$$\boldsymbol{t^t = \tau_{cr} = \pm\mu|t^n|} \quad (4)$$

Where $\boldsymbol{t^t}$ is the shear stress and $\boldsymbol{\mu}$ is the friction coefficient.

In this study, a concrete damage plasticity (CDP) law is used to represent tensile and compressive damage on bricks, under loading and unloading conditions. Additionally, this law is based on the incremental plasticity theory and is rate independent.

In the case of a masonry wall, the concrete damage plasticity model may be used to predict the behaviour of the wall under various loading conditions, such as blast or seismic loads [20]. The CDP model utilizes a yield function centred on the studies conducted by Lubliner et al. [21] and Lee et al [22].

Damage of a solid body can be defined as degradation phenomenon in material properties such as stiffness, strength, and anisotropy. According to [23], if the damage is defined by stiffness degradation, the elastic stiffness (C) can be written using the stiffness degradation parameter.

$$\boldsymbol{C = (1 - d)C_0} \quad (5)$$

Where d denotes the degradation and C_0 denotes the initial stiffness matrix.

The above equation can be rewritten in terms of the Young's modulus as equation (6). The concrete damaged plasticity model assumes that the reduction of the elastic modulus is given in terms of a scalar degradation variable d as

$$\boldsymbol{E = (1 - d)E_0} \quad (6)$$

Where $\boldsymbol{E_0}$ represents the Young's elasticity modulus initial value.

According to the existence of irreversible deformation/plastic strain, stiffness degradation models may be divided into two categories: elastic degradation models and plastic degradation models [24]. It is worth mentioned that if no damage is considered in the concrete (d=0), equation is reduced to:

$$\boldsymbol{\sigma = E_0\left(\varepsilon - \varepsilon^{pl}\right)} \quad (7)$$

where σ, $\boldsymbol{\varepsilon}$, and $\boldsymbol{\varepsilon}^{pl}$ represent respectively the stress, total strain, and plastic strain.

Furthermore, Lee et al [22] developed an equation that defines the yield function of concrete damage plasticity model as the following.

$$\boldsymbol{F(\bar{\sigma}, k) = \frac{1}{1-\alpha}\left(\sigma \bar{I}_1 + \sqrt{\frac{3}{2}}\,\|\bar{S}\| + \beta(k)\langle\overline{\sigma_{max}}\rangle\right) - c_c(k) \leq 0} \qquad (8)$$

Where:

$\boldsymbol{c_c(k)} = (\boldsymbol{\bar{\sigma}, k})$ is the material cohesion,

$\boldsymbol{\bar{I}_1}$ is the first stress tensor invariant,

$\|\boldsymbol{\bar{S}}\| = \sqrt{\boldsymbol{\bar{S}}} : \boldsymbol{\bar{S}}$ is the stress tensor deviator norm,

$\boldsymbol{\bar{S} = \bar{\sigma} - \overline{\sigma_m}}\, I$ is the deviator of effective stress,

$\boldsymbol{\overline{\sigma_m} = \frac{1}{3}\, tr\bar{\sigma}}$ is the mean effective stress,

$\boldsymbol{\overline{\sigma_{max}}}$ is the algebraic maximum of eigenvalues of effective stress tensor

From the above equation 8, the effective stress - total strain dependence for tension and compression is shown in figure 4 below.

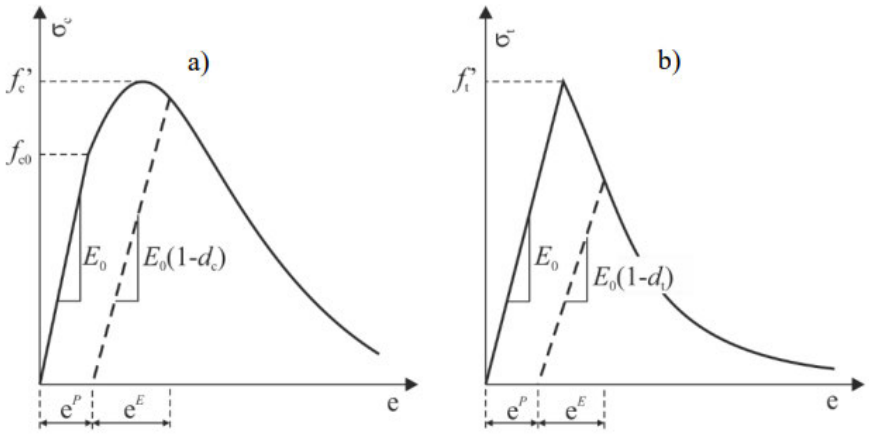

Figure 4: Dependence of stress on total strain for: a) compression and b) tension [25].

The material properties for the stones and mortar used for this investigation are presented in table 1 below.

Table 1. Mechanical properties of masonry unit and mortar [26]

Plasticity parameter	Value
Dilation angle	30
Eccentricity parameter	0.1
Bi and unidirectional compressive strength ratio	1.16

Stress ratio in tensile meridian	0.67
Viscosity parameter	0.001

The material properties for masonry unit that was adopted for this study included the Modulus of elasticity of 15 500 MPa, Poisson's ratio of 0.15, tensile strength of 1.05 MPa and the compressive strength of 10.5 MPa.

3.3 Basic modes of failure

The FEM models were built and modelled using commercial finite element software (ABAQUS) and the explicit solver was utilized. The different material properties used to model the masonry are listed in Table 1 above.

To take all basic failure modes into account, the modelling strategy proposed by [12] is followed. Figure 5 shows the basic failure mechanisms in masonry and the associated point on the failure surfaces proposed in this study.

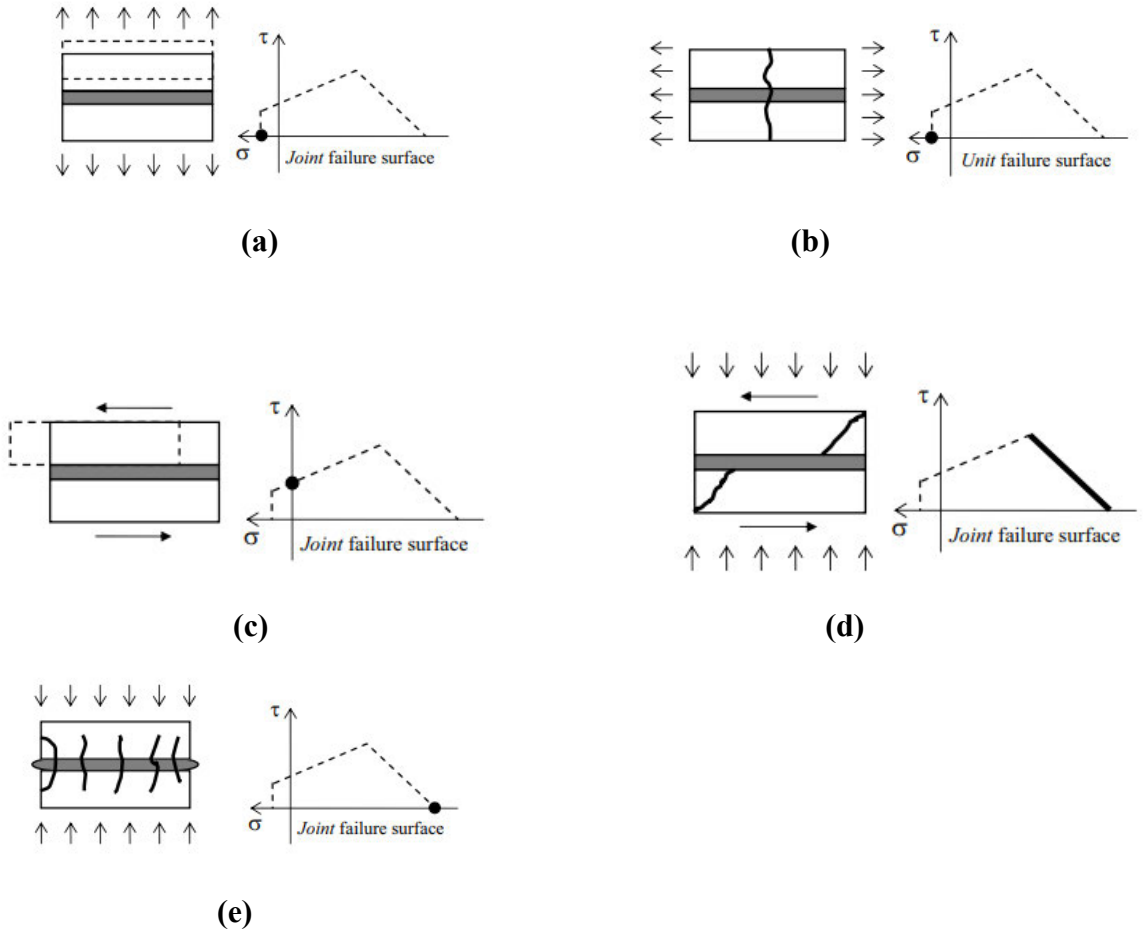

Figure 5: Basic failure modes in masonry as part of the modelling strategy. (a) Joint tensile cracking; (b) Cracking on unit in direct tension (c) Joint slip failure; (d) Unit diagonal tension cracking; (e) Masonry crushing [27]

4. Verification of the model

The proposed model is validated using already published literature for both in-plane and out-plane failure. As part of the novelty herein proposed in this study, comparison between the various brick bonding types will be made with specific reference to out-of-plane due to blast loading. The proposed model is validated using published results by other researchers with numerical and experimental studies.

4.1 In-plane response

The verification of the proposed model was verified using the failure mode from the experiment conducted by Vermeltfoort and Raijmakers [28]. In the experiment, a wall size of 990mm x 1000 mm, with 18 layers of solid clay bricks (dimensions 204 x 98 x 50 mm) was investigated. Furthermore, the tests considered vertical pre-compression pressure and a horizontal displacement loading as shown in Figure 6 below.

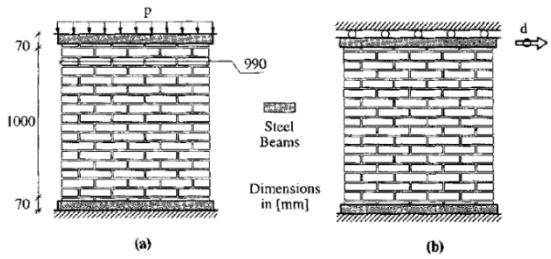

Figure 6: Loading of the specimen: (a) Vertical Loading; (b) Horizontal Loading [28]

In the experiment, a horizontal stress fracture that appeared at the bottom and top of the masonry wall signalled the beginning of the wall's failure mechanism. Following the appearance of a diagonal shear fracture and an increase in lateral displacement, the structure collapsed. Bricks began to shatter simultaneously with the stonework collapsing in the compacted toes.

The failure mechanism is show in figure 7 below which is compared with the failure pattern obtained from the numerical study.

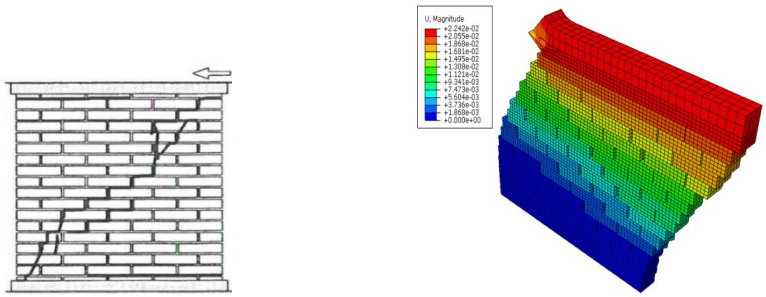

(a) **(b)**

Figure 7: Comparison of failure modes of walls: (a) Experimental failure patterns; (b) failure pattern from numerical model (scale factor = 20).

As seen in figure 7, the damage initiation and formation obtained from the numerical model is in close agreement with experimental model which there validates the model. Figure 8 below shows the damage patterns on the building caused by in-plane loading, it is worth noting that the direction of cracking follows that of the experimental model and numerical model.

Figure 8: Building damage due to in-plane loading.

4.2 Out-of-plane response

A running bond masonry wall subjected to a distributed blast pressure was investigated by Milani et al [29]. A 3-side constraint approach was used with the top position taken as free. Bricks in the 3D model used for validation were considered to have a stiff, endlessly resistant behaviour, while joints were subjected to the same Mohr-Coulomb failure criterion with the same tensile strength and friction angle as joints in the homogenised method.

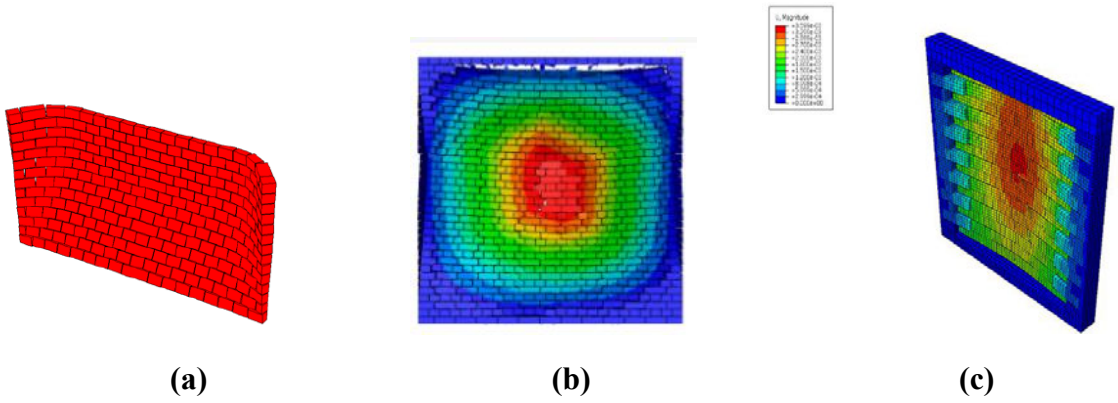

(a) **(b)** **(c)**

Figure 9:(a) out-of-plane response due to blast loading [28]; (b) out of plane response due to blast by [29] ;(c) Proposed model.

Figure 9 (b) depicts the deformation shape of a masonry wall subjected to 58.8kg TNT at a standoff distance of 5.5m from a study conducted by Zhang et al [30]. This study is comparable to the results obtained in this proposed work as can be seen in Figure 9 (c), where there is excessive deflection at the centre portion of the wall. Figure 10 shows the wall that was studied by Hao [31] who considered a 2880mm wide x 2820mm high wall which was fixed on all four sides.

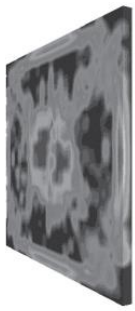

Figure 10: Simulation of the response to a surface blast due to a TNT explosive weight W = 200kg, located at 41m from blasting source [31]

At the distance of 41m, the study by [31] highlighted that the wall undergoes extensive damage but does not collapse. As expected, this study by [31] further highlighted that the increase in blast weight at the standoff distance of 41m leads to much higher deflection. The above comparison of the failure mode/pattern validates the proposed model as the wall's failure patterns are all in good agreement.

5. FEA Model

The wall was meshed using structural elements of 8 noded hexahedral linear brick element. The mesh size used for both brick and concrete beam was 20mm as shown in figure 11 d. The dynamic explicit solver was used for analysis under blast loading. With the aid of two reference points that were assigned depending on standoff distance from the site of reaction, the surface blast load was created using the CONWEP model as defined in ABAQUS. For the out-of-plane response, the wall was fixed on all four sides as compared to the in-plane investigation where the wall was fixed only at the base. The numerical analysis was carried out using an explosive weight of 50kg TNT at 20m. Figure 11 shows the wall patterns used in this study.

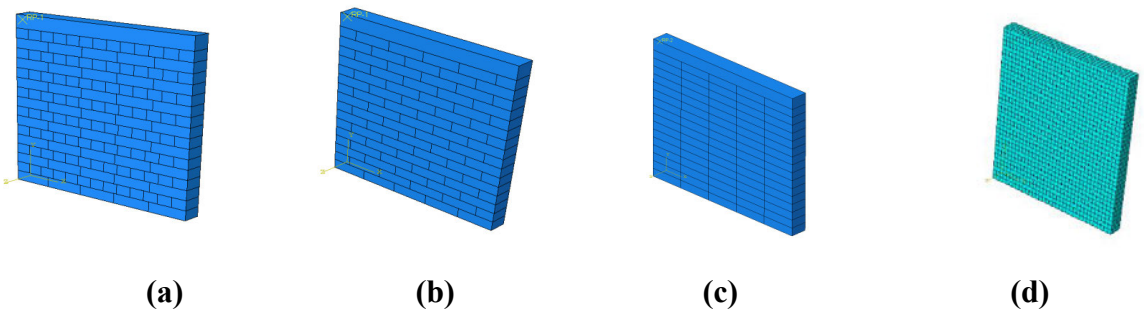

(a) **(b)** **(c)** **(d)**

Figure 11: Numerical Model of Masonry wall in ABAQUS: (a) English bond; (b) Stretcher bond; (c) Stack bond; (d) mesh model

The brick sizes that were used to develop the model were standard concrete brick size of 222mm (L) x 106mm (W) x 73mm (H). The modelled wall is 1110mm wide and 1268mm high including a beam of 100mm deep.

6. Results

6.1 In plane response of wall

The numerical analysis was performed on the wall with the pre-compression load of 0.25Mpa and horizontal displacement of 20mm that was applied on the concrete beam. The results for the three brick patterns are discussed below.

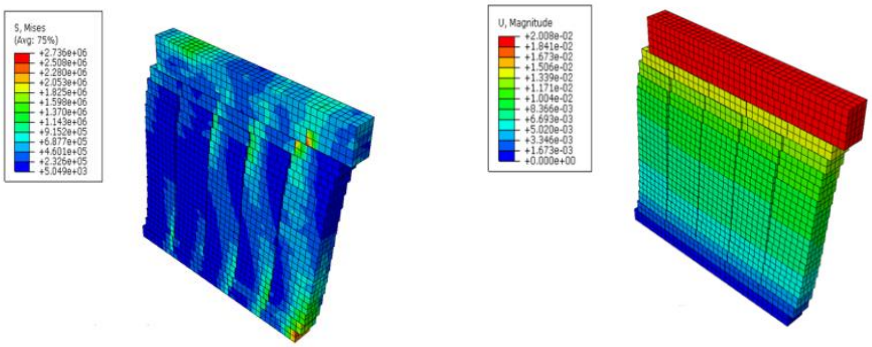

(a) **(b)**

Figure 12: (a) In-plane maximum Von-Mises stresses (S, Mises); (b) In-plane deflection of stack bond wall

The above figures show the opening of joints in the vertical direction. The non-linear behaviour of the stack bond wall is observed by initiation of cracks from the bottom and widen towards the upper part of the wall.

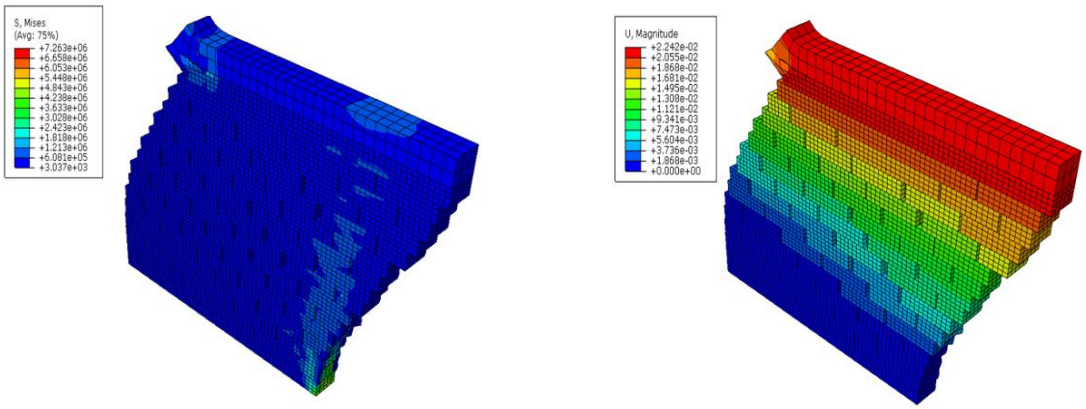

(a) **(b)**

Figure 13:(a) In-plane maximum Von-Mises stresses (S, Mises); (b) In-plane deflection of stretcher bond wall (scale factor= 20)

When compared with the stack bond, the stretcher bond wall has less deflection value. This brick pattern shows the diagonal cracking which is one of the expected modes of failure for walls that are subjected to in-plane loading. The tensile cracking leads to the diagonal stepped crack.

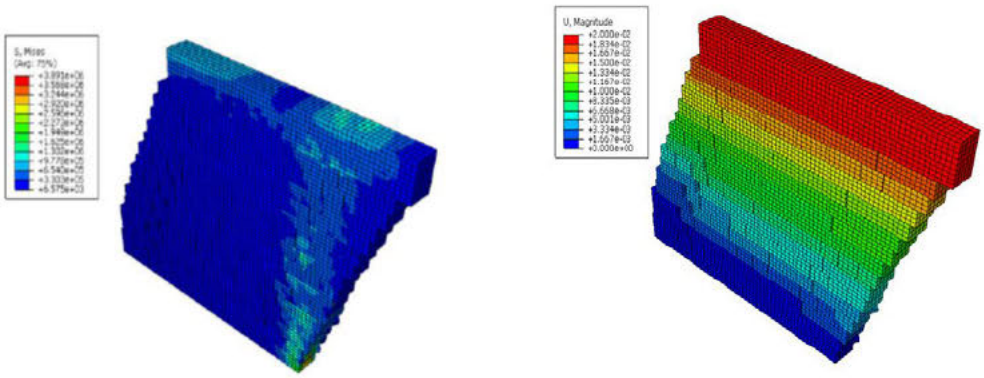

(a) **(b)**

Figure 14: (a) In-plane maximum Von-Mises stresses (S, Mises); (b) In-plane deflection of english bond wall (scale factor= 20)

The above results showed some similarity in terms of the mode of failure. Diagonal cracking in a form of staircase crack shape was observed on the English bond and Stretcher Bond. On the other hand, the stacker bond depicted de-attachment of joints in the vertical direction. All three walls depicted higher concentration of von-Mises stresses at the bottom corner of the wall. The comparison of wall's resistance is summarised on the graph below.

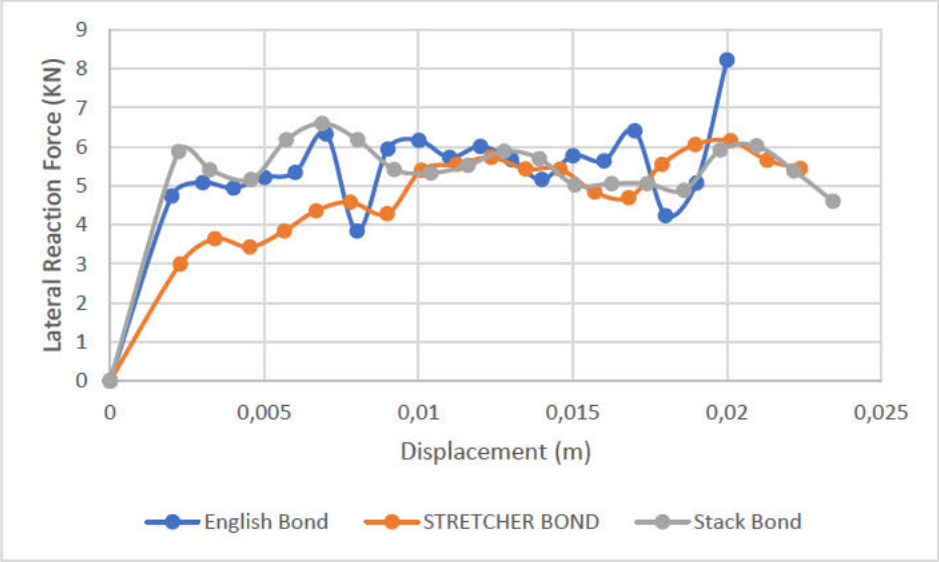

Figure 15: Comparison of resistance of wall against lateral displacement loading

From Figure 15, it can be observed that the English bond produced higher resisting forces when compared with the other two walls, mainly at the level of maximum displacements.

6.2 Out of Plane Results

This section discusses the results from the application of blast loading considering an explosive weight of 50kg TNT at a standoff distance of 20m. The results from the three different walls

are herein compared. The behaviour of the masonry wall in terms of Von-Mises stresses, defection concrete damage (tension and compression) is discussed in this section. The concrete damage plasticity model as discussed in section 3, was able to produce the compression and tensile damage of the wall.

6.2.1 English Bond

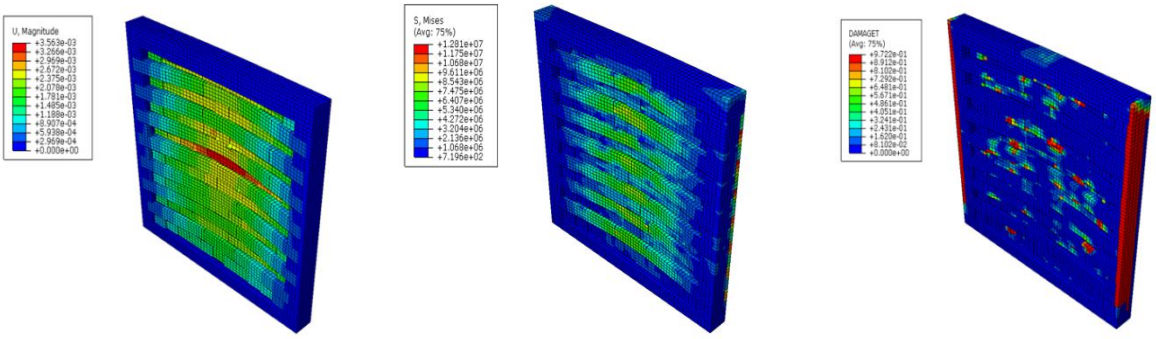

(a) **(b)** **(c)**

Figure 16: (a) Displacement of the wall at the end of the simulation (m), (b) Maximum Von-Mises stresses (S, Mises), (c) tensile damage variable distribution. (Scale factor = 30)

The English bond experiences minimal compression damage. Tension damage is observed under this bond type at the boundary positions and on some of the middle brick units. The deflection of the wall as expected is higher at the centre of the wall.

6.2.2. Stretcher Bond

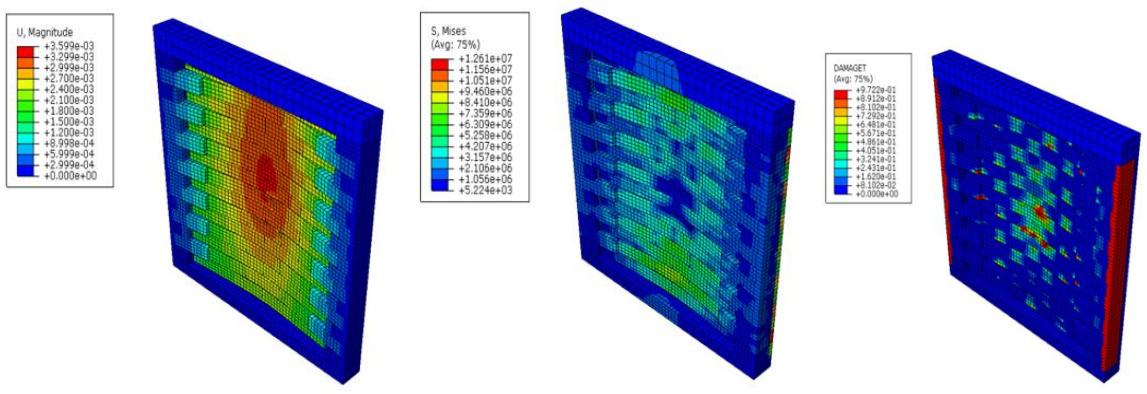

(a) **(b)** **(c)**

Figure 17: (a) Displacement of the wall at the end of the simulation (m), (b) Maximum Von-Mises stresses (S, Mises), (c) tensile damage variable distribution. (Scale factor = 30)

6.2.3. Stack Bond

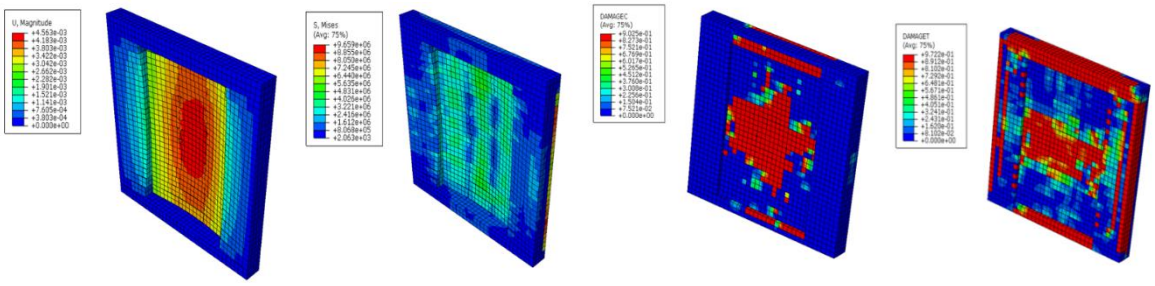

(a) **(b)** **(c)** **(d)**

Figure 18: (a) Displacement of the wall at the end of the simulation (m), (b) Maximum Von-Mises stresses (S, Mises) (c) compressive damage variable and (d) Maximum tension damage. (Scale factor = 30)

From an architectural point of view, stack bond can have a beautiful appearance, but it is typically seen to have a weaker binding pattern than other widely used bonds like English bond and stretcher bond. As can be seen in figure 18 (a), the first column/courses of bricks separate from the neighbouring bricks and it is worth noting that the vertical joints are easily prone to separation when subjected to lateral stresses, such as blast loads, which compromises structural integrity. Vertical cracking also happens. Stack bond masonry walls are vulnerable to vertical cracking at the vertical mortar joints because they lack horizontal support.

From the above results, it can be highlighted that the masonry head joint played a role in the out of plane response. It can be concluded that the English bond and stretcher bond have similar failure margins. The de-attachment of bricks in the vertical direction in the stack bond displayed a failure pattern that would be expected when there is a vertical expansion joint on the wall. Additionally, the location and magnitude of maximum von Mises stress amongst the three walls were within similar ranges and with all walls depicting maximum out of plane in the middle section of the wall.

From figure 18, it can be seen that the tension and compression damage for stack bond is much higher than the other two walls (stretcher bond and English bond). The displacement observed on the stack bond proves the importance of brick reinforcement in masonry wall.

The deflection of the three walls is summarized in figure 19 below, and as discussed above, the de-attachment of bricks (second column) from the fixed sides initiated a much higher relative displacement on the stack bond when compared with the other two walls.

The comparison below shows that the stack bond has slightly higher out of plane displacement when compared to the other two bonding patterns. In practice, the bedding reinforcement in the case of stack bond is crucial when used a structural/load bearing wall. The deformation due to blast load occurs within a short duration of time as can be observed in figure 19.

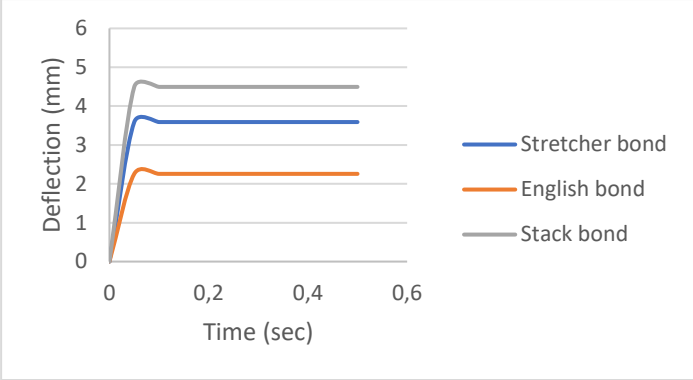

Figure 19: Deflection vs time for blast weight of 50kg TNT

7. Conclusions

This study concluded that there is a slight difference in the peak displacement at the centre of the wall for the English and stretcher bond. Under these two bonding patterns, when the blast load is lower it results in a lower wall centre displacement. The stack bond on the under hand displayed higher deflection values under both in plane and out-of-plane loading. The research results in this paper highlighted that the stack bond arrangement has the vertical joints are easily prone to separation when subjected to lateral stresses, such as blast loads, which compromises structural integrity. Also, Stack bond masonry walls are susceptible to vertical cracking at the vertical mortar joints because they lack horizontal support. The different brick patterns play a role in the blast resistance of the wall. This research work was able to highlight the importance of understanding the effect of different bonding patterns for structural walls.

Author Contributions: Conceptualization, S.G.T.; methodology, S.G.T.; formal analysis, S.G.T.; investigation, S.G.T. and G.A.D.; resources, G.A.D.; data curation, S.G.T..; writing—original draft preparation, S.G.T.; writing—review and editing, S.G.T., G.A.D., S.M.M and G.E.S.; visualization, S.G.T.; supervision, G.A.D. and G.E.S..; project administration, G.A.D. All authors have read and agreed to the published version of the manuscript."

Funding: This research received no external funding.

Data Availability Statement: Not applicable

Conflicts of Interest: The authors declare no conflict of interest.

References

1. Debnath, P.; Dutta S.C.; Mandal, P. Lateral behaviour of masonry walls with different types of brick bonds, aspect ratio and strengthening measures by polypropylene bands and wire mesh, *Structures Volume 49, March 2023, Pages 623-639*, **2023**, https://doi.org/10.1016/j.istruc.2023.01.155

2. Shrestha, J.K.; Pradhan, S.; Gautam, D. In-plane behaviour of various brick bonds in masonry walls, *Innovative Infrastructure Solutions* (2020) 5:58, **2020**, https://doi.org/10.1007/s41062-020-00306-x,

3. Bacigalupo,A .; Cavicchi,A.; Gambarotta,L. A simplified evaluation of the influence of the bond pattern on the brickwork limit strength, Advanced Materials Research Vols. 368-373 ,**2012**,pp 3495-3508, Trans Tech Publications, Switzerland doi:10.4028/www.scientific.net/AMR.368-373.3495 available at www.scientific.net, date accessed May 2023

4. Shah, S.A.R.; Arshad, H.; Farhan, M.; Raza, S.S.; Khan, M.M.; Imtiaz, S.; Gullnaz, S.; Qurashi, M.A.; Wassem, M. Sustainable Brick Masonry Bond Design and Analysis: An Application of a Decision-Making Technique, *Appl. Sci.* **2019**, 9, 4313; doi:10.3390/app9204313

5. Thango, S.G.; Stavroulakis, G.E.; Drosopoulos, G.A. Investigation of the Failure Response of Masonry Walls

Subjected to Blast Loading Using Nonlinear Finite Element Analysis. *Computation* **2023**, 11, 165. https://doi.org/10.3390/computation11080165

6. Elmenshawi, A.; Duchesne, D.; Paquette, J.; Mufti, A.; Jaeger, L.; Shrive, N. Elastic moduli of stone masonry based on static and dynamic tests. **2011.** Paper presented at the 11th NAMC, Minneapolis, USA.

7. D'Altri, A.M.; Miranda, S.; Castellazzi, G.; Sarhosis, V.A 3D Detailed Micro-Modelling Approach for the In-Plane and Out-Of-Plane Analysis of Masonry Structures, *Computers & Structures*. **2018,** 206: 18-30. https://doi.org/10.1016/j.compstruc.2018.06.007
8. Pasquantonio, R. D.; Parsekian, A.; Fonsecan, S; Shrive, G. Experimental and numerical characterization of the interface between concrete masonry block and mortar. 13(3): **2020**, 578-592. https://doi.org/10.1590/S1983-41952020000300008
9. Stankowski, T.; Runesson, K.; Sture, S. Fracture and Slip of Interfaces in Cementitious Composites Characteristics. **1993**, 119(2): 292-314. https://doi.org/10.1061/(ASCE)0733-9399(1993)119:2(292)

10. Weyler, R.; Oliver, J.; Sain, T; Cante, J. On the Contact Domain Method: A Comparison of Penalty and Lagrange Multiplier Implementations, **2012**, *Computer Methods in Applied Mechanics and Engineering*, vol. 205–208, p. 68–82.
11. Miranda Dias, J. L. Cracking due to shear in masonry mortar joints and around the interface between masonry walls and reinforced concrete beams. **2007**, *In Construction and Building Materials* (Vol. 21, Issue 2, pp. 446–457). Elsevier BV. https://doi.org/10.1016/j.conbuildmat.2005.07.016
12. Ngo, T.; Mendis, P.; Gupta, A.; Ramsay, J. Blast loading and blast effects on structures, An overview. *Electron J Struct Eng*, 7, 76–91. **2007**

13. Unified Facilities Criteria "UFC 3-340-02 Structures to Resist the Effects of Accidental Explosions", U.S. Army Corps of Engineers, Naval Facilities Engineering Command, Air Force Civil Engineer Support Agency. **2008**, available online https://www.wbdg.org/ffc/dod/unified-facilities-criteria-ufc/ufc-3-340-02, date accessed 01 May 2023
14. Lourenço, P.B Computational strategies for masonry Structures. **1996**, Doctoral thesis, Delft University of Technology, Delft University Press,

15. Lourenço, P. B. Computations on historic masonry structures. *Progress in Structural Engineering and Materials*, **2002**. 4, 301-319.
16. Lourenço.; Rots, J.G.; Blaauwendraad, J . Two Approaches for the Analysis of Masonry Structures: Micro and Macro-Modelling, Heron. **1995**, 40(4): 313-338. ISSN 0046-7316
17. Braimah, B, Blast load effects on historic masonry buildings, *Technical report*, Infrastructure Protection and International Security Department of Civil and Environmental Engineering Carleton University, **2013.**
18. Kömürcü, S.; Gedikli, A. Macro and Micro Modelling of the Unreinforced Masonry Shear Walls, *European Journal of Engineering and Natural Sciences*. **2019**, 3(2): 116-123. https://dergipark.org.tr/en/pub/ejens/issue/49410/369461
19. Drosopoulos, G.A.; Stavroulakis, G.E. A computational homogenization approach for the study of localization of masonry structures using the XFEM. Arch Appl Mech Vol. 88, **2018**, pp. 2135–2152. https://doi.org/10.1007/s00419-018-1440-4

20. Daniel, J.; Dubey, R. Finite Element Simulation of Earthquake Resistant Brick Masonry Building Under Shock Loading. Adv. Struct. Eng. **2014**, 81, 1027–1038. https://doi.org/10.12989/csm.2015.4.1.019
21. Lubliner, J.; Oliver, J.; Oller, S.; Oñate, E. A plastic-damage model for concrete", International Journal of Solids and Structures. **1989,** 25: 299-329. https://doi.org/10.1016/0020-7683(89)90050-4

22. Lee, J.; Fenves, G.L. Plastic-Damage Model for Cyclic Loading of Concrete Structures. Journal of Engineering Mechanics, **1998,** 124 (8): 892–900, , DOI: 1008 https://doi.org/10.1061/(ASCE)0733-9399(1998)124:8(892)
23. Lee, J. Theory and implementation of plastic-damage model for concrete structures under cyclic and dynamic loading.**1996**, PhD Dissertation. Berkeley, California, USA: University of California
24. Alhadid, M.M.A.; Soliman, A.M.; Nehdi, M.L.; Youssef, M.A. Critical overview of blast resistance of different concrete types, Magazine of Concrete Research, **2013**, 65(1), 1–10 http://dx.doi.org/10.1680/macr.13.00096

25. ABAQUS v. 6.14.2 User's Manual. Available online: http://130.149.89.49:2080/v2016/index.html (accessed on 7 May 2023).

26. Iuorio, O.; Dauda, J.A. Retrofitting Masonry Walls against Out-Of-Plane Loading with Timber Based Panels, *Appl. Sci*. **2021**, 11, 5443. https://doi.org/10.3390/ app11125443
27. Chaimoon, K, Numerical simulation of fracture in unreinforced masonry,**2007**, *PhD thesis*, School of Civil and Environmental Engineering, The University of New South Wales, Syndey, Australia, https://doi.org/10.26190/unsworks/17488
28. Vermeltfoort, A. T., Raijmakers, T., & Janssen, H. J. M, Shear tests on masonry walls, 6th North American Masonry Conference, 6-9 June 1993, Philadelphia, Pennsylvania, USA, **1993** (pp. 1183-1193). Technomic Publ. Co.
29. Milani, G.; Lourenço, P.B.; Tralli, A, homogenized rigid-plastic model for masonry walls subjected to impact, *Int. J. Sol. Struct*. Vol. 46(22-23), **2009**, pp. 4133-4149
30. Zhang, Y.; Hu, J.; Zhao, W.; Hu, F.; Yu, X. Numerical Study on the Dynamic Behaviours of Masonry Wall under Far-Range Explosions. *Buildings*, **2023**, 13, 443. https:// doi.org/10.3390/buildings13020443
31. Hao, D. Numerical Modelling of Masonry Wall Response to Blast Loads, *Australian Journal of Structural Engineering*. **2009** ,10(1):37-52. https://doi: 10.1080/13287982.2009.1146503

Chapter 6 - Prediction of the response of masonry walls under blast loading using Artificial Neural Networks

This chapter presents the research paper that developed machine learning models to predict the displacement and damage outputs of masonry walls exposed to blast loading using two input variables, namely, the blast weight and the standoff distance. The previous two chapters provided the numerical analysis of masonry walls against blast actions, however it was observed that using a commercial software to analyse the wall is time consuming/computational expensive. The need to provide machine learning methods for a fast-accurate prediction of the masonry wall response is achieved in this chapter as one of the innovations of this research.

This chapter is presented in the format of the published article.

To cite this article:

Thango, S.G., Drosopoulos, G.A., Motsa, M.M and Stavroulakis, G.E (2024). Prediction of the response of masonry walls under blast loading using Artificial Neural Networks. *Infrastructures,* 9, 5. https://doi.org/10.3390/infrastructures9010005

infrastructures

MDPI

Article

Prediction of the Response of Masonry Walls under Blast Loading Using Artificial Neural Networks

Sipho G. Thango [1], Georgios A. Drosopoulos [1,2,*], Siphesihle M. Motsa [1] and Georgios E. Stavroulakis [3]

[1] Discipline of Civil Engineering, University of KwaZulu Natal, Durban 4041, South Africa; 209523102@stu.ukzn.ac.za (S.G.T.); motsampho@gmail.com (S.M.M.)
[2] Discipline of Civil Engineering, University of Central Lancashire, Preston PR1 2HE, UK
[3] School of Production Engineering & Management, Technical University of Crete, 73100 Chania, Crete, Greece; gestavroulakis@tuc.gr
* Correspondence: gdrosopoulos@uclan.ac.uk

Abstract: A methodology to predict key aspects of the structural response of masonry walls under blast loading using artificial neural networks (ANN) is presented in this paper. The failure patterns of masonry walls due to in and out-of-plane loading are complex due to the potential opening and sliding of the mortar joint interfaces between the masonry stones. To capture this response, advanced computational models can be developed requiring a significant amount of resources and computational effort. The article uses an advanced non-linear finite element model to capture the failure response of masonry walls under blast loads, introducing unilateral contact-friction laws between stones and damage mechanics laws for the stones. Parametric finite simulations are automatically conducted using commercial finite element software linked with MATLAB R2019a and Python. A dataset is then created and used to train an artificial neural network. The trained neural network is able to predict the out-of-plane response of the masonry wall for random properties of the blast load (standoff distance and weight). The results indicate that the accuracy of the proposed framework is satisfactory. A comparison of the computational time needed for a single finite element simulation and for a prediction of the out-of-plane response of the wall by the trained neural network highlights the benefits of the proposed machine learning approach in terms of computational time and resources. Therefore, the proposed approach can be used to substitute time consuming explicit dynamic finite element simulations and used as a reliable tool in the fast prediction of the masonry response under blast actions.

Keywords: blast; masonry; in-plane deflection; out-of-plane deflection; explicit dynamic non-linear finite element analysis; machine learning; artificial neural network

Citation: Thango, S.G.; Drosopoulos, G.A.; Motsa, S.M.; Stavroulakis, G.E. Prediction of the Response of Masonry Walls under Blast Loading Using Artificial Neural Networks. *Infrastructures* **2024**, *9*, 5. https://doi.org/10.3390/infrastructures9010005

Academic Editor: Daniel V. Oliveira

Received: 17 November 2023
Revised: 11 December 2023
Accepted: 21 December 2023
Published: 25 December 2023

1. Introduction

Masonry is commonly used in the construction of non-structural and structural walls in residential and commercial buildings in developing and developed countries. The behavior of masonry walls when subjected to in-plane and out-of-plane actions has been investigated for the past decades. Blast loading may lead to the collapse of such buildings. Researchers such as Hao [1], Davidson et al. [2], Knock et al. [3], and Masi et al. [4] conducted laboratory and field blast tests to develop empirical relations of masonry wall damage and blast loading conditions. There is, however, limited data on field tests for walls subjected to blast loading and that is mainly due to safety and cost considerations. Numeral analysis of walls has then become popular and has been proven to provide reliable results. According to Hao [1], the numerical approach generally simplifies the masonry wall to a single degree-of-freedom (SDOF), and from this simplification the wall's response under blast loading is calculated by investigating the dynamic responses of the SDOF system. The model's definition is said to influence the computational time each model will take to generate the set of results. In their study, Dorn et al. [5] were able to reduce the

computational time and computer memory by assuming the bricks to be rigid and only subjecting the mortar to failure.

As part of the ongoing effort of reducing the computational cost, Pande et al. [6] and Pietruszczak et al. [7] derived the corresponding elastic moduli for brick masonry from the elastic properties of individual components and assumed the masonry material as an orthotropic elastic-brittle material. Research on numerical modelling of masonry under dynamic excitations or blast loading, also integrating micro- and macro-modelling approaches, has garnered increasing interest in recent years. The motivation for this study emanates from the international drive to better understand the behavior of masonry walls under out-of-plane and in-plane loading, in the context of data-driven mechanics. Therefore, the main goal of this paper is to extend existing knowledge by introducing machine learning techniques in predicting the response of masonry walls under different blast loading and standoff distances.

First, parametric explicit dynamic simulations are conducted for a masonry wall, adopting varying blast weight and stand-off distances. The out-of-plane deflection is used as output in the generated dataset. The wall is simulated within non-linear finite element analysis. Unilateral contact and friction laws are introduced to capture discrete damage (opening-sliding) in the interfaces between masonry blocks. A concrete damage plasticity model is also used to capture tensile and compressive damage to the bricks. Explicit dynamic simulations are done using commercial finite element software.

To run and automatically control the parametric finite element simulations, MATLAB R2019a and Python scripts are developed. Once the datasets are developed, ANNs are used to train and test the data. The error is recorded, and tests to random input values are conducted to highlight the efficiency of the method.

The paper is structured as follows: In Section 2 of this article, the relevant literature review is presented. In Section 3.1, failure modes of masonry walls are provided and modeling approaches that can be used to capture these modes are briefly discussed. This part includes, among others, information on the geometry of the walls, the material constitutive description, and details of the blast load simulation. In Section 3.2, the blast wave propagation is discussed. Sections 3.3 and 3.4 provide an overview of artificial neural networks and the architecture of the adopted network. Sections 3.5 and 3.6 detail the adopted methodology and the finite element models which are used for the development of the dataset. In Section 3.7, the details of the finite element model are presented. In Sections 3.8 and 3.9, the contact mechanics and the wall's response are provided. In Sections 4 and 5, results and discussions derived from the proposed network are provided. Lastly, in Section 6, the conclusions of this investigation are presented.

2. Literature Review

Literature findings on the topic of blast actions on masonry walls are discussed in this section. Su et al. [8] performed a numerical investigation of unreinforced masonry walls subjected to blast loads. In their study, a distinctive model, in which mortar and brick units of masonry are discretized individually was used to model the performance of masonry and the contact between the masonry. On the other hand, Ishfaq et al. [9] numerically studied the out-of-plane behavior of confined dry-stacked masonry walls under blast loading. Their study considered four different test cases using a charge weight of 4 k, 8 kg, 12 kg, and 19 kg of Wabox explosive.

Masi et al. [4] investigated the dynamic behavior of non-standard curvilinear masonry geometries under blast loading using the discrete element method. This approach allowed the consideration of detailed mechanical and geometrical properties of masonry. One of the important findings from their study was that masonry joints with zero dilatancy result in greater out-of-plane deformations and decreased membrane deformations. Additionally, it was discovered that cohesion and tensile strength have very little bearing on the structural reaction. Investigating the effect of material properties on the blast response of walls is of utmost importance. Anas et al. [10] conducted an experimental study on clay-brick

and concrete block unreinforced walls. Their study highlighted that the effect of brick strength and mortar had an insignificant role to play on the maximum mid-span deflection under reflected pressures that are above 2 MPa. The same study concluded that increasing the Young's modulus of masonry is an effective way of reducing the maximum mid-span deflection.

A study by Zhang et al. [11] investigated the dynamic behavior of a clay-brick masonry wall under a blast weight of 21.5 kg TNT at 4.0 m standoff and 50.8 kg TNT at 5.5 m standoff. According to the study findings presented in this paper, the thickness of the wall and its boundary connection with the frame have a major impact on how blast resistance is developed. This study further concluded that the reaction and damage pattern of walls exposed to medium- and far-range explosions are significantly influenced by the wall's boundary constraints, length, breadth, thickness, and other dimensional parameters.

Similarly, Thango et al. [12] investigated the failure response of masonry walls subjected to blast loading using nonlinear finite element analysis. This investigation aimed in highlighting potential collapse mechanisms by testing different blast load parameters, namely, the weight of the explosive and the standoff distance between the source of the explosion and the structure. Explosive weights of 100 kg TNT, 200 kg TNT and 1150 kg TNT were considered with the varying standoff distances which included distances such as 20 m, 50 m, and 100 m. Additionally, Thango et al. [12], investigated the influence of an opening (window) on the wall and the results highlighted that the present of an opening may reduce the effect of the blast action by decreasing the out-of-plane response of the structure.

Recently, the rapid advances in data processing techniques and the emergence of different artificial intelligence approaches have led to the development of different applications for masonry walls. According to Jasmine et al. [13] and Thai [14], Machine Learning (ML) is a major subfield of artificial intelligence (AI) that deals with the study, design, and development of algorithms that can learn from the data itself and make predictions using the learned data. Additionally, machine learning methods use programmed algorithms to optimize a performance standard based on previously accumulated data [15]. There are different types of machine learning algorithms, which have been adopted in applications related to structural engineering, such as Artificial Neural Networks (ANN), Support Vector Machines, Nearest Neighbors and Random Forests. These methods can deal with a significant large amount of data. Data for such studies is acquired in situ or using numerical models.

Friaa et al. [16] used ANNs to predict the elastic membrane and bending constants of the equivalent Love–Kirchhoff plate of hollow concrete blocks masonry wall. Drosopoulos and Stavroulakis [17] used the ML approach in multi-scale computational homogenization to obtain the masonry wall's non-linear response. In Cascardi et al. [18] an analytical model for predicting the shear strength of Fiber Reinforced Mortars (FRM) masonry by using the ANN approach is proposed and proven to be able to predict the shear strength of the FRM walls.

Zhang et al. [19] adopted ANN techniques to predict the cracking patterns of masonry wallets that are subjected to vertical loading. Also, studies by Zhou et al. [20] aimed to use ANN to predict the failure of a wall panel subjected to lateral loading using laboratory data. In the study conducted by Plevris and Asteris [21], ANN was applied to approximate the failure surface of a brittle anisotropic material. In their study, the ANN was trained using the available experimental data.

Chomacki et al. [22] used ML methods to predict the damage of the residential houses that are exposed to the industrial environment of mines. In their study, four machine learning methods were considered, namely, the Probabilistic Neural Network, Support Vector Machine, Naive Bayes Classification and Bayesian Belief Network. Amongst the four methods, it was highlighted that the selection of the Bayesian Belief Network was the most effective approach. This raised the importance of ML methods for efficient structural or damage assessments and design activities.

In the study conducted by Remennikov et al. [23], an ANN was used to predict the effectiveness of blast wall barriers. Experimental data sets for a wide range of scaled wall heights and a large area of scaled space behind the wall were adopted to train and validate the ANN. A total of 285 measurements were used in their study and the cross-validation techniques were adopted in which the training set was employed to decide the connection weight, whereas the validation set was used to evaluate the performance of the model. This study highlighted the feasibility of using ANN for fast prediction of barrier wall's response against blast loading.

Bewick et al. [24] developed a neural-network model-based engineering tool to estimate the peak pressure, impulse, time of arrival, and time of duration of blast loads on buildings protected by simple barriers. Their study used 91 experimental datasets in which 81 simulations were used to train the network and the other 10 simulations were used to verify and validate the accuracy of the network. It was highlighted that due to the dispersion of the available training data, the model had a constrained range of application even though it demonstrated strong correlation with the data. This study showed the development of an ANN methodology for a range of values for the variables of charge weight, charge to barrier standoff, barrier to structure standoff, barrier height, and location on the structure face as well as roof loads. This work also highlighted that given sufficient data and training, neural networks can provide efficient solutions to nonlinear problems to any degree of accuracy.

A study conducted by Huang et al. [25] used a dataset of 76 explosion observations to develop a machine learning model that will be able to predict the damage scale of buildings subjected to a fertilizer plant explosion. This study evaluated three machine learning models which included k-Nearest Neighbour, ANN, and gradient boosting (a sub technique of decision trees). The input parameters in this study included the building category, building structure, wall surface material, distance from the blast centre, year built, and the shockwave overpressure. It was concluded that the gradient boosting and the ANN models offered better prediction accuracy. The importance of ML models was highlighted in this work as being a tool that can assist government decision makers, architects, and engineers in selecting the most resilient structure design and material for buildings.

Salem et al. [26] used 100 experimental data for blast performance of a masonry wall. In their study, four different ML models were tested and assessed. The models were developed using linear, polynomial, and random forest regressions, and an artificial neural network. Comparing the different models, it was concluded that the artificial neural network was the most reliable model. This study highlighted the ANN's ability to generate the blast curves (P-I curves) faster than traditional methods. The P-I diagram produced is thought to be a quicker and less expensive method for further resilience evaluations.

Khaleghi et al. [27] utilized the ANN to examine how unreinforced masonry walls responded to in-plane loading. This study examined how a wall's reduced ability to support weight may result in structural deterioration. A number of 49 different configurations were considered and a set of designed experiments were used to generate numerical simulations for dataset creation. The ability of ANNs to precisely forecast the initial stiffness and loss in load capacity resulting from unreinforced masonry wall piercing was determined by this study. The peak load and initial stiffness were used as the inputs of the ANN.

Existing prediction techniques, such as numerical methods, call for a solid foundation in computer modeling, as well as a significant investment in time and resources. Similarly, analytical models are dependent on assumptions based on the complex pattern of the structural configuration. The ability to predict damage patterns has recently made data-driven approaches more popular. Comparative studies have been done to evaluate the accuracy of machine learning approaches. The study conducted by Chopra et al. [28] proved that neural networks had the highest predictive accuracy.

Various researchers have developed ANN models to predict masonry wall response mainly considering in-plane actions. The behaviour of masonry has been numerically and experimentally studied by many researchers but to the authors' best knowledge there

have not been many attempts to apply ML techniques for the prediction of masonry response under blast loading. Thus, although studies highlighting conventional, finite element analysis solutions on masonry response against blast actions can be found on literature, it seems that less studies are identified, introducing machine learning techniques to investigate blast actions. This article aims to contribute to this area by proposing a machine learning formulation that can be adopted to predict fast and accurately the response of masonry walls under blast actions.

3. Material and Methods

3.1. Failure Mechanisms of Masonry

Typically, load-bearing masonry wall panels exposed to in-plane lateral and vertical loads will exhibit either flexural or shear behavior, each with a distinct set of related failure mechanisms. Figure 1 below depicts the failure modes for walls that are subjected to in-plane loading.

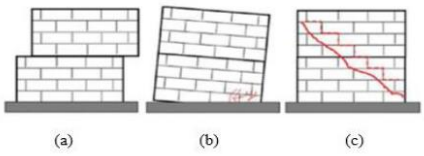

Figure 1. Typical in-plane failure modes of masonry walls: (**a**) sliding shear failure; (**b**) rocking; and (**c**) diagonal cracking [29].

Due to the residual tensile strength of the brickwork material, the behavior caused by an out-of-plane stress, such as an explosion, shares some similarities with flexural behavior [29]. Walls that are subjected to out-of-plane loading such as blast loading, will often have the orientation of the internal stresses within the wall and the resulting crack pattern developed is dictated by the boundary conditions or the position of its supported edges. Figure 2 shows the various types of wall support shapes and the associated out-of-plane flexure cracking patterns.

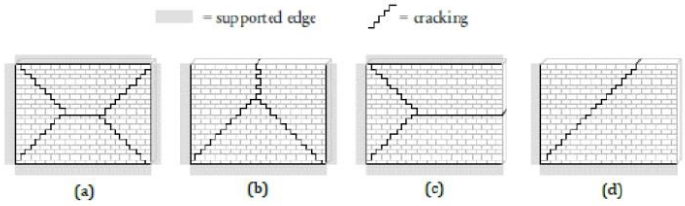

Figure 2. Typical cracking patterns for out-of-plane loaded two-way spanning walls with (**a**) O-shaped, (**b**) U-shaped, (**c**) C-shaped, and (**d**) L-shaped supports [30].

3.2. Wave Propagation

In a blast, wave propagation describes how energy from an explosion spreads out and impacts nearby structures. Mining activities that entail blasting have been considered as case study for this paper. When an explosion happens, a shock wave is produced that travels through the air quickly, causing a significant rise in pressure and temperature [31]. Various researchers have argued that a shock wave can cause significant damage to buildings, especially if they are near the blast.

According to Baumgart [32], the strength and direction of the shock wave depend on various factors, including the size and type of the explosive device, the distance between the explosion and the building, and the near terrain. When designing buildings for blast resistance, it is important to consider how the shock wave will propagate through the

structure, and to design walls, floors, and roofs that can withstand the pressure and forces generated by the blast. Low-cost rural houses are unlikely to have its design or construction taking into account such loading. Figure 3 depicts the typical blast wave propagation curve.

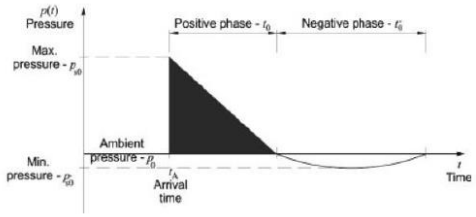

Figure 3. Typical blast wave propagation curve [33].

When a shock wave hits a structure, reflection occurs, which is described by the reflection coefficient c_r:

$$C_r = \frac{p_{ref}}{p_{inc}}. \quad (1)$$

where p_{ref} is the reflected pressure and p_{inc} the incident pressure, respectively. Understanding the wave propagation curve is critical in analysing the blast loading on structures. To determine the magnitude of peak overpressure, two major factors are utilized: the charge weight and the standoff distance.

3.3. An Overview of Neural Network

Artificial Neural Network (ANN) is a machine learning technique composed of a system of interconnected neurons [14,34]. ANN is built on a collection of connected nodes known as artificial neurons, which are basically the prototypical neurons found in the genetic animal brain. Furthermore, using learning algorithms, the interconnected nodes can have the ability to recognize the hidden patterns and correlations in the given raw data and can even cluster and classify it over some time through the learning process [35].

The networks consist of neurons which are basic units in this operating system. Each artificial neuron, or node, is connected to others and has a corresponding weight and threshold. The development process of the model includes data collection and training the data set. Training data is used by neural networks to develop their accuracy over time. Since many of the links between inputs and outputs in real life are non-linear and complex, it is crucial that ANNs be able to learn and represent non-linear and complex interactions, hence the training and aiming of high accuracy levels of output received.

According to Asteris et al. [36], ANNs are information-processing models arranged for a specific application through a training process. Once the network is well trained, a specific output is obtained from specified input data. The common advantage of ANN is that it can learn from experience, so that it is possible to train the network to recognise certain patterns to improve its performance or better understand or predict the modes of failure in structures.

There are different types of neural networks. They are often classified depending on their structure, data flow, neurons used and their density, layers, and their depth activation filters. These types include Convolutional Neural Network, Multilayer Perceptron, Radial Basis Functional Neural Network, Feedforward Neural Network, and Modular Neural Network.

3.4. The Architecture of an Artificial Neural Network

In this paper, the feedforward backpropagation neural network developed in MATLAB R2019a is used. The feedforward ANN's structure has three forms of layers, namely input, hidden, and output layers. They are mostly used in pattern generation, pattern recognition, and classification. A feedforward neural network has the capability to correlate vector

inputs with vector outputs, provided that the parameters involved have been suitably calculated [37]. Predictions are formed during the feedforward phase of an ANN based on the values in the input nodes and the weights. This is relevant to this study, where the out of plane deflection of the masonry wall is intended to be recognised or predicted by the trained ANN. Figures 4 and 5 show a typical ANN and its layers.

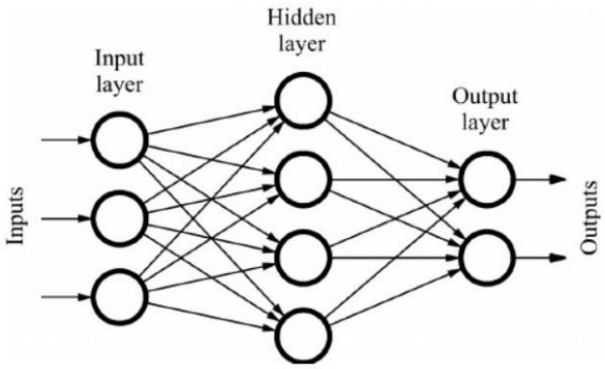

Figure 4. Feedforward ANN design architecture.

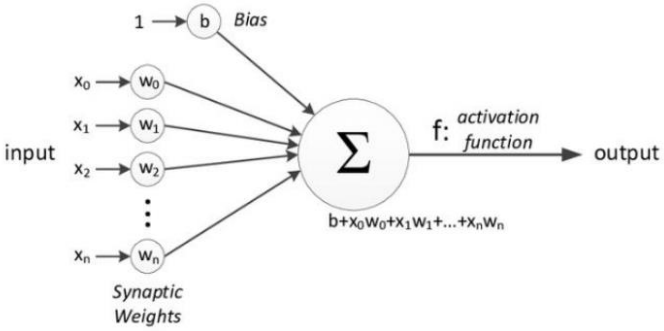

Figure 5. Input-to-output operations at each perceptron layer.

As shown in Figure 5, the neurons are connected by synapses, and the signals travel in one way, i.e., from input to output only in the Feedforward Neural Network. In this ANN type, there is no feedback or loops, and the output of any layer does not affect that same layer in such networks.

According to Liu [38] the neural network can be single-layer or multilayer, although after training, a neural network with a single hidden layer and a single output node can approximate nearly any functional relationship. This paper adopted a single hidden layer neural network due to few input and output parameters. The number of hidden-layer neurons affects the calculation accuracy as well as the learning efficiency. The choice on the number of hidden-layer neurons also considered the crucial observation made by Qi [39], where fewer hidden-layer neurons lead to underfitting, while several hidden-layers lead to the reduction of learning efficiency and results in an overfitting issue.

The ANN model consists of three layers, namely, the input layer, hidden layer, and output layer. The input layer accepts inputs in a variety of programming-provided forms, while the hidden layer, which is commonly known as the secreted-up layer, is positioned in between the input and output layers. In this framework, the ANN model performs all

the calculations to discover covered up highlights and designs. Lastly, the output layer contains the final values from the input that has gone through an arrangement of changes utilizing the hidden layer, which at last comes about in a yield that is passed on utilizing this layer.

Following the above definition of layers, ANN takes the input and computes the weighted sum of the inputs and includes a bias. This computation is represented in the form of a transfer function.

A single layer in a feedforward neural network can be described using Equation (2) below:

$$y_i = f_{(i)}\left(W_{(i)} \cdot y_{(i-1)} + b_{(i)}\right), i = 1, 2 \ldots\ldots, n_{layers} \quad (2)$$

where y is the output vector of the ith layer, W and b are weight and bias vectors, and f is the activation function. Adopting the supervised learning method, the error function may be determined using the mean squared error defined as given by the Equation (3) below:

$$MSE = \frac{1}{n}\sum_{j=1}^{n}\left(Y_j - {Y^*}_j\right)^2 \quad (3)$$

where n is the number of output nodes, Y is the network output, and Y^* is the actual expected value.

The performance of the ANN is further evaluated using the correlation coefficient (R). The R-value is calculated using Equation (4) below:

$$R = \frac{\sum_{i=1}^{n}(m_i - \overline{m})(p_i - \overline{p})}{\sqrt{\sum_{i=1}^{n}(m_i - \overline{m})^2 \sum_{i=1}^{n}(p_i - \overline{p})^2}} \quad (4)$$

where m_i represents experimental or numerical data values, p_i represents predicted values, n is the number of samples, and $\overline{m}$ and $\overline{p}$ are the mean values of m and p, respectively.

3.5. Adopted Methodology

In the present study, numerically generated data from commercial finite element software was used. This data consisted of 95 numerical simulations/samples. The data comprised of input parameters, namely, standoff distance, and blast weight/charge. The output parameter is the out-of-plane displacement at the centre of the wall. This study utilised a multi-layered feed-forward neural network to examine data that was generated numerically and a Python script to modify the input variables without opening the finite element software. Using the MATLAB R2019a/SIMULINK tool, a neural network model was developed.

The stage of data gathering and processing entails transforming the chosen data into a comprehensible format so that the machine learning analysis may quickly access and use the data. This involves formatting, cleaning, and sampling the data. Considering the standoff distance, the authors concluded that standoff distances that were greater than 100 m had less damage on the wall though some in-plane failure was noticed. The dataset therefore focused mainly on parameters that had significant in-plane and out-of-plane response. The datasets were classified into three categories: learning, verification, and evaluation. Splitting of data was such that the learning sample comprised 80% of the dataset, and 20% used for verification and evaluation. The dataset consisted of simulations using blast weights ranging from 100 kg TNT to 1700 kg TNT with varying standoff distances. The flowchart of the artificial neural network is shown in Figure 6 below.

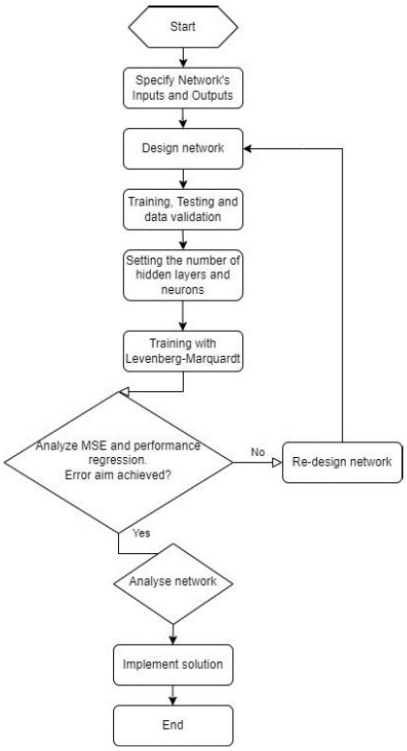

Figure 6. Flowchart of the adopted methodology.

Table 1 lists the network parameters for the proposed model. Ten hidden layer neurons and one output neuron make up the network. The training function adopted in the training network is the Levenberg–Marquardt backpropagation (TRAINLM).

Table 1. Neural network parameters.

Network	Hidden Layer	Hidden Neurons	Output Nodes	Training Function	Learning Function
Feed Forward	1	10	1	Trainlm	Tansig-Purelin

3.6. Finite Element Model for Data Simulation

This study adopted the approach of simplified micro modelling, which did not model the mortar thickness (zero thickness is assumed). Instead, the contact law adopted replicated the effect of mortar between the bricks. The masonry units are represented by continuum elements, while between masonry units normal and tangential contact surfaces are introduced to represent the mortar layer. Using commercial finite element software, the interface between the blocks was defined as surface-to-surface contact with zero tensile resistance. Since the tensile strength of the mortar is very low, this is an appropriate assumption as indicated also by a number of studies [12]. The dimensions of each masonry unit considered in this paper are 390 mm × 140 mm × 190 mm. This solid structural concrete masonry unit size is commonly used in low-cost housing. Figure 7 below shows the dimensions of the wall. It is noted that the numerical model used in this article to

generate the dataset, that will then be used to train the artificial neural network, has been validated in [12], by comparing the results of this model with the literature.

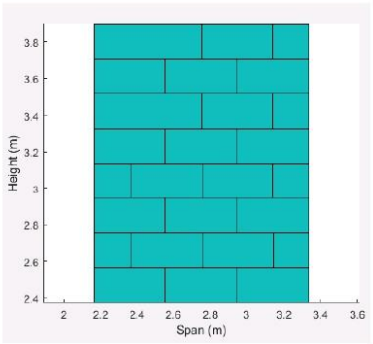

Figure 7. MATLAB plot of the vertices that make up the wall.

3.7. Details of the Finite Element Model

Figure 8 below shows the mesh which was adopted in the finite element model. Three-dimensional, eight-node linear brick elements were used, with the element side equal to 40 mm. A total number of 4800 elements was used for the model.

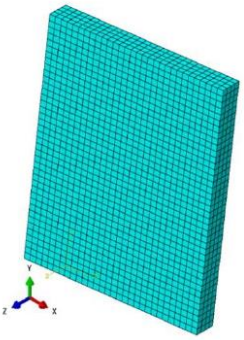

Figure 8. Mesh of the considered masonry walls.

The boundary conditions of the wall were fixed in three translational degrees of freedom, according to the coordinate system shown in Figure 8. Thango et al. [12] in their study assumed the restraining effect on the top side of the walls in the Z direction as attributed to the assumption that an upper slab or roof will provide the restraint in that direction. A similar assumption was adopted for this study.

The loading of the model was applied in two load steps. In an initial, pre-existing step a vertical pressure of 0.25 MPa is applied to the top side of the structure. In the first load step, a horizontal shear (in-plane) displacement of 10 mm is applied to the top side of the walls. In the second load step, the blast loading is applied.

3.8. Contact Mechanics and Material Properties

Material models were developed to examine the structural behavior of the unreinforced masonry wall. The Concrete Damage Plasticity (CDP) law was used for the analysis to capture damage occurring in the material. CDP is a constitutive model used to simulate the failure behaviour of concrete under loading and unloading conditions.

Figure 9 below shows the compressive and tensile stress–strain curves that were used in this study to define the compressive and tensile failure response of the masonry units on the numerical models.

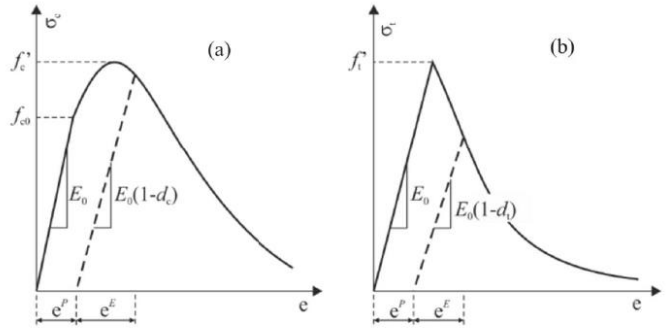

Figure 9. Stress-strain curves adopted for the masonry units under (**a**) compression and (**b**) tension [40].

The uniaxial tensile damage and uniaxial compressive damage parameters were developed using the post-failure stress as a function of cracking strain. The cracking strain is equal to the total strain minus the elastic strain of the undamaged material [40]. The inelastic strains are calculated using Equation (5) below:

$$\varepsilon_{in} = \varepsilon_t - \varepsilon_{el} \tag{5}$$

where ε_{in} represents the inelastic strain, ε_t denotes the "total strain", and ε_{el} denotes the "elastic strain". According to [37], the damage parameter that is utilised to capture the failure at peak load is shown below in Equation (6):

$$d_c = 1 - {}^{\sigma_c}/_{\sigma_c'} \tag{6}$$

where d_c represents the damage parameter in compression, while σ_c is the compressive strength of masonry unit after the peak stress. The ultimate compressive strength of masonry is denoted by σ_c'.

Equation (7) is used to calculate the plastic strain:

$$\varepsilon_c^{pl} = \varepsilon_c^{in} - \frac{d_c}{1 - d_c} \cdot \frac{\sigma_c}{E_0} \tag{7}$$

In terms of the tensile behaviour, the strain is calculated using Equation (8), which is obtained from the ultimate value of the tensile stress:

$$\varepsilon_{cr} = \varepsilon_t - \varepsilon_{el} \tag{8}$$

where ε_{cr} represents the cracking strain. The damage parameter and the plastic strain are calculated using Equations (9) and (10) below:

$$d_c = 1 - {}^{\sigma_t}/_{\sigma_t'} \tag{9}$$

$$\varepsilon_t^{pl} = \varepsilon_t^{in} - \frac{d_t}{1 - d_t} \cdot \frac{\sigma_t}{E_0} \tag{10}$$

Some additional material properties adopted within the concrete damage plasticity law are provided in Tables 2 and 3.

Table 2. Mechanical properties of masonry unit and mortar [41].

Plasticity Parameter	Value
Dilation angle	30
Eccentricity parameter	0.1
Bi and unidirectional compressive strength ratio	1.16
Stress ratio in tensile meridian	0.67
Viscosity parameter	0.001

Table 3. Material properties [41].

Material	Modulus of Elasticity [MPa]	Poisson's Ratio	Tensile Strength [MPa]	Compressive Strength [MPa]
Masonry Unit	15,500	0.15	1.05	10.5

3.9. Wall's Response

Figure 10 below shows the typical response of the masonry wall under blast loading. This was generated using finite element analysis as part of the dataset creation process. This is similar to Figure 2, which depicted modes of failure under in-plane and out-of-plane loading, thus validating the model.

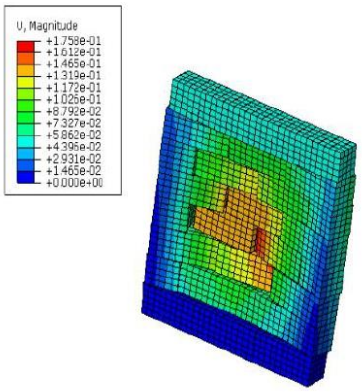

Figure 10. Solid wall loaded with charge weight of 1150 kg at 50 m.

4. Results

4.1. Out-of-Plane Response

The performance and training accuracy of the developed ANN is discussed in this section. The model consisted of two input variables, namely, the blast weight in terms of kg TNT and the standoff distance in metres. The trained ANN is aimed at predicted the in-plane and out-of-plane deformation of the chosen node or location on the wall. The mid-section of the wall was chosen. Using MATLAB R2019a/finite element analysis interface, 95 numerical simulations were generated. The choice of the number of datasets was based on the sample size from the available literature such as the Gaopale [42] where a total of 104 blasting datasets was provided by Orapa Diamond mine for their study to apply ANN to predict blast-induced ground vibration. The authors used 95 simulations as the first trial.

It may be inferred from an analysis of the results collected during the training, testing, and validation phases that ANN models are sufficiently competent to distinguish between

input and output variables while making predictions that are relatively accurate. To investigate the training accuracy of the proposed ANN model, results on regression plots and the training state of the designed ANN were investigated. As per the plots below, the performance of the model for training, testing and validation were found to be acceptable. These acceptable correlation results confirm the relationship between model output values vs. the actual target deflection values. Figure 11 shows the simulation process. As can be seen in Figure below, the data division that was chosen for this model is random and this data sampling method prevents the data modelling process from being bias towards different possible data characteristics. The performance evaluation parameter (mean squared error, MSE) is also known as mean square deviation. The MSE is calculated as the average of the squared alterations between the predicted value and the actual values in the model. A value close to zero as the MSE is generally considered acceptable. In ANN, a gradient is used to measure how much the output of a function changes if there are adjustments in the inputs [43]. In this case, for the gradient descent algorithm to reach the local minimum, the learning rate was set to an appropriate value of 0.0338, which was considered as neither too low nor too high. Validation check is employed to terminate the learning of the ANN and the amount of validation checks will depend on how many times the neural network is iterated. The Mu value is utilized to control the weights of the neurons during the training, specifically on the updating process. The algorithms and progress parameters are further shown in Figure 12.

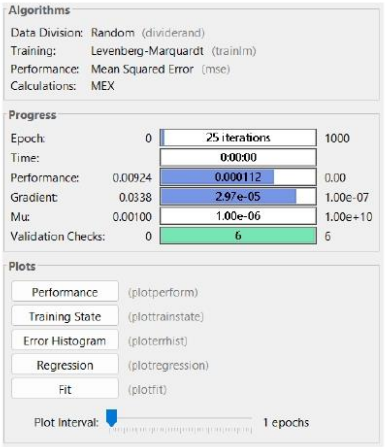

Figure 11. ANN Model training.

The coaching efficiency graph in Figure 12 demonstrates unequivocally that the ANN's learning capacity is appropriate. The plot for performance of training includes the gradient, momentum parameter and validation check which are then plotted against the number of epochs.

Figure 13 depicts the decreasing trend of MSE for the test, training, and verification sets. When the number of iterations reached 19, the MSE of the verification set dropped to the minimum value of 0.000068441, thus achieving the reliable training effect. When the number of iterations got to 19, the training reached the highest number of failures and was stopped.

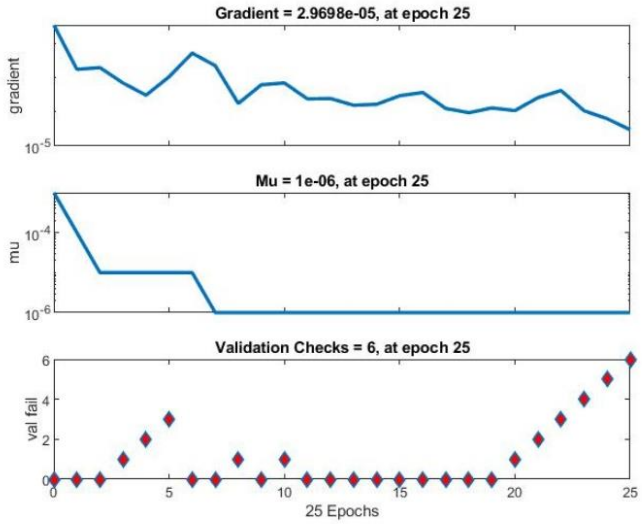

Figure 12. Validation in the training process

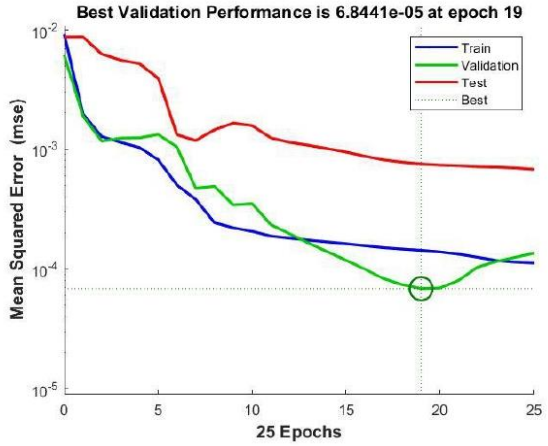

Figure 13. Performance of the training process.

The distribution of the errors made by the neural network on the testing instances is displayed in error histograms. The histogram displays the difference between the anticipated values and the desired values. According to Mtsweni [44], after the training phase, the error histogram is a useful tool for assessing the accuracy of error distributions based on ANN predictions. Figure 14 shows a normal distribution centred at zero for each output variable, and this confirms the decent performance and good error distributions of the developed ANN model.

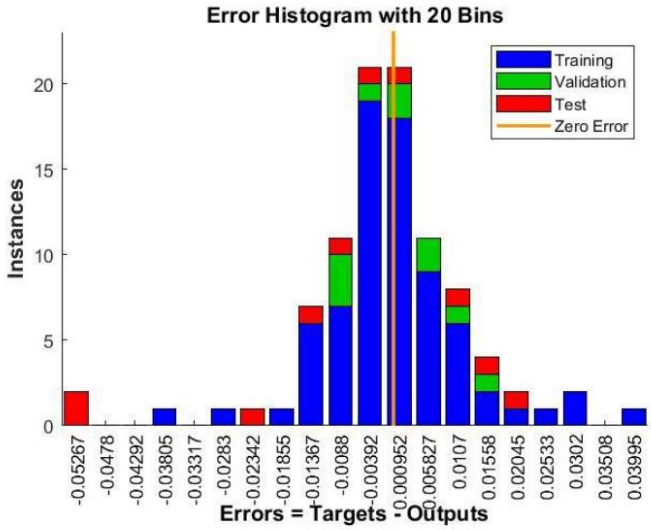

Figure 14. Graphical plot of error histogram for 20 bins.

Figure 15 summarizes the regression plots at the end of the training phase. The predictive performance of the wall deflection under the blast load obtained from the ANN framework is shown in Figure 15, where the coefficient of correlation (R) during training, validation, testing, and combination of three phases were recorded as 0.96737, 0.97981, 0.95596, and 0.96381, respectively. In a similar study conducted by [22], the overall coefficient of correlation (R) that was obtained for a dataset of 478 cases was 94.77%. These are comparable to the proposed study, which has proven to offer acceptable prediction with a reasonable number of number of datasets. In the study conducted by [38], the correlation coefficient for validation of dataset was 0.98011 which is comparable to the present study (R = 0.97981) and to the overall R = 0.99037, which is comparable to R = 0.96381. This validated the training method that was adopted for this study. One of the common checks is that the data must fall on a 45-degree line where the network outputs equal the targets for a perfect fit. As can be seen in the figure below, most data fall along the 45-degree line, and this indicates that the fit by regression is acceptable for all data sets.

To confirm the feasibility of using the above-proposed model in the fast prediction of masonry wall's response, a random value of blast weight was chosen, and standoff distances varied but did not contain any of the distances used as part of training the model. Figure 16 below shows the plot of z-displacement vs. standoff distances for some of the simulations that were used for the training and validation of the model. The randomly selected blast weight showed good prediction, as can be seen on the graph. Firstly, it can be observed that the proposed ANN is able to show the relationship between the displacement and the standoff distance. The damage severity reduces with the increased blast weight. The proposed ANN can be adopted in predicting the masonry wall's response.

Additional random predictions were also performed. These are presented in Table 4 below.

Figure 17 depicts the out-of-plane deflection of explosive weights 120 kg and 160 kg that were used for random prediction.

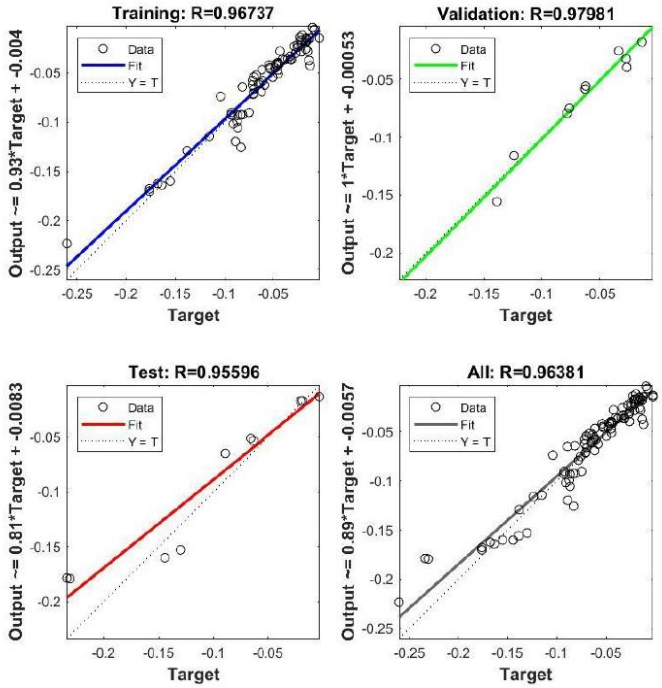

Figure 15. Prediction performance of the output variable (out-of-plane displacement).

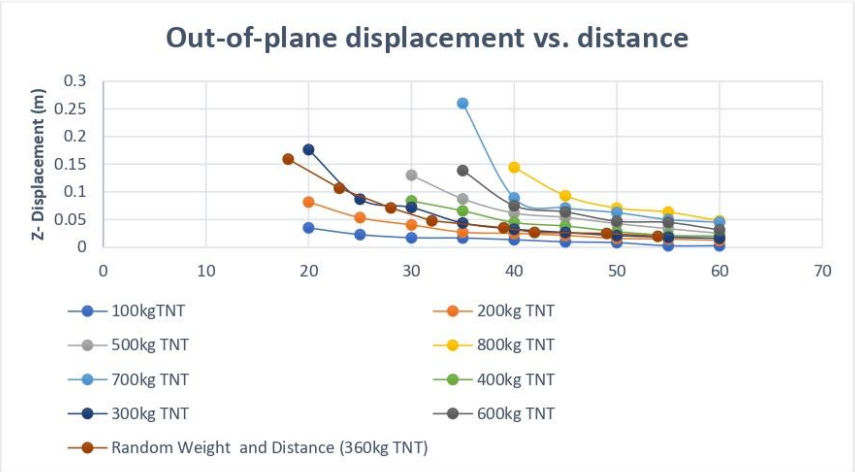

Figure 16. Prediction performance of the proposed model: Displacement vs. standoff distance.

Table 4. Out-of-plane response prediction.

Blast Weight (kg TNT)	Standoff Distance (m)	Actual Out-of-Plane (m)	Predicted Out-of-Plane(m)	Percentage Error	FEA TIME (cpu Time)	Ann Time
120	43	-1.32×10^{-2}	-1.24×10^{-2}	6.4%	1915.2 s	6.5 s
160	26	-3.99×10^{-2}	-4.01×10^{-2}	0.4%	1926.6 s	6.5 s

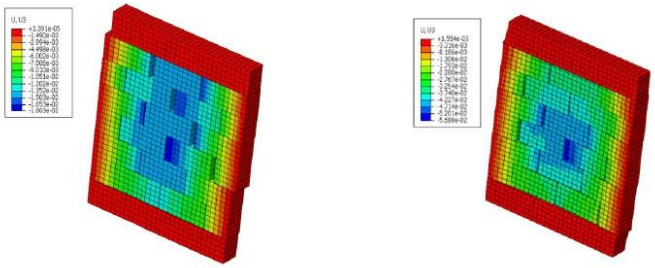

(**a**) (**b**)

Figure 17. Predicted out-of-plane response: (**a**) 120 kg TNT at 43 m standoff, (**b**) 160 kg TNT at 26 m standoff.

4.2. Effect of Blast Weight/Standoff Distance

In order to analyse the effect of blast weight and standoff distance, Figure 18 clearly shows that the out-of-plane response is greatly influenced by the explosive weight and the standoff distance. This can be seen by an increasing exponential graph. On the other hand, Figure 19 depicts the relationship between the ratio of the explosive weight and the distance vs. in-plane deflection. From this figure it can be concluded that there is no direct relationship between the two variables, however, it can be highlighted that a higher ratio leads to less in-plane deflection which is the opposite of the results presented in Figure 18. Thus, a higher explosive weight at a closer standoff distance results in more out-of-plane and less in-plane deflection.

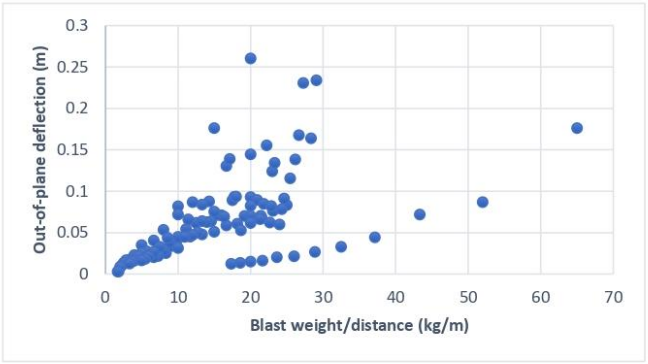

Figure 18. Ratio of Blast weight/distance vs. out-of-plane response of wall.

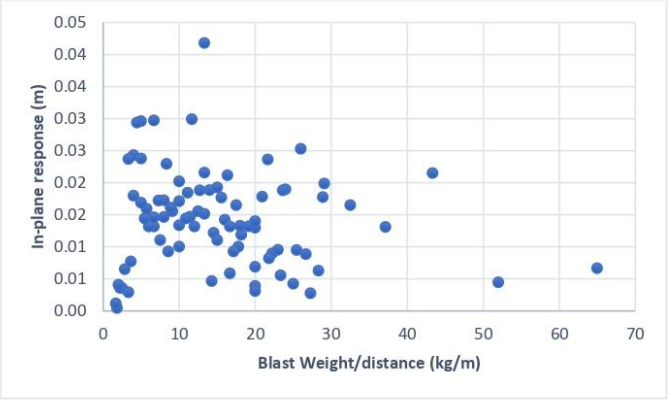

Figure 19. Ratio of Blast weight/distance vs. in-plane response of wall.

5. Discussion

Machine learning has gained popularity in the field of structural engineering. Researchers have conducted research on the prediction of masonry wall response, but the majority focuses on the in-plane loading. Upon reviewing literature, it was found that limited efforts are found in machine learning for blast loading. In this study, an innovative approach was adopted to predict the response of masonry under blast loading. Additionally, this study utilized the unilateral contact-friction and damage mechanics laws, which are adopted to capture masonry's failure modes, and these are strongly non-linear, and this increases the computation cost for one numerical simulation. This article proposed a scheme that uses machine learning techniques that can be adopted, to predict parameters of the mechanical response of the wall under blast actions, by drastically reducing computational cost. This is achieved by training and then using an artificial neural network.

The generation of datasets in this study entailed varying the blast weights and the standoff distance. The present study utilized the wall definition and properties from the study that was conducted by Thango et al. [12]. Other researchers such as Zhang et al. [8,9,11] highlighted the influence of standoff distance and the size of the explosive weight on the response of masonry wall. With reference to Figure 18, it can be seen that the out-of-plane response is greatly influenced by the explosive weight and standoff distance. Figure 16 also shows for majority of explosive weights, a closer standoff distance will lead to higher out-of-plane deflection.

In this study, the accuracy of the proposed ANN framework was evaluated using the coefficient of correlation (R) during training, validation, and testing. Generally, acceptable results offer an R value close to one which shows the model's ability to predict the output given a set of data (input). An overall value of 0.96381 which indicated that the fit by regression is acceptable. The studies conducted by [22] and [38] obtained similar regression results using the quantity of datasets that were compared to the proposed study.

According to Table 4, it has been found that the proposed model is highly capable of predicting deflection given the random input values (blast weight and standoff distance). In addition to that, the proposed model is able to offer results within seconds which is one of the advantages that this model will contribute as part of the practical applications in structural engineering.

6. Conclusions

In this article, a machine learning approach is proposed to predict the structural response of masonry walls under blast actions. First, a non-linear finite element model is used to provide the failure response of masonry, considering unilateral contact-friction interfaces

between masonry stones and a damage mechanics law. Then, parametric simulations are conducted to generate a dataset that is finally used to train an artificial neural network.

Solution of the non-linear finite element model is computationally expensive, in terms of the computational time and resources needed, even for one simulation. This is attributed to the non-linear constitutive descriptions, which are adopted to capture the real failure response of the wall, including the discrete failure mode between masonry stones and continuum failure in the mass of stones.

Therefore, the article aims to provide an efficient machine learning tool that can be used for a first, fast prediction of the out-of-plane deflection of masonry walls under blast loads. In particular, after the generation of the dataset from parametric non-linear finite element simulations, training of the artificial neural network is implemented. As shown in the article, the trained neural network is then able to provide a fast prediction of the response of the masonry wall due to random blast properties (blast weight and standoff distance), avoiding time consuming numerical simulations and heavy computational cost.

The accuracy of the trained artificial neural network is satisfactory, as given by relevant regression plots. Tests to random input variables (not included in the dataset used to train the artificial neural network) also depict a satisfactory accuracy, as compared to finite element analysis.

In addition, the proposed process is able to automatically generate parametric finite element simulations to create the dataset using Python and MATLAB R2019a scripts in collaboration with commercial finite element software.

The study can be extended and overcome current limitations by introducing in the machine learning scheme random geometries of the masonry wall, while also considering the random sizes and patterns of the masonry stones. The influence of modelling the mortar joint between stones, using for instance cohesive zone laws, is another future investigation. Finally, numerical solutions can be evaluated on advanced materials that can be used to protect masonry walls under blast actions. For instance, auxetic materials, with negative Poisson's ratio can be numerically tested by developing proper finite element models [45,46].

Author Contributions: Conceptualization, S.G.T. and G.A.D.; methodology, S.G.T. and G.A.D.; formal analysis, S.G.T.; investigation, S.G.T. and G.A.D.; resources, G.A.D.; data curation, S.G.T. and S.M.M.; writing—original draft preparation, S.G.T.; writing—review and editing, S.G.T., G.A.D., S.M.M. and G.E.S.; visualization, S.G.T.; supervision, G.A.D. and G.E.S.; project administration, G.A.D. All authors have read and agreed to the published version of the manuscript.

Funding: This research received no external funding.

Data Availability Statement: Data are contained within the article

Conflicts of Interest: The authors declare no conflicts of interest.

References

1. Hao, D. Numerical Modelling of Masonry Wall Response to Blast Loads. *Aust. J. Struct. Eng.* **2009**, *10*, 37–52. [CrossRef]
2. Davidson, J.S.; Porter, J.R.; Dinan, R.J.; Hammons, M.I.; Connell, J.D. Explosive testing of polymer retrofit masonry walls. *J. Perform. Constr. Facil. ASCE* **2004**, *18*, 100–106. [CrossRef]
3. Knock, C.; Horsfall, I.; Champion, S.M.; Harrod, I.C. The bounce and roll of masonry debris. *Int. J. Impact Eng.* **2004**, *30*, 1–16. [CrossRef]
4. Masi, F.; Stafanou, I.; Maffi-Berthier, V.; Vannucci, P. A Discrete Element Method based-approach for arched masonry structures under blast loads. *Eng. Struct.* **2020**, *216*, 110721. [CrossRef]
5. Dorn, M.; Nash, M.; Anderson, G.; Anderson, G. Computer prediction of the damage to and collapse of complex masonry structures from explosions. In *Structures Under Shock and Impact VI*; WIT Press: Billerica, MA, USA, 2000; pp. 277–286.
6. Pande, G.N.; Liang, J.X.; Middleton, J. Equivalent elastic moduli for brick masonry. *Comput. Geotech.* **1989**, *8*, 243–265. [CrossRef]
7. Pietruszczak, S.; Niu, X. A mathematical description of macroscopic behavior of brick masonry. *Int. J. Solids Struct.* **1992**, *29*, 531–546. [CrossRef]
8. Su, Y.; Wu, C.; Griffith, M. Mitigation of blast effects on aluminum foam protected masonry walls. *Trans. Tianjin Univ.* **2008**, *14*, 558–562. [CrossRef]

9. Ishfaq, M.; Ullah, A.; Ahmed, A.; Ali, S.; Ali, S.M.; Uddin, M.; Shahzada, K. Numerical Approximation of Blast Loads on Confined Dry-Stacked Masonry Wall. *Math. Probl. Eng.* **2021**, *2021*, 2394931. [CrossRef]
10. Anas, S.; Alam, M.; Umair, M. Experimental studies on blast performance of unreinforced masonry walls: A state-of-the-art review. *Asps Conf. Proc.* **2022**, *1*, 1791–1802. [CrossRef]
11. Zhang, Y.; Hu, J.; Zhao, W.; Hu, F.; Yu, X. Numerical Study on the Dynamic Behaviors of Masonry Wall under Far-Range Explosions. *Buildings* **2023**, *13*, 443. [CrossRef]
12. Thango, S.G.; Stavroulakis, G.E.; Drosopoulos, G.A. Investigation of the Failure Response of Masonry Walls Subjected to Blast Loading Using Nonlinear Finite Element Analysis. *Computation* **2023**, *11*, 165. [CrossRef]
13. Jasmine, P.H.; Arun, S. Machine learning applications in structural engineering—A review. *IOP Conf. Ser. Mater. Sci. Eng.* **2021**, *1114*, 012012. [CrossRef]
14. Thai, H.-T. Machine learning for structural engineering: A state-of-the-art review. *Structures* **2022**, *38*, 448–491. [CrossRef]
15. Almustafa, M.K.; Nehdi, M.L. Machine learning model for predicting structural response of RC slabs exposed to blast loading. *Eng. Struct.* **2020**, *221*, 111109. [CrossRef]
16. Friaa, H.; Hellara, M.L.; Stefanou, I.; Sab, K.; Dogui, A. Artificial neural networks prediction of in-plane and out-of-plane homogenized coefficients of hollow blocks masonry wall. *Meccanica* **2020**, *55*, 525–545. [CrossRef]
17. Drosopoulos, G.A.; Stavroulakis, G.E. Data-driven computational homogenization using Neural Networks. *J. Comput. Cult. Heritage* **2020**, *14*, 1–19. [CrossRef]
18. Cascardi, A.; Micelli, F.; Aiello, M.A. Analytical model based on artificial neural network for masonry shear walls strengthened with FRM systems. *Compos. Part B Eng.* **2016**, *95*, 252–263. [CrossRef]
19. Zhang, Y.; Zhou, G.; Xiong, Y.; Rafiq, M. Techniques for Predicting Cracking Pattern of Masonry Wallet Using Artificial Neural Networks and Cellular Automata. *J. Comput. Civ. Eng.* **2010**, *24*, 161–172. [CrossRef]
20. Zhou, G.; Pan, D.; Xu, X.; Rafiq, Y. Innovative ANN Technique for Predicting Failure/Cracking Load of Masonry Wall Panel under Lateral Load. *J. Comput. Civ. Eng.* **2010**, *24*, 377–387. [CrossRef]
21. Plevris, V.; Asteris, P. Anisotropic failure criterion for brittle materials using artificial neural networks. In Proceedings of the COMPDYN 2015/5th ECCOMAS Thematic Conference on Computational Methods in Structural Dynamics and Earthquake Engineering, Crete Island, Greece, 25–27 May 2015.
22. Chomacki, L.; Rusek, J.; Słowik, L. Machine Learning Methods in Damage Prediction of Masonry Development Exposed to the Industrial Environment of Mines. *Energies* **2022**, *15*, 3958. [CrossRef]
23. Remennikov, A.M.; Rose, T.A. Predicting the effectiveness of blast wall barriers using neural networks. *Int. J. Impact Eng.* **2007**, *34*, 1907–1923. [CrossRef]
24. Bewick, B.; Flood, I.; Chen, Z. A Neural-Network Model-Based Engineering Tool for Blast Wall Protection of Structures. Air force Research Laboratory, Materials and Manufacturing Directorate. 2010. Available online: https://apps.dtic.mil/sti/tr/pdf/ADA520929.pdf (accessed on 24 July 2023).
25. Huang, Z.; Cai, L.; Kollipara, T. Blast Hazard Resilience Using Machine Learning for West Fertilizer Plant Explosion. *J. Perform. Constr. Facil.* **2021**, *35*, 04021062. [CrossRef]
26. Salem, S.; Torky, I. Incooperating machine learning for rapid blast resilience assessment. In Proceedings of the European Conference on Computing in Construction Ixia, Rhodes, Greece, 24–26 July 2022.
27. Khaleghi, M.; Salimi, J.; Farhangi, V.; Moradi, M.; Karakouzian, M. Application of artificial neural network to predict load bearing capacity and stiffness of perforated masonry walls. *Civil. Eng.* **2021**, *2*, 48–67. [CrossRef]
28. Chopra, P.; Sharma, R.K.; Kumar, M. Prediction of Compressive Strength of Concrete Using Artificial Neural Network and Genetic Programming. *Adv. Mater. Sci. Eng.* **2016**, *2016*, 7648467. [CrossRef]
29. Proença, J.M.; Gago, A.S.; Vilas Boas, A. Structural window frame for in-plane seismic strengthening of masonry wall buildings. *Int. J. Archit. Herit.* **2018**, *27*, 2031–2047. [CrossRef]
30. Vaculik, J.; Griffith, M.C. Out-of-plane load—Displacement model for two-way spanning masonry walls. *Eng. Struct.* **2017**, *141*, 328–343. [CrossRef]
31. Sochet, I. Blast effects of external explosions. In Proceedings of the Eighth International Symposium on Hazards, Prevention, and Mitigation of Industrial Explosions, Yokohama, Japan, 5–10 September 2010; HAL Open Science: Lyon, France, 2010; p. hal-00629253.
32. Baumgart, C.M. The Effects of Advanced Structural Materials to Mitigate Explosive and Impact Threats. Master's Thesis, Missouri University of Science and Technology, Rolla, MO, USA, 2014; p. 7320. Available online: https://scholarsmine.mst.edu/cgi/viewcontent.cgi?article=8319&context=masters_theses (accessed on 8 July 2023).
33. Dragani'c, H.; Sigmund, V. Blast Loading on Structures. *Tech. Gaz.* **2012**, *19*, 643–652.
34. Solís-Pérez, J.E.; Hernández, J.A.; Parrales, A.; Gómez-Aguilar, J.F.; Huicochea, A. Artificial neural networks with conformable transfer function for improving the performance in thermal and environmental processes. *Neural Netw.* **2022**, *152*, 44–56. [CrossRef]
35. Maren, R.J.; Harston, C.T.; Pap, R.M. *Handbook of Neural Computing Applications*; Academic Press, Inc.: San Diego, CA, USA, 1990.
36. Asteris, P.G.; Argyropoulos, I.; Cavaleri, L.; Rodrigues, H.; Varum, H.; Thomas, J.; Lourenço, P.B. Masonry Compressive Strength Prediction Using Artificial Neural Networks. In *Communications in Computer and Information Science*; Springer International Publishing: Berlin/Heidelberg, Germany, 2019. [CrossRef]

37. Stavroulakis, G.E.; Drosopoulos, G.A.; Muradova, A. Data-driven, data-based and artificial intelligence methods in com-putational mechanics. In Proceedings of the 3rd Coordinating Engineering for Sustainability and Resilience, Irbid, Jordan, 6–9 May 2022.
38. Liu, F.; Zhang, Z.; Gao, Y.; Xin, K.; Yan, M.; Huang, X.; Duan, Y.; Huang, C. Prediction method of blast load on underground structure surface based on neural network. *AIP Adv.* **2023**, *13*, 045110. [CrossRef]
39. Qi, C.; Yang, S.; Yang, L.-J.; Han, S.-H.; Lu, Z.-H. Dynamic Response and Optimal Design of Curved Metallic Sandwich Panels under Blast Loading. *Sci. World J.* **2014**, *2014*, 1–14. [CrossRef]
40. *ABAQUS*, version 6.14.2; User's Manual. Available online: http://130.149.89.49:2080/v2016/index.html (accessed on 10 April 2023).
41. Iuorio, O.; Dauda, J.A. Retrofitting Masonry Walls against Out-Of-Plane Loading with Timber Based Panels. *Appl. Sci.* **2021**, *11*, 5443. [CrossRef]
42. Gaopale, K.; Rodrigo, J.S.; Seitshiro, T. Application of Artificial Neural Networks to Predict Blast-Induced Ground Vibration in a Diamond Mine. In Proceedings of the BIUST Research and Innovation Symposium 2019 (RDAIS 2019), Palapye, Botswana, 4–7 June 2019; Botswana International University of Science and Technology: Palapye, Botswana, 2019.
43. Bhavatarini, N.; Syed, M.B.; Syed, T.A. *Deep Learning: A Practical Approach*; Milestone Research Publications: San Diego, CA, USA, 2022.
44. Mtsweni, S. Performance Optimization Modelling of a Horizontal Roughing Filter for the Treatment of Mixed Greywater. Ph.D. Thesis, Durban University of Technology: Durban, South Africa, 2021. Available online: https://openscholar.dut.ac.za/bstream/10321/3727/3/Mtsweni%20Sphesihle-20410988_Redacted.pdf (accessed on 9 August 2023).
45. Kalubadanage, D.; Remennikov, A.; Ngo, T.; Qi, C. Close-in blast resistance of large-scale auxetic re-entrant honeycomb sandwich panels. *J. Sandw. Struct. Mater.* **2021**, *23*, 4016–4053. [CrossRef]
46. Bohara, R.P.; Linforth, S.; Nguyen, T.; Ghazlan, A.; Ngo, T. Anti-blast and -impact performances of auxetic structures: A review of structures, materials, methods, and fabrications. *Eng. Struct.* **2023**, *276*, 115377. [CrossRef]

Chapter 7 – Conclusions and recommendations

The results from this study provided a methodology relying on finite element analysis and machine learning to derive the response of masonry walls under blast loading. Factors that govern the structural behaviour of masonry walls under blast actions, including the impact of horizontal forces, as well as the influence of changing the blast weight or the standoff distance, were also investigated. This chapter summarises the findings and recommends possible future work that can extend this study.

In chapter 4, the response of masonry walls under static in-plane and blast loads, is investigated using non-linear finite element analysis. In order to simulate the damage in the interfaces between the masonry units, unilateral contact-friction interfaces are applied depicting opening and sliding failure. This study was able to determine the tensile and compressive damage in the blocks by adopting a concrete damage plasticity model available in the software. The proposed scheme was applied to a solid masonry wall and to a wall with an opening (window).

The collapse mechanism due to varying blast weights and standoff distances was also investigated in this study using FEA. Three load cases and two masonry walls were considered, namely, (1) Solid masonry wall loaded by vertical pressure, shear displacement and blast load, (2) Solid masonry wall loaded by vertical pressure and blast load, (3) Masonry wall with an opening loaded by vertical pressure, shear displacement and blast load. From the different loading cases, it was concluded that when there is no shear displacement loading, the response is dominated by the out-of-plane flexural deflection, attributed to the blasting action. Another result of this work is that the existence of a window or other opening in the wall may lessen the impact of the blast action by lowering the structure's out-of-plane reaction. The reason for this, is that due to the opening being located at the middle of the wall, the blast load is not applied to this critical (for out-of-plane flexure) middle part of the surface of the wall. Accordingly, the study demonstrates that in order to seriously harm the building, the blast action needs to happen at a closer standoff distance than the solid wall.

In chapter 5, the effect of brick patterns on the masonry wall’s response is investigated. The influence of brick bonding patterns has been investigated by various research under in plane loading. This study aimed at contributing to the body of knowledge by comparing the different bonding patterns under blast loading and the findings were intended at highlighting the importance of selecting the applicable pattern when blast loading is anticipated. Three bonding

patterns were considered in this study, namely, English bond, stretcher bond and stack bond. This investigation concluded that there is a slight difference in the peak displacement at the centre of the wall for the English and stretcher bond. The stack bond displayed higher deflection values than the other two bonding patterns under both in plane and out-of-plane loading. Also, stack bond masonry walls are susceptible to vertical cracking at the vertical mortar joints because they lack horizontal support. The different brick patterns play a role in the blast resistance of the wall. It was highlighted that the stack bond arrangement with the vertical joints is easily susceptible to separation when subjected to out of plane stresses, such as blast loads, which compromises structural integrity. This study was able to highlight the importance of understanding the effect of different bonding patterns for structural walls that are subjected to out-of-plane loading such as blast actions.

In chapter 6, a data-driven approach using machine learning methods to predict the masonry response under blast loading is considered. Using 95 numerically generated datasets from FEA, an artificial neural network was developed. This model was able to accurately predict the out-of-plane response of the wall under varying loading conditions.

This study aimed at gaining insight and exploration the applicability of Neural networks as the fast-predicting tool for masonry walls subjected to blast loading. The artificial neural network (ANN) techniques have proven to offer prompt prediction of masonry response under blast loading. The development of datasets was done using numerical simulations. The linkage of MATLAB scripts, Python scripts and ABAQUS was implemented done in this study. This linkage provided an approach to run automatically, several ABAQUS models through MATLAB/Python, without having to open the FEA software. In the scripts, all boundary conditions were added, including the unilateral laws to simulate the contact-friction between the masonry units. The parametric study considered under the machine learning approach included varying the blast load weight and the standoff distance. This was implemented through MATLAB coding.

MATLAB's Levenberg-Marquardt training technique was utilized to construct the neural networks that predicted the structural behaviour. A total number of 95 simulations were used to train the model. The 80-10-10 rule was used to train the neural networks with one hidden layer that consisted of 10 neurons. In terms of the regression graphs, the data points were mainly centred on the 45° line which confirmed an acceptable fit and good generalization between the targets and network predictions. In this study, the *R* correlation coefficients were

all greater than 0.9 for the training, testing, validation and all data sets which proved the model's ability to accurately predict the output.

This research was able to provide failure patterns of masonry walls when subjected to blast actions which can be useful to structural engineers who are tasked with investigating the possible causes of blast actions on buildings. Furthermore, the choice of brick bonding pattern shall be done taking into account the response of each bonding pattern against in-plane and out-of-plane loading. It is worth highlighting that this research was able to provide valuable information that can be used for structural health monitoring with specific reference to post blast effect on residential houses in the close proximity to open cast mining activities which requires some level of understanding on the factors that contribute to failure mechanisms on masonry walls. The proposed machine learning model from this study will be able to promptly predict the expected response of the walls given the blast weight and the standoff distance. This can be used for planning or for assessment purposes by engineers.

Recommendations for future research

The research study presented in this thesis investigated the masonry wall's response under blast loading using nonlinear finite element methods and data driven methods. Considering the broadness of this subject area, some aspects are uncovered. Recommendations for future research are presented below:

- Image recognition deep learning tools can be adopted to correlate existing damage of the masonry walls with their response against blast actions. Input in those machine learning algorithms will be the image of existing walls and output the failure response.
- As some low-cost houses are still built using rubble masonry, an investigation of a rubble wall's response under blast loading can provide valuable information on the suitability of such walls in areas that are prone to blast loads.
- The concept of applying advanced composite materials to protect masonry walls against blast actions can be investigated. For example, auxetic materials depicting negative Poisson's ratio could be tested numerically, as protecting materials.

APPENDIX A

(Python script to create multiple Finite element models without opening ABAQUS every time each job is completed) . The analysis framework is established using Python.The numerical FE model is established in ABAQUS/CAE. The ABAQUS/CAE is required to run the files.

```
from part import *
from material import *
from section import *
from assembly import *
from step import *
from interaction import *
from load import *
from mesh import *
from optimization import *
from job import *
from sketch import *
from visualization import *
from connector Behavior import *
import glob
import numpy as np
import os
        #Created by S Thango (for his Phd Studies)
        #-------------------------------------------------------------------------------------------------------
-----
for vv in range(1, 10):


        #importing CAE file.
        os.chdir(r"E:\Sipho Thango_UKZN\Aug4")
        openMdb(pathName='E:\Sipho Thango_UKZN\Aug4\jan22 50020FixedWITHP.cae')
        #: The model database "E:\Sipho Thango_UKZN\Jan23\jan22 50020FixedWITHP.cae"
has been opened.
        session.viewports['Viewport: 1'].setValues(displayedObject=None)
        p = mdb.models['Model-1'].parts['Part-1']
        session.viewports['Viewport: 1'].setValues(displayedObject=p)
```

```
        #changing stand-off distance
        #Stand-off distance increasing in multiples of 5.

        va=vv*5+15;
        a = mdb.models['Model-1'].rootAssembly
        session.viewports['Viewport: 1'].setValues(displayedObject=a)
        session.viewports['Viewport: 1'].assemblyDisplay.setValues(
                optimizationTasks=OFF, geometricRestrictions=OFF, stopConditions=OFF)
        a = mdb.models['Model-1'].rootAssembly
        a.features['RP-1'].setValues(zValue=va)
        a = mdb.models['Model-1'].rootAssembly
        a.regenerate()
        a = mdb.models['Model-1'].rootAssembly
        a.regenerate()

        #-------------------------------------------------------------------------------------------------
-----
        # This sorts out the naming of the Jobs created.
        #The location where the Jobs\results are stored.
                AAA = r"E:\Sipho Thango_UKZN\Aug4\\";

        # search text files starting with the word "Job"
        #BBB = AAA + "Job" + "*.odb" ;   - creates . odb files
        BBB = AAA + "Job" + "*.inp" ;

        # List of the files that match the pattern
        CCC = glob.glob(BBB);

        DDD = np.size(CCC);
        EEE = 'Job-' + str(DDD+1);
        #-------------------------------------------------------------------------------------------------
-----
```

```
        # Creating INP file


        mdb.models['Model-1'].rootAssembly.regenerate()
        mdb.Job(atTime=None, contactPrint=OFF, description='', echoPrint=OFF,
                explicitPrecision=SINGLE, getMemoryFromAnalysis=True,
historyPrint=OFF,
                memory=90, memoryUnits=PERCENTAGE, model='Model-1',
modelPrint=OFF,
                multiprocessingMode=DEFAULT, name=EEE,
nodalOutputPrecision=SINGLE,
                numCpus=1, numGPUs=0, queue=None, scratch='', type=ANALYSIS,
                userSubroutine='', waitHours=0, waitMinutes=0)
        #----------------------------------------------------------------------------------------------------
-----
        # Solve Job
        #mdb.jobs[EEE].submit(consistencyChecking=OFF)
        mdb.jobs[EEE].writeInput(consistencyChecking=OFF)
        #----------------------------------------------------------------------------------------------------
-----
```

APPENDIX B

(Python script to extract deformations to be used as dataset for training of the network). A node group is created on ABAQUS, each node has x,y and z parameters defined. For each completed job, the python script is able to call for deformations on the specified node of the model.

#Created by S Thango (for his Phd studies)

Importing Abaqus odb files

*from abaqus import **

*from abaqus Constants import **

import odb Access

import section

import region Toolset

import display Group MdbToolset as dgm

import part

import material

import assembly

import step

import interaction

import load

import mesh

import optimization

import job

import sketch

import visualization

import xyPlot as xyPlot

import display Group Odb Toolset as dgo

import connector Behavior

*from cae Modules import **

from driver Utils import execute On Cae Startup

import display Group Mdb Toolset

import display Group Odb Toolset

*from abaqus import **

*from abaqus Constants import **

*from cae Modules import **

```
from driver Utils import execute On Cae Startup


from abaqus import *
from abaqus Constants import *
import numpy as np
#-------------------------------------------------------------------------------------------------------
        #The location where the Jobs\results are stored.
for x in range(1, 1862):
    AAA = r"E:\Sipho Thango_UKZN\Aug6\\";
    BBB = "Job-"+str(x);
        #search text files starting with the word "Job"
    CCC = AAA + BBB + ".odb" ;
    DDD = BBB + "_deformation.txt";


    odb = session.openOdb(CCC)
        #Creating a loop
        # Create a variable that refers to the last frame of the first step.
        #lastFrame = odb.steps['Step-1'].frames[-1]
    lastFrame = odb.steps['Step-1'].frames[-1]


        # Create a variable that refers to the displacement 'U' in the last frame of the first step.
        #Surface deformation
    displacement = lastFrame.fieldOutputs['U']
    centerInner = odb.rootAssembly.nodeSets['REFNODE']
    centerDisplacementInner = displacement.getSubset(region=centerInner)
    #SURFACE
    D1x = []
    D1y = []
    D1z = []
    for v in centerDisplacementInner.values:
        D1x.insert(0, v.data[0])
```

```
    D1y.insert(0, v.data[1])
    D1z.insert(0, v.data[2])

dataInner= np.array([D1x,D1y,D1z]).transpose()

with open(DDD, "w") as f:
    np.savetxt(f, dataInner, fmt='%1.50f')
```

APPENDIX C

(MATLAB Code for developing and training ANN). The dataset from ABAQUS was saved as an excel file (Blast weight and standoff distance). On MATLAB, the dataset was then split for training, validation and testing.

```
% Solve an Input-Output Fitting problem with a Neural Network
% Script generated by Neural Fitting app
% Created 6-Aug-2023 17:05:26
% Created by S Thango (as part of his Phd studies)
% This script assumes these variables are defined:
%   data_1 - input data (Blast weight and standoff distance)
%   data_2 - target data (out of plane displacement)
x = data_1';
t = data_2';
% Choose a Training Function
% For a list of all training functions type: help nntrain
% 'trainlm' is usually fastest.
% 'trainbr' takes longer but may be better for challenging problems.
% 'trainscg' uses less memory. Suitable in low memory situations.
trainFcn = 'trainlm';  % Levenberg-Marquardt backpropagation.
% Create a Fitting Network
hiddenLayerSize = 10;
net = fitnet(hiddenLayerSize,trainFcn);
% Setup Division of Data for Training, Validation, Testing
net.divideParam.trainRatio = 80/100;
net.divideParam.valRatio = 10/100;
net.divideParam.testRatio = 10/100;


% Train the Network
[net,tr] = train(net,x,t);
% Test the Network
y = net(x);
e = gsubtract(t,y);
performance = perform(net,t,y)
```

```
% View the Network
view(net)
% Plots
% Uncomment these lines to enable various plots.
%figure, plotperform(tr)
%figure, plottrainstate(tr)
%figure, ploterrhist(e)
%figure, plotregression(t,y)
%figure, plotfit(net,x,t)
```

APPENDIX D

(MATLAB code for prediction of deformation). This code was used to randomly predict an output given a random blast weight and standoff distance.

```
% CREATED BY SIPHO THANGO (As part of his Phd Studies)
% Script generated by Neural Fitting app
% Created 10-Aug-2023 22:23:17
%
% This script assumes these variables are defined:
%
%   INP - input data.
%   OUT - target data.
%INP is the input data used for training the network
%OUT is the output data used as part of training the model
x = INP';
t = OUT';

% Choose a Training Function
% For a list of all training functions type: help nntrain
% 'trainlm' is usually fastest.
% 'trainbr' takes longer but may be better for challenging problems.
% 'trainscg' uses less memory. Suitable in low memory situations.
trainFcn = 'trainlm';  % Levenberg-Marquardt backpropagation.

% Create a Fitting Network
hiddenLayerSize = 10;
net = fitnet(hiddenLayerSize,trainFcn);

% Setup Division of Data for Training, Validation, Testing
net.divideParam.trainRatio = 80/100;
net.divideParam.valRatio = 10/100;
net.divideParam.testRatio = 10/100;

% Train the Network
[net,tr] = train(net,x,t);

% Test the Network
y = net(x);
e = gsubtract(t,y);
performance = perform(net,t,y)

% View the Network
view(net)

% Plots
% Uncomment these lines to enable various plots.
%figure, plotperform(tr)
%figure, plottrainstate(tr)
```

```
%figure, ploterrhist(e)
%figure, plotregression(t,y)
%figure, plotfit(net,x,t)
%Load optimization data. This section allows for random prediction of outputs
  op=Optimizationmatlab';
 % to predict the outcome,for a sample x
 a=net(op(:,17))
```